NASA TECHNICAL MEMORANDUM

NASA TM X-53124

September 3, 1964

NASA TM X-53124

LUNAR ENVIRONMENT: AN INTERPRETATION OF THE SURFACE OF THE MOON AND ITS ATMOSPHERE

by JOHN R. ROGERS AND OTHA H. VAUGHAN, JR.
Aero-Astrodynamics Laboratory

NASA

George C. Marshall
Space Flight Center,
Huntsville, Alabama

NASA - GEORGE C. MARSHALL SPACE FLIGHT CENTER

Technical Memorandum X-53124

September 3, 1964

LUNAR ENVIRONMENT: AN INTERPRETATION OF THE SURFACE OF THE MOON AND ITS ATMOSPHERE

By

John R. Rogers and Otha H. Vaughan, Jr.

SPACE ENVIRONMENT GROUP
AERO-ASTROPHYSICS OFFICE
AERO-ASTRODYNAMICS LABORATORY

TECHNICAL MEMORANDUM X-53124

LUNAR ENVIRONMENT: AN INTERPRETATION OF THE SURFACE OF THE MOON AND ITS ATMOSPHERE

By

John R. Rogers* and Otha H. Vaughan, Jr.

George C. Marshall Space Flight Center

Huntsville, Alabama

ABSTRACT

10304

This MSFC report on the lunar environment represents the first of a series of reports entitled Space Environment Criteria Guidelines. Subsequent reports will discuss matters pertinent to other space environments including (1) the earth's atmosphere above 100 km; (2) the atmosphere and surface of Mars; (3) the atmosphere of Venus; (4) the radiation environment of space; (5) the meteoroid environment of space; and (6) the magnetic and gravitational fields of the earth, moon, and the planets. The present study and these future studies are intended for use by MSFC in future lunar and space programs. These studies as presently envisaged will compliment work being done on space environments at other government and contractor facilities.

Under the heading of lunar topographic features comparative analyses have been made of several geological classifications of lunar features based on inferred age relationships. Also, a discussion of the major landforms, Continents and Maria, is included. The genetic classification, based on inferred geological origin of the various lunar landforms, attempts to compare by analogy certain lunar features with their interpreted terrestrial counterparts.

Otha

---

* Engineering Specialist, Brown Engineering Company.

A deliberate attempt has been made to be objective and to draw from the entire spectrum of lunar geological knowledge some specific conclusions regarding the somewhat controversial origins of lunar features. A practical approach has been taken in identifying certain features as predominantly impact in origin versus volcanic since it is realized that many decisions have to be made now regarding future lunar surface vehicles and missions. An independent judgment has been made concerning the genetic significance of certain lunar features and in such cases the authors of this report assume full responsibility for their tentative conclusions.

Since design criteria for a stationary vehicle will not suffice for future missions involving mobility, this report provides design criteria parameters for both mobile and stationary vehicles. A need exists for reliable small scale data to obtain a lunar surface criteria based on "real-case" conditions instead of "worst-case" assumptions.

ACKNOWLEDGEMENTS

The authors wish to express appreciation to the following persons whose individual contributions made this report possible: R. E. Smith, Chief, Space Environments Group, Aero-Astrophysics Office; W. W. Vaughan, Chief, Aero-Astrophysics Office, Aero-Astrodynamics Laboratory; and Everett D. Jackson, United States Geological Survey, Houston, Texas.

FIGURE 1. FULL MOON

(Courtesy University of Chicago Press)

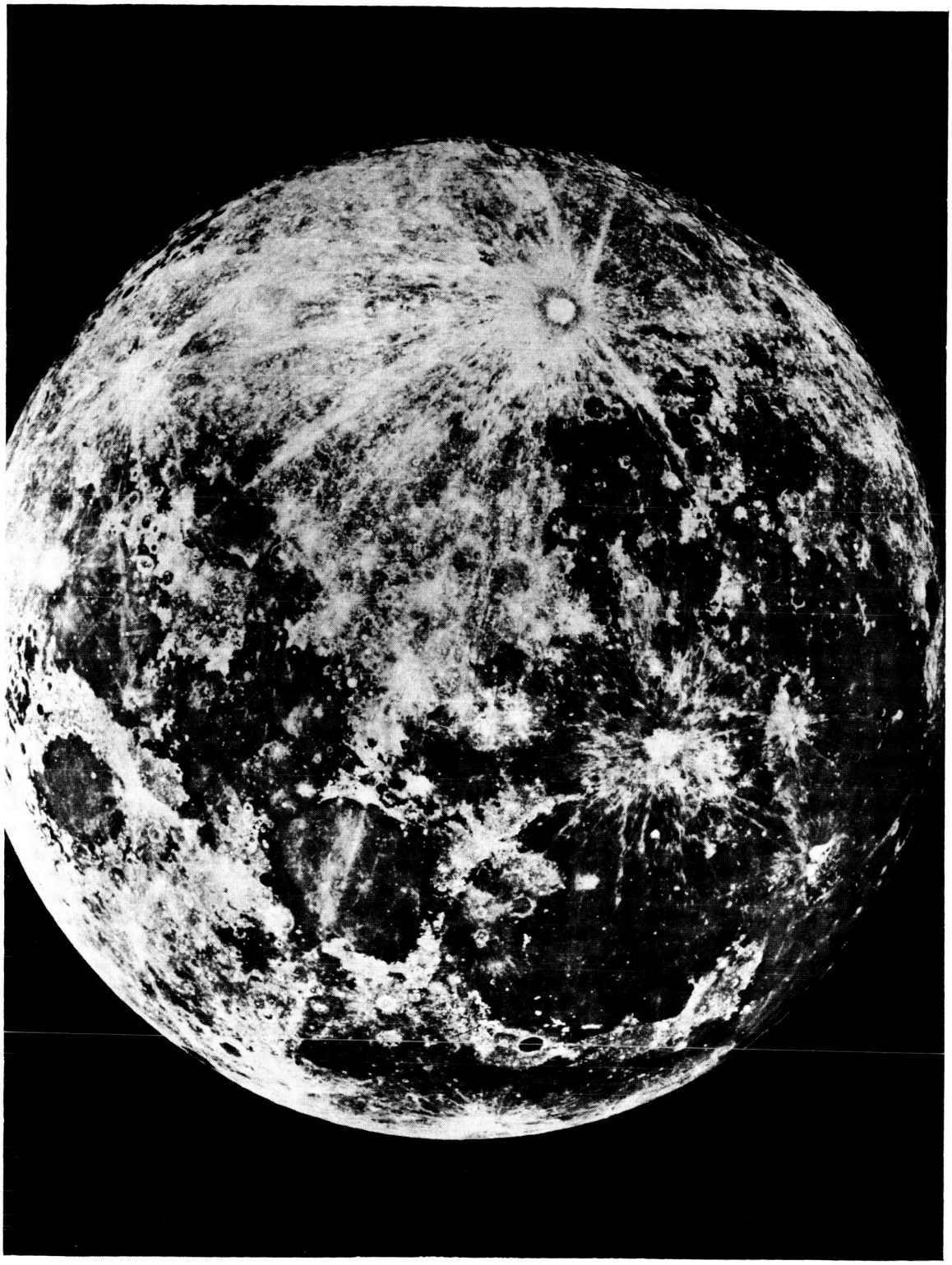

TABLE OF CONTENTS

LIST OF ILLUSTRATIONS

LIST OF ILLUSTRATIONS (Cont'd)

LIST OF ILLUSTRATIONS (Cont'd)

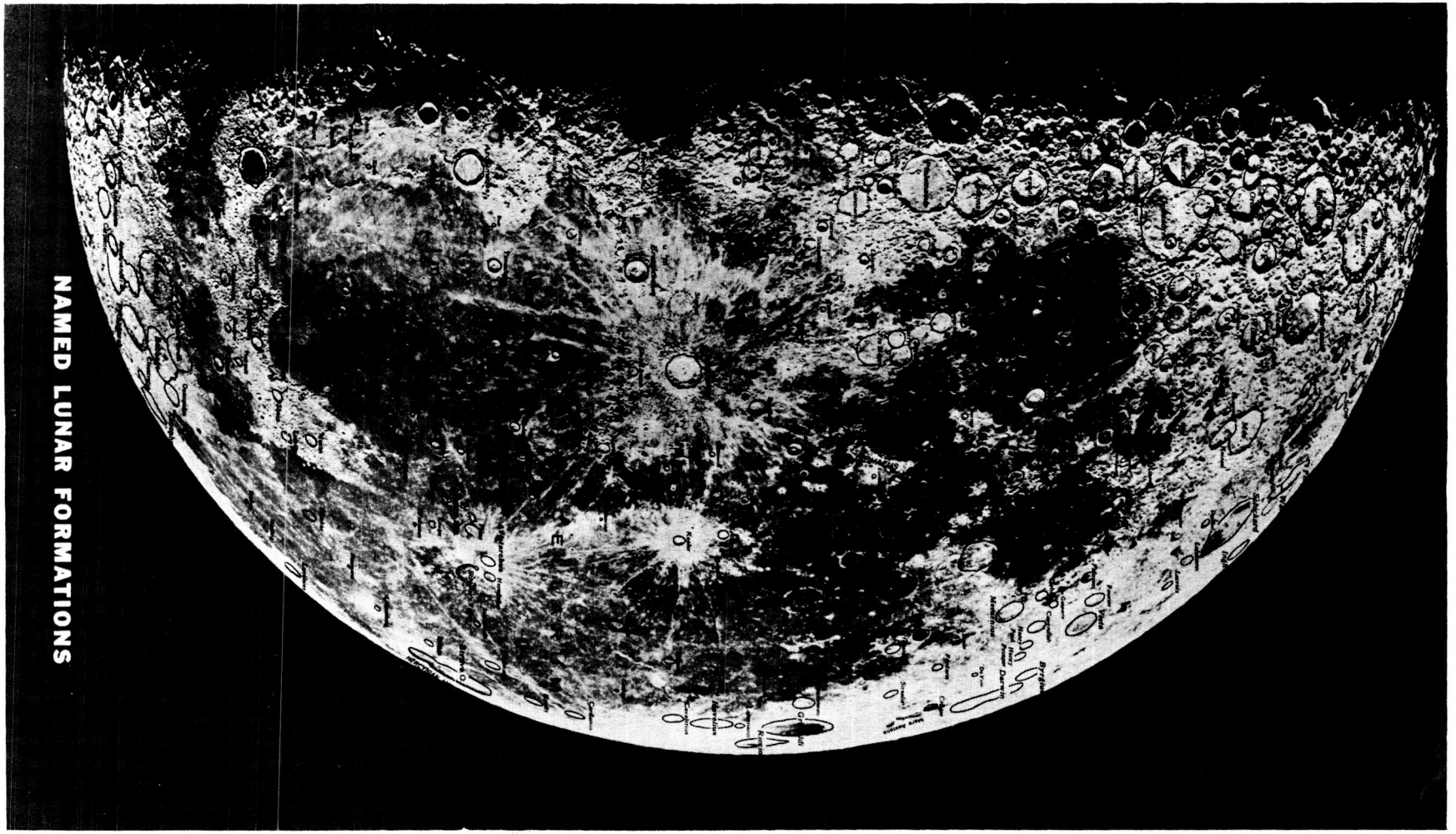

FIGURES 2-3: NAMED LUNAR FORMATIONS

(Courtesy of University of Arizona Press)

TECHNICAL MEMORANDUM X-53124

LUNAR ENVIRONMENT: AN INTERPRETATION OF THE SURFACE OF THE MOON AND ITS ATMOSPHERE

SUMMARY

This report on the lunar environment is the first of a series of reports entitled Space Environment Criteria Guidelines. Subsequent reports will discuss matters pertinent to other space environments including (1) the earth's atmosphere above 100 km; (2) the atmosphere and surface of Mars; (3) the atmosphere of Venus; (4) the radiation environment of space; (5) the meteoroid environment of space; and (6) the magnetic and gravitational fields of the earth, moon, and the planets. The present study and these future studies are intended for use by MSFC in future lunar and space programs. These studies as presently envisaged will complement work being done on space environments at other government and contractor facilities.

Under the heading of lunar topographic features, comparative analyses have been made of several geological classifications of lunar features based on inferred age relationships. Also, a discussion of the major landforms, Continents and Maria, is included. The genetic classification, based on inferred geological origin of the various lunar landforms, attempts to compare by analogy certain lunar features with their interpreted terrestrial counterparts.

A deliberate attempt has been made to be objective and to draw from the entire spectrum of lunar geological knowledge some specific conclusions regarding the somewhat controversial origins of lunar features. A practical approach has been taken in identifying certain features as predominantly impact in origin versus volcanic since it is realized that many decisions have to be made now regarding future lunar surface vehicles and missions. An independent judgment has been made concerning the genetic significance of certain lunar features, and in such cases the authors of this report assume full responsibility for their tentative conclusions.

Since design criteria for a stationary vehicle will not suffice for future missions involving mobility, this report provides design criteria parameters for both mobile and stationary vehicles. A need exists for reliable small scale data to obtain a lunar surface criteria based on "real-case" conditions instead of "worst-case" assumptions.

This report was prepared under NASA Government order No. NAS8-5285.

I. INTRODUCTION

Presently, the moon and its associated problems occupy a significant portion of the research effort in the space sciences. Definite answers must be provided to the significant problems regarding the moon's surface if adequate design criteria are to be established for future lunar exploration. This document provides the designer of both lunar colonies and roving vehicles with the state of the art in lunar technology in the subjects most significant for their particular design purposes. Secondly, it is expected that this document will be useful to those individuals charged with the responsibility for future lunar mission studies.

An attempt is made at objectivity since some of the lunar problems are of a cosmological nature and others are of an engineering nature. That there should be a distinction between these two broad fields of research is not only significant, but necessary if a proper conceptual engineering design is to be achieved at this stage in lunar exploration.

II. STATEMENT OF THE PROBLEM AREAS

As of the time of this writing, the design parameters for Project Apollo have already been defined and no significant new knowledge concerning the lunar environment has been obtained since the design criteria for the Apollo Lunar Excursion Module (LEM) were put into effect.[1] However, this is only a temporary condition, and with the successful lunar landing of future Ranger and Surveyor spacecraft, this situation should change rapidly.

At the present time, it might be easier to compile a list of what we do not know about the moon than to compile one of what we know about it. For example, in the area of cosmological problems, we do not know (1) the chemical composition, (2) the exact mechanism of crater or Maria formation, (3) the density and thermal distribution of the interior, (4) the existence of water or other minerals required for the sustenance of life, or (5) the true nature of the small-scale features of lunar surface, e.g., dust, vesicles, "fairy castle," surface roughness, hardness, etc.

[1] On the morning of July 31, 1964, the Ranger VII successfully relayed back to earth the first close-up photographs of the lunar surface. The resolution of these photographs is estimated as 2000 times better than the best earth-based photographs. These photographs and their implications of the lunar surface small-scale structure and engineering parameters will be discussed in Section VIII of this report.

The major engineering problem encountered in establishing lunar surface design criteria is that too little is known concerning the small-scale features. If a conservative view is adopted and the engineer tries to design for a "worst-case" moon, it has been assumed that the two main problems are an abnormally low bearing strength exhibited by theoretical types of lunar soil models and a relatively high percentage of the surface covered by slopes of more than 15 degrees in the landing area caused by local protuberances, e.g., boulders, crater pits, etc.[2] The Apollo design criteria are basically for a Lunar Excursion Module (LEM) which can land and take off on a "worst-case" moon without turning over due to landing on a high slope or sinking deeply into a structurally weak soil mixture. However, the Apollo design and engineering parameters may not be satisfactory for future scientific missions because the LEM vehicle is designed only to land and take off on the lunar surface. The post-Apollo design must allow for mobility. This will be true regardless of whether a mobile laboratory or a lunar base is established as the Apollo follow-up mission.

As soon as the post-Apollo mission concept is defined, it will be necessary to re-examine the Apollo lunar surface design criteria based on the new mission concept and objectives. Hopefully, by that time, our knowledge of the lunar environment will have progressed sufficiently so that design parameters may be based on the realities that exist for the lunar surface, rather than on "worst-case," engineering expediencies. A design based on a "real-case" moon would offer much more flexibility and adaptability than could ever be afforded by a theoretical lunar surface model.

To be sure, environmental problems exist on the moon other than those associated with the moon's surface. These problems are related to the moon's meteoroid, radiation and thermal environments. The moon's total environment is the sum of these discrete environments. However, this document deals primarily with the surface environments and atmosphere. The moon's radiation and meteoroid environment will be included in future sections.

[2]Initial results from Ranger VII indicate that only about 10 percent of the Mare surface is covered by crater pits and rock fragments and that the percentage of crater pits and rock fragments in the lunar rays is sufficiently high enough to preclude selecting landing sites on them.

One of the main problems facing the systems designer is evaluating the various environmental factors in terms of future system design. This type of evaluation will likely be made on the basis of engineering trade-offs. For example, the radiation and meteoroid environments will require more consideration in terms of shielding, gross weight, etc., for manned missions than for unmanned ones. This document does not attempt to define specific parameters for design since these will vary from mission to mission. Instead, a broad coverage of all lunar surface environmental parameters as they are known today is presented.

Where there are differences of opinion or where a criterion is based on an interpretation of cosmological arguments, e.g., the logical consequences of impact versus volcanic origin of major lunar features, this document will identify these opinions and interpretations. In fact, the problem of interpretation is of such fundamental importance that a deliberate attempt has been made to separate the lunar surface features into a number of distinct categories, e.g., a classification, based on several schemes. It is hoped that this method of analysis will not only help the designer avoid the handicap of "hazy" thinking associated with mixing unrelated concepts, but that at the same time it will lay the foundation for a possible genetic classification of lunar features. A genetic classification will result, not only in better design concepts, but also in a better understanding of the moon as a body of scientific interest.

The philosophy adopted in this guideline is that design criteria are much more effective as they approach the true conditions that they are intended to describe. In lieu of sufficient knowledge of a subject, e.g., small-scale structure of the moon's surface, assumptions must be made regarding the nature of the moon's surface. It is of the utmost importance that we be aware whether we are dealing with a known condition or an assumed one. It is intended that the analyses of the lunar surface on the following pages lead to a clearer understanding of both of these conditions.

III. LUNAR ATMOSPHERE

It has been stated numerous times that the moon has a tenuous atmosphere. Certainly by comparison to the earth's atmosphere, this is a true statement and the atmosphere on the moon could more appropriately be compared to the vacuum of space with all of its associated problems, e.g., sublimation of lubricants and some polymeric materials, and vaporization of liquids. Other problems associated with this environment involve heat transfer under conditions where there are no convection currents and where conduction properties are not well known.

It would be incorrect to state that the moon has no atmosphere since some gaseous emissions have been detected. The pressures and densities are very low by earth's standards, and the effects of these gases on future design will probably be small. Judging from the effects of the lunar atmosphere as an active agent of weathering on large scale lunar surface features, it may be stated that the atmosphere will have a negligible effect on future spacecraft except for problems associated with the effects of vacuum on components and materials. The lack of atmosphere, furthermore, allows the moon's surface to be fully exposed to the effects of the radiation and micrometeoroid environment, and for all practical purposes, these environments may be regarded as greatly enhanced by comparison to their effects on earth.

A. Density

Based on density measurements involving radio star occulations, it has been determined that the gas density of the moon is less than 10^{-12} and possibly 10^{-13} times the mean density at the earth's surface. The lowest value yet obtained using this method, which is regarded as the most sensitive available, is less than 10^{-15} times that of the earth value [1].

The results of an analysis by Öpik [2] of the density of the daytime lunar atmosphere are shown in Table 1.

B. Composition

Lunar gaseous composition has been estimated using theoretical consideration by Öpik [2] as consisting primarily of H_2O and CO_2 with some admixed H_2. Other observers have theorized traces of SO_2, Krypton and Xenon due to outgassing of lunar volcanoes.

C. Pressure

Lunar atmospheric pressure is estimated at 10^{-13} times the earth's mean sea level pressure. Table 1 shows the results of a study by Öpik on the composition of the lunar atmosphere [2].

TABLE 1. MOLECULAR DENSITIES OF COMMON LUNAR GASES

SPECIES	DENSITY, MOLECULES per cm^3
H_2	0.12×10^5
H_2O	1.4×10^5
CO_2	$1.4 - 3.4 \times 10^5$
Various	0.1×10^5
All	3.5×10^5

D. Sources of Gases

The sources for gases on the lunar surface are either internal or external. Internally, gases may result from outgassing due to lunar volcanism, or externally, they may result from the dynamic interaction between solar wind protons or solar electromagnetic radiation with the lunar surface materials or by outgassing of occluded gases from lunar soils in vacuum. Present indications are that little or no true current volcanic activity exists on the lunar surface. One possible exception to this latter statement can be found in the work of Soviet Astronomer Dr. N. A. Kozyrev of the Pulkova Observatory. On the night of November 3, 1958, Kozyrev observed gaseous emissions accompanied by a reddish glow from the crater Alphonsus which he recorded spectrographically. The identified emission bands are C_2 molecules at 4735 Å, 4713 Å, and 4696 Å, C_3 molecules at 5165 Å, 5130 Å, and C_3 bands of comet spectra at between 4100 Å and 3950 Å [3]. Although this information is significant, it is not definitive since the results have been interpreted in several ways. Those lunar scientists who regard volcanism as the most significant geologic process on the moon consider this as a significant lunar eruption, while those scientists who believe that meteoroid impact is the chief geologic process argue that it could have been caused by impact of a carbide-containing meteoroid into a water-bearing soil, or it could simply be due to the release of occluded gases from meteoritic material under high vacuum conditions. In addition, Shorthill [4] has recently noted that the temperatures of the interior of some lunar craters are higher than the adjacent low-lying areas both before and after a lunation. This observation is likewise open to several interpretations.

E. Loss of Gases

The moon's generally slight atmosphere is due to the fact that its low gravitational acceleration allows most gases to achieve escape velocity easily. Kinetic energy, imparted to the molecules by thermal radiation, accelerates the molecules to escape velocities. This process is more effective on light gases than the heavier ones, and it is generally believed that the loss of gases from the moon has occurred largely by this process.

IV. TOPOGRAPHIC FEATURES

A. General Considerations

Lunar topographic features, like earth features, lend themselves to several methods of classification. One type of landform classification is based on inferred age of the lunar feature in question. Observations of age relationship are useful for those individuals who are interested in the moon's geologic history and the natural consequences derived from a consideration of the time and origin of lunar features.

Another type of classification is based on the scale of the lunar feature in question. Broadly speaking, lunar features are either macroscopic or microscopic, depending on the ability of a competent observer to view them from an astronomical observatory. The macroscopic features are those which can be seen and photographed under ordinary "seeing" conditions, and the microscopic features are those which are smaller than the resolving power of most telescopes. The characteristics of small-scale lunar features are inferred and based largely on theoretical considerations. For design purposes, however, the microscopic features are of primary importance, and at present, the most significant lunar experiment would be to increase our knowledge of the microscopic features.

A genetic classification of lunar topographic features is based on the interpreted geological development of the feature in question. The state-of-the-art of lunar technology is such that the major lunar landforms, i.e., craters, Maria, etc., could have been formed by either large scale volcanism or extensive meteoroid bombardment in the geologic past. The issues involved in this scientific argument have far greater consequences than if they were merely academic questions. Indeed, it is fair to say that the future direction of the lunar exploration program hinges on the correct geological interpretation. It seems germane, therefore, to point out a few of the natural consequences which derive from all of these theories and to point out the design considerations that are significant for each of them.

B. Geological Classifications of Lunar Features Based on Inferred Age Relationships

To construct a geologic map of the moon's surface, it is necessary to formulate a hypothesis for establishing the criterion which will be used for determining the relative ages of lunar topographic features. Possible inferences regarding relative age relationships might be based on the relative "sharpness" of the rim material of a lunar crater or the relative brightness of ray material. By inductive reasoning, we might say that the relative "sharpness" of rim material should be related to age, since the older an object is, the longer it has been exposed to weathering and erosion which are the chief aging processes on the moon. Similarly, it can be inferred that the brighter the rays the younger the feature from which they came, since it is known that radiation darkens most materials with time. The rates and efficiency of the processes of erosion and weathering on the moon are not known with a high degree of accuracy. Neither are the agents responsible for lunar erosion and weathering processes well known, although several recent laboratory studies indicate that solar wind bombardment [5], and frequent meteoroid and micrometeoroid bombardment [6] constitute lunar erosion processes. In the presence of ultra-high vacuum, such as exists

on the moon, the clastic or detrital material derived from meteorite bombardment could be reconstituted into various arrangements of mineral grains quite unlike those with which we are familiar on earth. But even with a less than adequate knowledge of the lunar weathering and erosional processes, it seems safe to assume that they do exist and probably have throughout lunar history.

Other observations which indicate relative age relationships on the lunar surface are overlapping or truncated crater rims (Figure 23); partially buried craters, known as "ghost" craters (Figure 24); light colored ray material spread out over pre-existing surfaces; and relative ages of the post-Maria and pre-Maria craters with the Maria. None of these previous observations indicate the absolute age of any lunar features. The only absolute age for the moon is 4.5×10^9 years, and this is based on the assumption that the moon and earth and certain meteoroids are all the same age. Therefore, in classifying lunar features by age, we are concerned with establishing a method for determining the relative ages exhibited by lunar topographic features. Several schemes have been proposed to classify lunar features according to inferred age relationships. These proposed methods of age classification will be reviewed briefly in the following paragraphs.

1. United States Geological Survey's Original Classification

The United States Geological Survey, in its publication entitled Engineer Special Study of the Surface of the Moon, 1961 [7], divided the lunar rocks into three major categories based on relative age. Their classification presupposes that the Maria were formed long after the moon formed and that all of the Maria were formed about the same time. This assumption has led to the concept of the Maria as a time-stratigraphic formation. A time-stratigraphic formation has boundaries based on geologic time, i.e., with synchronous boundaries [23]. With this classification, the rocks have been divided into pre-Maria, Maria, and post-Maria based on their relative ages.

a. Pre-Maria

According to the U.S.G.S., the pre-Maria rocks are largely accretionary material composed of stony meteoroids. Most of this meteoritic material has been broken up and fragmented to a very fine grain size. In addition, breccias and layers of ejecta are expected in the lunar highlands. Volcanic and other igneous rocks are not regarded as significant in the area of the pre-Maria outcrops. The predominant large-scale features in the lunar highlands, or pre-Maria areas, are craters caused by impact.

b. Maria

The Maria, by contrast, are interpreted as lava flows composed of thick basalt sheets. These vast flows vary in thickness from several thousand feet in the centers of the Maria to a feather-edge pinch-out at the margins. The Maria probably occurred over a short period of time, rather late in the development of the moon as evidenced by the relatively few post-Maria craters. Large impacts of planetoidal or asteroidal dimensions were required to produce the large structural basins which are now occupied by the lava flows of the circular Maria, e.g., Imbrium, Serenitatis, Nectaris, Humorum, and Crisium (Figures 2 and 3).

c. Post-Maria

The post-Maria deposits, according to the U.S.G.S. original classification, consist largely of ejecta derived from impacting meteoroids. Just as in the highlands, finely divided accretionary material and brecciated rocks are anticipated in post-Maria features. Post-Maria craters, however, are best observed in the Maria where they are more or less randomly distributed on the surface. However, post-Maria craters in the lunar highlands are obscured by the thousands of pre-Maria craters.

The youngest of the post-Maria craters are those which contain associated systems of rays. Rays are interpreted as ejecta sprayed from an impact crater. The optical properties of the rays indicate that they may be composed of volcanic glass. They apparently form a thin, low-relief, veneer-like material on the Maria surface. Because of the low lunar gravity and the near absence of an atmosphere, ray-forming material was spread out in a radial distribution over large parts of the lunar surface.

It is conceded that some post-Maria features may be truly volcanic in origin, particularly the chain craters.

2. United States Geological Survey's Newest Classification

More recently (1962), the U.S.G.S. has subdivided the lunar surface rocks into five systems of rock units [8, 18]. Arranged according to age (from oldest to youngest) these are pre-Imbrian, Imbrian, Procellarian, Eratosthenian, and Copernican. This terminology is now being used by the U.S.G.S. on their lunar geological maps. Maps have been prepared for several regions on the moon including Kepler (Figure 30), Copernicus (Figure 29), Letronne, Archimedes (Figure 31). Figures 4 and 5 are examples of the recent geologic map of the Kepler region.

The lunar geological systems are defined as follows:

a. Pre-Imbrian System

The pre-Imbrian rocks exist in the lunar highlands, e.g, the Apennine Mountains in the Archimedes Region (Figure 31). This pre-Imbrian material is composed of ejecta, breccia, and possibly volcanic or other igneous rocks.

b. Imbrian System

The Imbrian deposits of the Kepler region are interpreted as ejecta blanket material and breccia, e.g., those occurring in patches to the south and east of Kepler (Figure 11). The Imbrian deposits of the moon are derived chiefly from ejecta from the region of Mare Imbrium and they rest stratigraphically on pre-Imbrian deposits.

c. Procellarian System*

This material is made up mostly of thick sheets of basaltic lava flows which rest stratigraphically on the Imbrium deposits and which form the rocks of this vast lunar Maria. Procellarian deposits are relatively dark and smooth and have a surface of low relief containing a few low ridges, domes, and an occasional fault scarp (Figures 24 and 25). The ridges may attain a height of 100 m and typically have lengths of 15 to 30 km (Figures 25, 29, and 35). However, in some cases, ridges range up to 200 km (Figures 29 and 35) in length.

d. Eratosthenian System

This system is represented on the Kepler map (Figure 5) by many of the smaller craters, notably Encke C, Encke F, Suess F, Moestlin H, Kepler C, etc. Elsewhere on the moon, Eratosthenian craters include Eratosthenes (Figure 29), Reinhold, and Landsburg.

The main characteristics of the Eratosthenian age craters are that they are rayless and are superposed on Procellarian deposits.

e. Copernican System

Deposits of this age include material derived from the major ray craters on the moon such as Copernicus, Tyco, Kepler, etc. The ray material is characterized by its unusually high reflectivity. The features of typical Copernican craters, such as Kepler, include the following: ray material, crater rim material, crater floor material, and slope material. Ray material is a light-colored veneer of crushed

*On the most recent preliminary geologic maps, the Procellarian System is classified as a subdivision of the Imbrian System.

By
R. J. Hackman

1962

GEOLOGIC MAP OF THE KEPLER REGION OF THE MOON

PREPARED BY THE U.S. GEOLOGICAL SURVEY IN COOPERATION
WITH THE NATIONAL AERONAUTICS AND SPACE ADMINISTRATION
AND THE USAF AERONAUTICAL CHART AND INFORMATION CENTER

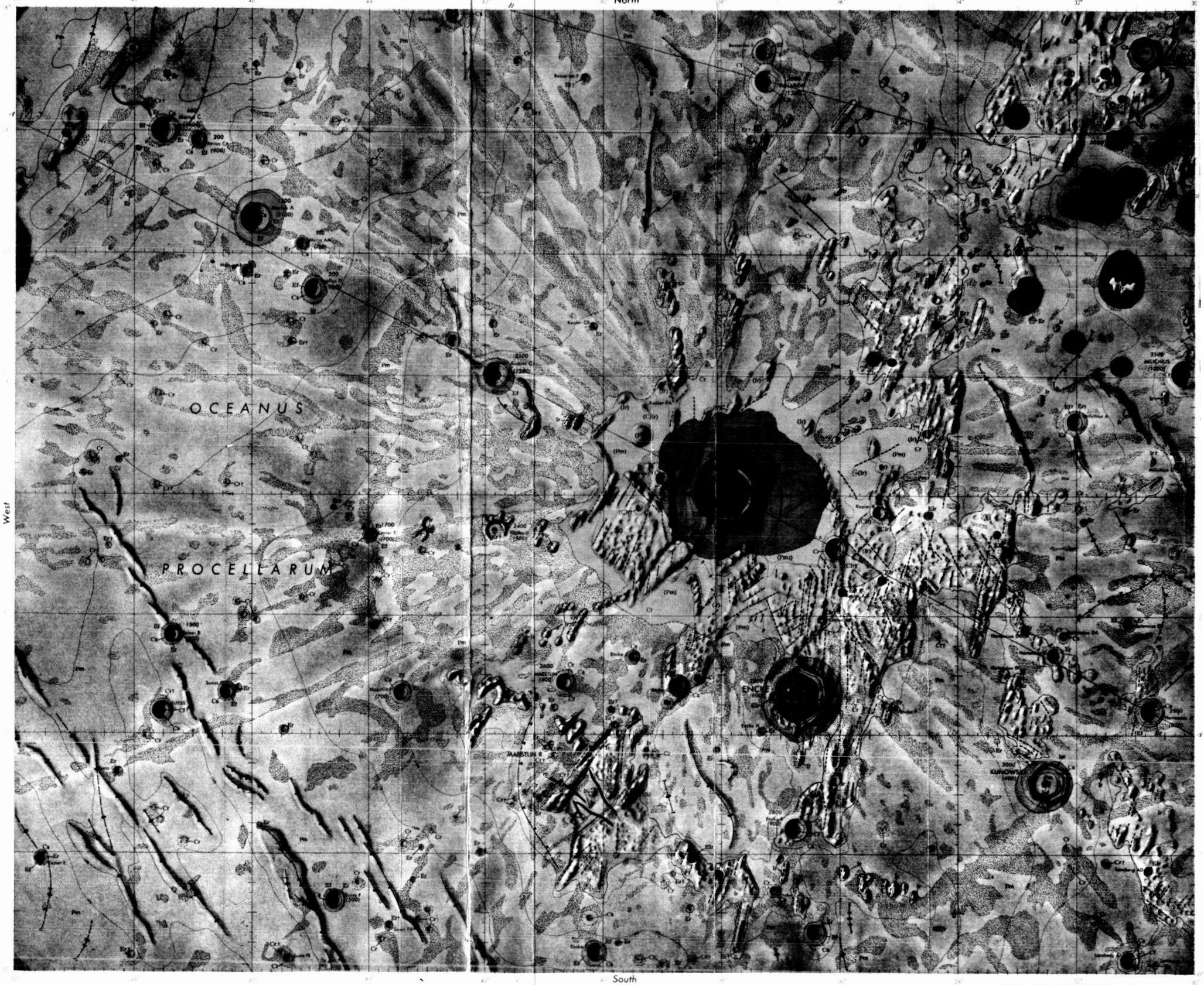

GEOLOGY OF THE MOON
KEPLER REGION
I-355 (LAC-57)

EXPLANATION

Material exposed on the surface of the Moon is heterogeneous. In albedo and most other physical characteristics that have been determined with the use of optical and radio telescopes this material varies from one part of the Moon to another, and the variations are partially correlated with differences in topography. Discontinuities are present in the areal variation which permit the surface material to be divided into map units, each exhibiting a limited range of photometric properties associated with a limited range of topographic characteristics. Each map unit is further characterized by a distinctive pattern of distribution, and the patterns of certain units are in places superimposed on the patterns of other units. From the relations of superposition it is possible to determine the relative ages of the units or the sequence in which they were formed.

For the purpose of geologic mapping a classification has been adopted in which map units are grouped according to sequence or relative age. The major subdivisions of this classification are called systems (Shoemaker, 1961; Shoemaker and Hackman, in press) and subdivisions of the systems are called series. The systems and series are arranged below in the order of relative age, the youngest at the top and the oldest at the bottom.

The boundaries or contacts and photometric and topographic characteristics of the map units have been determined by a combination of visual examination of photographs, telescopic observation, and traversing of photographs with a continuously recording microdensitometer. Relative reflectivity is described for full moon illumination. The photometric properties observed are those only of the material exposed at the surface. The distribution of certain units that are concealed or partly concealed by superimposed material has been inferred entirely from topographic characteristics.

Certain elements of the lunar topography suggest the presence of a variety of structural features in the Moon's crust. Their positions are indicated on the map with special symbols.

Each map unit and each type of probable structure has been given a descriptive name. A genetic name, where warranted, is given in parentheses beneath the descriptive name for certain map units and for probable structural features as well. A more detailed genetic interpretation follows the description of each unit and probable structure. These interpretations are based partly on analogy with terrestrial features and partly on analysis of the detailed interrelations of the features on the Moon and are necessarily speculative. The cross-sections incorporate these speculative interpretations. Discrimination and mapping of the units and determination of their sequence, however, is independent of the genetic interpretations placed on them.

The geologic mapping has been carried out to the precision obtainable with existing telescopic technique. As more detailed information is acquired through lunar exploration, further refinement of the chronologic sequence of map units will be possible, and greater precision in the discrimination and location of geologic units and structures is to be expected.

References cited

Shoemaker, E. M., 1961, Interpretation of lunar craters, in Kopal, Zdenek, ed., Physics and Astronomy of the Moon: London, Academic Press, p. 283-358.

Shoemaker, E. M., and Hackman, R. J., in press, Stratigraphic basis for a lunar time scale: Internat. Astron. Union Symposium 14, The Moon, Proc., London, Academic Press.

COPERNICAN SYSTEM

Ray material

Telescopic characteristics:

Reflectivity generally high but grades to that of surrounding material. Local contrast in reflectivity generally large; lateral variations locally abrupt; characterized by bright patches and streaks. Ray material is superimposed on parts of all other units except dark halo material. Except for satellitic craters, topography controlled by underlying units

Interpretation:

Probably chiefly crushed rock. Forms thin patchy layers in most places probably not more than a meter thick

Cr **Crater rim material**
(Ejecta blanket)

Telescopic characteristics:

Reflectivity moderate to very high. Local contrast in reflectivity moderate to large; lateral variations commonly abrupt. Areas of relatively low reflectivity around craters larger than 25 kilometers in diameter mapped as Crd. Topography around large craters is hummocky near crest of rim and includes low hummocks or low subradial ridges on rim flanks. Around small craters topography is smooth. Crater rim material grades to ray material away from craters

Interpretation:

Probably chiefly crushed rock with large blocks. Forms hummocky layers ranging from about a meter to about 600 meters in thickness

Crater floor material
(Breccia?)

Telescopic characteristics:

Reflectivity generally high to very high. Local contrast in reflectivity moderate; lateral variations generally abrupt. Topography generally smooth or flat in craters less than 16 kilometers across and partly flat and partly hilly to hilly in larger craters

Interpretation:

Probably chiefly crushed rock with large blocks. Probably forms deep lenses inside small and large craters

Slope material
(Talus?)

Telescopic characteristics:

Reflectivity high to very high. Occurs mostly on smooth slopes ranging from 20° to 40°

Interpretation:

Probably partially sorted fragments ranging in size from dust to large blocks

Crater rim material
(Ejecta blanket)

Telescopic characteristics:

Reflectivity low to moderate. Local contrast in reflectivity moderate; lateral variations generally gradual. Topography around large craters is hummocky near crest of rim and includes low hummocks or low subradial ridges on rim flanks. Around small craters topography is smooth

Interpretation:

Probably chiefly crushed rock with large blocks. Forms hummocky layers ranging from about a meter to 200 meters in thickness

Crater floor material
(Breccia?)

Telescopic characteristics:

Reflectivity low to moderate. Local contrast in reflectivity small. Topography generally smooth or flat in craters less than 16 kilometers across and partly flat and partly hilly to hilly in larger craters

Interpretation:

Probably chiefly crushed rock with large blocks. Probably forms deep lenses inside small and large craters

ERATOSTHENIAN SYSTEM

Crater rim material
(Ejecta blanket)

Telescopic characteristics:

Reflectivity low to moderate. Local contrast in reflectivity small to moderate; lateral variations generally gradual. Topography around large craters is hummocky near crest of rim and includes low hummocks or low subradial ridges on rim flanks. Around small craters topography is smooth. Crater rim material grades to ray material away from craters

Interpretation:

Probably chiefly crushed rock with large blocks. Forms hummocky layers ranging from about a meter to 600 meters in thickness

Crater floor material
(Breccia?)

Telescopic characteristics:

Reflectivity low to moderate. Local contrast in reflectivity small. Topography generally smooth or flat in craters less than 16 kilometers across and partly flat and partly hilly to hilly in larger craters

Interpretation:

Probably chiefly crushed rock with large blocks. Probably forms deep lenses inside small and large craters

PROCELLARIAN SYSTEM

Dome material

Telescopic characteristics:

Reflectivity low and local contrast in reflectivity small. Occurs on domes up to 30 kilometers across and up to 300 meters high generally with a small crater at the summit

Interpretation:

Probably chiefly volcanic flows; may include volcanic ash. Common low reflectivity and low slopes suggest dominantly basaltic composition

Pm **Mare material**

Telescopic characteristics:

Reflectivity generally low with small local contrast and gradual to abrupt lateral variation. Forms extensive, relatively smooth horizontal surfaces abruptly terminate against many topographic forms

Interpretation:

Probably volcanic flows. Great extent and relatively smooth topography suggest thick sheets of basalt or ignimbrite. Forms layers ranging from a feather edge to a few thousand meters in thickness

IMBRIAN SYSTEM

Archimedian Series

Crater rim material
(Ejecta blanket)

Telescopic characteristics:

Reflectivity low to moderate. Local contrast in reflectivity small to moderate; lateral variations generally gradual. Topography around large craters is hummocky near crest of rim and includes low hummocks and low subradial ridges on rim flanks. Around small craters topography is smooth

Interpretation:

Probably chiefly crushed rock with large blocks. Forms hummocky layers ranging from about a meter to 200 meters in thickness

Crater floor material
(Breccia?)

Telescopic characteristics:

Reflectivity low to moderate. Local contrast in reflectivity small. Topography generally smooth or flat in craters less than 16 kilometers across and partly flat and partly hilly to hilly in larger craters

Interpretation:

Probably chiefly crushed rock with large blocks. Probably forms deep lenses inside small and large craters

Apenninian Series

Regional material
(Ejecta blanket?)

Telescopic characteristics:

Reflectivity ranges from very low to moderate with generally moderate local contrast and gradual lateral variations. Topography characterized by numerous hills and depressions two to four kilometers across

Interpretation:

Probably chiefly crushed rock and great blocks derived mainly from the region of Mare Imbrium. Forms a layer probably ranging from a few meters to about 1000 meters in thickness. Layer is probably heterogeneous in composition. Areas where Apenninian layer may be generally very thin and pre-Imbrian material locally exposed are shown with ruled pattern

MERCATOR PROJECTION
SCALE 1:1,000,000 AT 11°06'45"

10 0 STATUTE MILES 50
16° 8° 0°
10 0 KILOMETERS 50
16° 8° 0°

Rill and chain-crater material

Telescopic characteristics:

Material of generally low to moderate reflectivity lying within narrow linear depressions with associated small craters or within linear series of craters

Interpretation:

Probably includes breccia, fault blocks, and volcanic rocks. Age not definitely established but probably chiefly Eratosthenian

Copernican satellitic craters
(Secondary impact craters?)

Telescopic characteristics:

Small, relatively shallow craters occurring in rim material and rays around large Copernican craters. Satellitic craters are commonly composite or elongate with very low rims or no observable rims

Interpretation:

Craters formed by impact of fragments ejected from large, primary craters

Contact

Dashed where approximately located

Indefinite contact

(Pm)
(Ir)

Concealed contact

Queried where location is uncertain
Symbols in parentheses indicate concealed units:
(CEr) *Copernican and Eratosthenian crater rim material, undifferentiated*
(CIr) *Copernican to Archimedian crater rim material, undifferentiated*
(CIf) *Copernican to Archimedian crater floor material, undifferentiated*

U D

Offset of surface
(Fault)

Showing foot of scarp separating regions of similar topography. U, upthrown side; D, downthrown side. Dotted where concealed

Lineament
(Probable fault or fracture)

Partially or completely covered. Inferred from linear topographic features

Mare ridge

Showing crest line. Tapered end indicated by arrowhead. Dashed where approximately located. Queried where probable. Probably underlain by anticline, possibly the site of a volcanic extrusion

Rounded mare scarp

Showing trace of foot of scarp. Barbs point in direction of slope. Dashed where approximately located. Queried where probable. Probably a flow front or monocline

Outer limit of telescopically observable low hummocks or low subradial ridges on Copernican crater rim material

rock, rim material (ejecta blanket) is composed of crushed rock mixed with large blocks, floor material is composed of crushed brecciated rock with large angular blocks, and slope (talus) material is composed of angular unsorted fragments of rim material [8].

3. Bensko's Classification of Lunar Geological Time

Bensko [9], writing in the Handbook of Astronautical Engineering, has classified the lunar formations into five eras (from oldest to youngest): Eoselenic, Archaeoselenic, Paleaeoselenic, Mesoselenic, and Cenoselenic. The nomenclature for these eras is adapted from the classical earth eras of geologic time.

a. Eoselenic and Archaeoselenic

The two earliest lunar eras, the Eoselenic and Archaeoselenic, comprise the primeval history of the moon. According to Bensko, the rocks of the large circular basins (Figures 20 and 21) and walled plains were formed during this time. Also the lunar fracture and joint systems, internal volcanic activity, outgassing, and large-scale cosmic impact all occurred during this time.

b. Paleaeoselenic

The Paleaeoselenic era is interpreted as the time of formation of the large Maria basins. The large Maria, if they were caused by impact, must have occurred before the oldest earth's sedimentary rocks were formed since there is nothing in the earth's geologic record to correspond to this catastrophic event. Secondly, the Maria did not occur simultaneously since some Maria show evidence of isostatic adjustment, whereas with others, formation in a rigid crust is indicated. Bensko suggests that these observations may indicate that the Maria were formed just before and after the moon became rigid.

c. Mesoselenic

The Mesoselenic era is characterized by erosion by micrometeoroids, radiation, etc., and the continued pulverizing and granulation of lunar surface material. In general, this process had the effect of leveling off the surface just as erosion does on earth, but to a lesser extent.

d. Cenoselenic

The Cenoselenic era was the time of formation of the lunar faults, rilles, and young craters and associated ray systems. The glassy ray material is gradually darkened and obliterated by radiation, and its presence indicates a relatively recent event on the lunar surface.

4. Shoemaker's Correlation of the Lunar and Geologic Time Scales

It is desirable to obtain, if possible, a quantitative approximation of the absolute age of lunar features to compare lunar history with earth history. The U.S.G.S. original classification assumed the Maria to be young based on the relatively few post-Maria craters. This estimate has no real basis in fact, since the frequency of impact distribution was not considered. Later, Shoemaker of the U.S.G.S. used Harrison Brown's impact frequency of meteoroid bodies presently falling upon the earth. Brown's formula for maximum impact frequency is as follows:

$$f = \left[\frac{6.9 \times 10^{11}}{(10^6 \text{ km}^2)(10^9 \text{ years})(\text{gm}^{-0.80})}\right] M^{-0.80},$$

where f = total impact frequency of bodies of mass $> M$, and M is the mass of the impacting body in grams. Shoemaker multiplied Brown's formula by an appropriate factor to compensate for the lesser lunar gravity. By counting the Maria craters and assuming a relatively constant rate of influx, Shoemaker attempted to calculate the age of the Maria.

Studies performed by Hackman of the U.S.G.S. (quoted in Reference 18) indicate that he counted 24.2 craters per 10^5 km^2 on Mare Crisium (Figure 2) to 54 craters per 10^5 km^2 on Mare Nubium (Figure 3) with an average of about 45 craters per 10^5 km^2 on all the visible Maria surface. Table II shows a compilation of Hackman's data for the lunar Maria. With the exception of Mare Crisium (Figure 2) all of the lunar Maria have, within a few percent, the same number of post-Maria craters on them. Baldwin [35] attempts to explain this apparently anomalous condition of Mare Crisium by suggesting that the Mare is too near the limb for optimum viewing, and by careful study he obtained a figure of 39 craters per 10^5 km^2, for Mare Crisium. From these data, he argues that the Maria are synchronous, or nearly so, and can be used as a time-stratigraphic horizon.

By combining Hackman's crater counts with Brown's flux rates, Shoemaker estimates that the Maria surfaces, or the Procellarian System, are 4.5×10^9 years old or approximately as old as the oldest rocks on earth.

One problem with Shoemaker's work is found in his assumption that the post-Maria influx rate of meteoroid material has been constant, and that the pre-Maria impact rate was much higher. This supposition was required to account for the thousands of pre-Maria craters. Baldwin argues that there is no real basis for this assumption and, in fact, argues that the flux of meteoroid infall has been on a continuous decline and that, therefore, the Maria are less than 4.5×10^9 years old.

TABLE II. Size Frequency Distribution of Primary Impact Craters on the Lunar Maria

Area	Approximate square kilometers	Number of craters, according to size: Crater diameter in miles 1	2	4	8	16	32	64	128	Craters per $10^6 km^2$
Mare Imbrium	864,000	199	117	37	10	5	1	0		42.8
Lacus Somniorum	64,500	103	68	41	15	5	2	0		46.5
Mare Frigoris	439,000									
Mare Serenitatis	318,000	88	41	7	1	1	0	0		43.7
Mare Fecunditatis	311,000	56	34	28	6	3	1	1		41.5
Mare Tranquillitatis	402,000	89	57	39	11	6	0	1		50.5
Palus Epidemiarum	28,800	111	64	27	11	0	1	0		54.0
Mare Humorum	107,000									
Mare Nubium	261,000									
Mare Nectaris	96,400	26	16	2	1	0	0	0		46.7
Mare Crisium	165,000	20	10	6	4	0	0	0		24.2
Total	3,056,700	692	407	187	59	20	5	2		44.9

5. Summary of Classifications Based on Inferred Age Relationships

Table III is a summary and comparison of the major trends and differences of opinion expressed in these various schools of thought concerning the relative ages of lunar topographic features.

The following observations have been made concerning these various concepts of lunar geologic history.

a. All three theories are in agreement concerning the major relative ages of lunar formations, viz. pre-Maria, Maria, post-Maria.

TABLE III

Comparison of Theories of Age Relationships
Exhibited by Lunar Formations

	U.S.G.S. [7] Original Classification	Bensko, MSFC [9]	Shoemaker, et al [10] and U.S.G.S. newest Classification
Pre-Maria	Predominantly impact produced structures and topographic features.	Eoselenic and Archaeoselenic eras were times of intense fracturing of lunar surface by strong tidal forces; internal activity plus cosmic impact.	Period of intense meteoroid bombardment, a "sweeping up" of coarse solid material. Includes pre-Imbrian and Imbrian Systems.
Maria	Occurred late in lunar history due to presence of relatively few post-Maria craters; composed of impact produced lava flows.	Probably at least 1.7 x 10^9 years old (Paleoselenic era) based on theory that Maria are older than earth's sedimentary rocks; presents evidence that Maria formed about the time moon became rigid body.	Estimated that Maria are at least 4.5 x 10^9 years old based on frequency of impact estimate on earth compared to the moon. Includes Procellarian System.
Post-Maria	Predominantly impact craters produced in recent geologic times; rayed craters are the youngest.	Mesoselenic and Cenoselenic eras. Times of formation of ray craters, faults, rilles and widespread leveling, etc.	Frequency of impact has been assumed to be fairly constant over this time interval. Includes Eratosthenian and Copernican Systems.

b. Both the U.S.G.S. original classification [7] and Shoemaker, et al. [10] have conceived of the Maria as time-stratigraphic markers in the geologic sense. Bensko [9] believes that the formation of the Maria were not contemporaneous.

c. U.S.G.S. original classification [7] believes the Maria are geologically young; Bensko [9] states that they are probably at least 1.9×10^9 years old; and Shoemakers' thesis [10] rests on the assumption that they are at least 4.5×10^9 years old.

d. All of the authors are in general agreement concerning the significance of impact meteoroids as a geologically active process in crater and Maria formation, but all are vague concerning the role and nature of volcanism as an active process on the moon.

C. Major Areas of the Lunar Surface

1. Relations Between Structures and Landforms on the Lunar Surface

It is perhaps significant that the origin of most landforms, regardless of whether they are on the earth or on the moon, can be attributed to alternate interpretations. The most effective way of determining, and often the only definitive way to determine the origin of landforms on earth, is by means of field investigations. Obviously, in the case of the moon, field investigations are not yet feasible. In lieu of a definitive method of solving problems concerning the nature of the lunar landforms and lunar surface variations, it is proposed that several scientifically sound hypotheses be considered at this time. As our knowledge increases, some of these hypotheses can be eliminated and our interpretation will become more precise.

The purpose of the following discussion is to consider geomorphology, the study of landforms,and to apply this discipline to the landforms on the lunar surface. This approach to the problem should provide the proper direction and framework for an understanding of lunar landforms as new and better data on the moon continue to come in.

a. Circular Basins

It is known that the circular landforms so common with the lunar craters can be developed in several ways on earth. Perhaps the most common terrestrial basin-type circular structure occurs when stratified rocks are downwarped by compressional forces. This phenomenon can be performed on practically any scale by a variety of forces. By contrast, the formation of a topographic basin on top of a structural dome is most often attributed to weathering and erosion of rocks of different hardness following structural upwarping and is known as the

inversion of topography. It is presently believed that erosional processes exist on the lunar surface to a much smaller degree than on earth and without sufficient erosive energy to result in the inversion of topography (Figure 6).

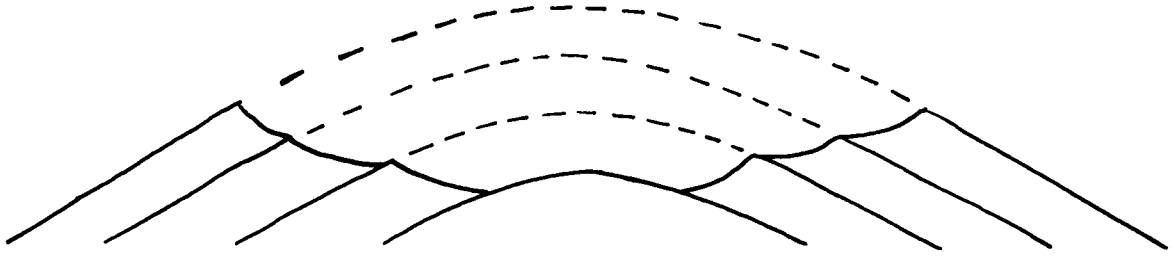

FIGURE 6. TOPOGRAPHIC BASIN WITHIN STRUCTURAL DOME - INVERSION OF TOPOGRAPHY

b. Domes

It is noteworthy that the lunar domes are still domal and have not evolved by the process of erosion into basins or crater-like structures. Examples of phenomena that can cause domal structures on earth include compressional folding by vertical forces such as intrusion of salt domes or igneous plugs. Intrusive activity may be the cause of domes on the lunar surface. Similarly, the expansion of overlying rocks due to the serpentinization of olivine in the subsurface has been suggested for the origin of lunar domes [11].

c. Internal versus External Origin of Lunar Topographic Features

The origin of a particular structure may be due either to internal forces as in the examples of domal structure above, or external forces, as in the case of craters due to impacting meteorites, but probably not due to both as in the case of the example of inversion of topography. The external forms of certain structures may be identical in gross outline, and yet be produced by entirely different geological processes. It will be within the province of this document to point out alternate hypotheses for these various features and to discuss possible criteria for recognizing them and determining their implications for the lunar environment criteria.

Other lunar structures which may have a relationship to topographic features include those due to crustal movement caused by faults and folds; igneous activity with resulting volcanic cones, calderas, etc.; and erosion which produces crater terraces. These features and their geomorphic development will be discussed in subsequent sections.

2. Continents (Highlands)

These broad areas occupy about 60 percent of the visible surface of the moon. They are composed of rugged topography with predominantly light-colored rocks. These areas contain a great concentration of ringed plains and craters as well as linear features of unknown origin. The continents may be analogous to continents on earth, and in this respect they stand topographically higher than the Maria. The predominant boundary between Continent and Maria is sharp and commonly marked by escarpments. Heights of these escarpments may vary from several hundred to several thousand meters [12].

The U.S.G.S. [7] describes the continents, or lunar highlands as almost completely covered by 30,000 craters, with perhaps over a million in all. The surface is believed to be extremely rough and almost entirely in slopes, except perhaps in the bottom of craters. The slopes vary from 5° to 25°, averaging about 10°.

The material in this region is characterized as fragmental material, which is composed of unsorted ejecta and breccia, and also some volcanic material.

Salisbury [13] in discussing the lunar environment indicates that, according to the volcanic theory, the highlands should exhibit (a) a complex of overlapping collapse structures, (b) extrusive vesicular lavas, (c) intrusive dikes and sills, and possibly (d) large lava caverns. By contrast, if the highlands are predominantly due to impact, their structure should consist of highly fractured basement rock overlaid by discontinuous layers of rubble, rock flows, and meteoritic materia

3. Maria

These large features range in size from 300 to 800 km in diameter [9]. Two classes have been defined: circular and irregular. The circular Maria include Imbrium, Crisium, Nectarus, Humorum, and, to a lesser extent, Serenitatis (Figures 2 and 3). Irregular Maria (Figures 2 and 3) include Tranquillitatis, Fecunditatis, Nubium, and Procellarum [14]. The Maria constitute 40 percent of the area of the visible lunar disk, but only about 4 percent of the backside [2]. The surfaces of the Maria appear to be very smooth at the visible scale, but it must

be remembered that our ability to resolve features on the Maria is limited to structures larger than 1 km.

The term "Maria" refers to the strong resemblance these features have with terrestrial ocean basins filled with water. Smaller areas than the Maria, but of a similar nature, are called Lacus (for lakes), Sinus (for bays), and Palus (for swamps), although it is realized these names have no genetic justification. Eventually, such terminology should be replaced by consistent genetically-based terminology, but this should await further knowledge of these areas [12].

Since the following features are related to the Maria, a discussion of them is appropriate at this point.

a. Surfaces

The Maria surfaces are flat and featureless down to the limit of optical resolution (max. slopes 2-3°) [15].

b. Domes and Anticlines

Low domes and anticlines occur with slopes of from 2-4° [15]. They consist of slight elevations which appear as blisters on the Maria surface. Small openings on the summits of some of these have led various authors to suggest lunar degassing or shield volcanic origins [16]. Salisbury [11] writes that they may be due to volumetric increase in material due to serpentinization of olivine, while Bensko [9] points out the possibility of igneous intrusion, or large ejecta blocks covered with smaller debris and dust.

c. Random Craters

Random craters [15] are present which range from below the limit of optical resolution up to 60-80 km in diameter, but these are much less numerous than in the continental regions (see Table II).

d. Ridges

Ridges which exhibit long sinuous patterns lie parallel to the Maria border (Figures 25, 29, and 35). These ridges range in height up to 100 m, in width up to 20 km, and in length up to several hundred kilometers. Some of these structures exhibit a discontinuous subparallel arrangement resembling en echelon faulting [12]. The Serpentine Ridge is an example of this type of feature.

e. Fault Scarps

Fault scarps with concentric patterns occur around the borders of the Maria. Linear normal fault scarps have been noticed. The classic example of this type of fault on the moon is the Straight Wall which is 130 km long and 250 m high and which trends northwest to southeast in the western part of Mare Nubium (Figure 24).

f. Radial Structures

In the case of some of the circular Maria, e.g., Mare Imbrium (Figure 11), mountain ridges radiate from the direction of the center [17]. These mountains are truncated by the Maria plain (Figures 26, 28, 30, 31).

g. Ejecta Blankets

Ejecta blankets caused by crater explosions are composed of rough, blocky unsorted ejecta and breccia which have been deposited on the floor of the areas adjacent to the Maria.

h. Subsequent Flooding

The Maria appear to be filled with congealed lava. Concerning this, Urey [17] wrote that the "secondary processes such as the flow of lava from the collision Maria" may have been the agent responsible for filling them. Further, "the energy of the great collisions, even if the velocities were subsonic, is quite sufficient to produce some melting." According to U.S.G.S. interpretation [7], the material indigenous to the Maria, or lowlands, is composed mainly of lava flows of basalt-type lava, which may be covered by loose material. Of the major theorists, only one, Gold (quoted by Reference 15) of Cornell University, visualizes the Maria as formed by some substance other than lava. Gold is a proponent of the hypothesis that the Maria are filled with dust.

V. GENETIC CLASSIFICATION OF LUNAR TOPOGRAPHIC FEATURES

A. Large-Scale Lunar Features

1. Structures and Landforms Produced Predominantly by Impact Phenomena

Craters occur only one-tenth as frequently in the Maria as in the highlands. Their shapes range from circular to subcircular to polygonal and their sizes vary from 288 km in diameter to below the limit of optical resolution [15].

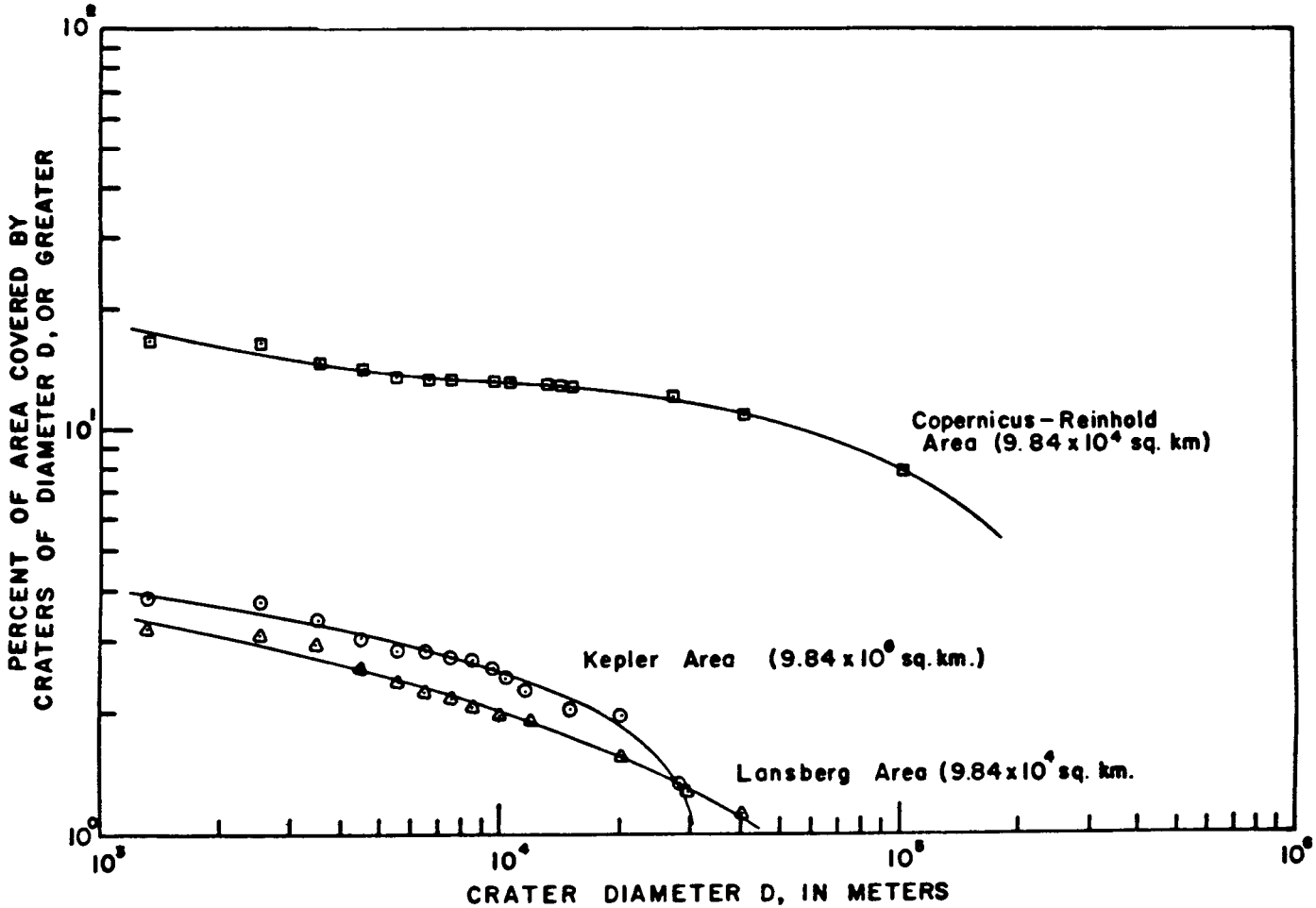

FIGURE 7: PERCENTAGE OF THE MOON'S SURFACE IN AREA OF THE OCEAN OF STORMS POPULATED BY VISIBLE CRATERS (Ref. 27)

The number of craters increases as an inverse exponential function of their diameters [16], and thus, by extrapolation to the smaller sizes, it is argued that the moon's surface is covered by a vast number of small craters below the limit of optical resolution. Niedze [2], in a special study of the moon, has observed that there are over 300,000 craters on the visible side of the moon with diameters of 1.6 km or greater.

By contrast, Bensko and Cortez [27] have made several studies on the Ocean of Storms to ascertain the order of magnitude of the subtelescopic distribution of craters. On the basis of their studies in which they extrapolated percentages of crater distribution below the limit of visibility (Figure 7), the authors conclude that the "Moon's surface does not become infinitely rougher because of the assumed influx of smaller cosmic debris."

Craters exhibit a generally inverse relationship between crater diameter and depth. The depth/diameter ratio varies from 0.02 for 100 km diameter craters to 0.1 for 10 km diameter craters [15].

The following features and relationships describe the morphology of craters.

a. Rims

Inner slopes of rims generally have high slopes, approximately 35-40 degrees, while outer slopes of rims have slopes of only a few degrees. Rim material will probably exhibit inverted stratigraphy in the debris units from the original bedrock strata [18].

b. Floor

Impact crater floors are generally depressed below the ground level (see Figure 18). This relationship appears to be so general for craters of impact origin as to form a possible criterion for distinguishing impact craters from volcanic calderas. Floor material may be composed of brecciated finely divided rock in the deeper craters, and in the filled craters, it may contain lava or dust deposits.

c. Walls

Crater walls are composed of material making up the adjacent terrain, and therefore, are probably different in the Maria than in the lunar highlands. The high inner slopes of the rims indicate that the wall material has a shear strength higher than most granular materials on earth since the inner slopes are as high or

or higher than the angles of repose of most granular materials on earth. Vacuum welding and sputtering effects of solar wind bombardment may enhance the strength of this material.

d. Ejecta Blankets

Material ejected from a crater center by either explosion or impact will result in the deposition of a widespread sheet of unsorted angular rock fragments with sizes ranging from clay (.004 mm) to boulders (256 mm). An example of this type of the ejecta blanket pattern has been obtained from nuclear explosion craters (Figure 8).

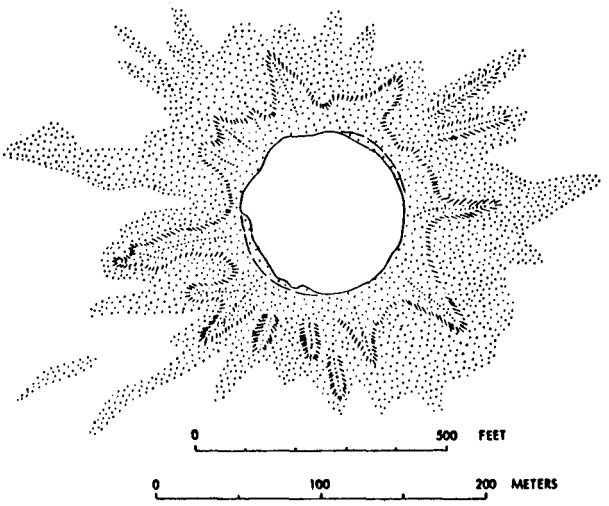

FIGURE 8. EJECTION PATTERN AT TEAPOT ESS NUCLEAR EXPLOSION CRATER [19]

Similarly, material ejected at low angles (6 to 14 degrees) forms the continuous ejecta blanket surrounding the rim of Copernicus [19].

e. Secondary and Satellite Craters

Studies of the Copernicus region on the moon (Figures 9 and 10) indicate that fragments ejected at angles ranging from 14 to 22 degrees form the secondary impact craters (the gouges) and the rays [19].

Ejection angles ranging from 22 to 43 degrees result in a relatively small volume of material which is widely scattered over the lunar surface. Material ejected at angles above 43° is sent into escape trajectories [19] if the explosive impact energy is sufficient to cause this material to achieve escape velocity.

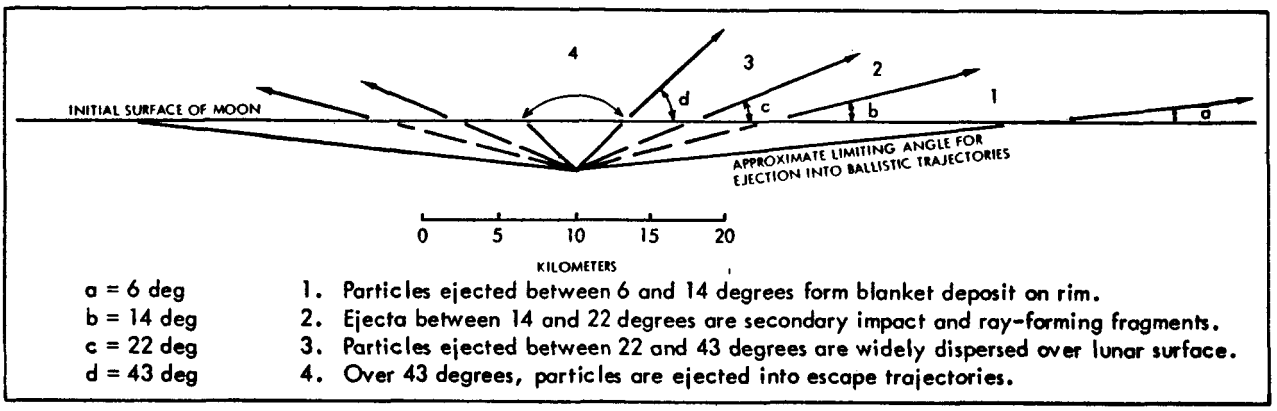

FIGURE 9. PROVENANCE OF FRAGMENTS EJECTED FROM COPERNICUS

Figures 10 and 29 show the effects of fragments ejected from the center of Copernicus on the surrounding lunar terrain. Figure 10 shows that all the fragments are situated in a circular belt around the crater center with an inner radius of approximately 50 kilometers and an outside radius of 160 kilometers. Nine hundred and seventy-five secondary impact craters surround Copernicus. The criteria used to select secondary impact craters are (1) markedly elongated shapes, (2) shallow depth compared to most small craters outside the ray system, and (3) an extremely low rim or the absence of a visible rim.

f. Rays

Rays are composed of material ranging from clay to boulder size which produces a debris pattern radiating outward from the crater center. Many writers have noted that ray material exhibits a very low relief, but at a low angle of illumination it has been determined that the surface of the rays is rough [19]. It appears that ray forming materials are actually ejected in clusters or clots and are ejected in the same range of angles as secondary impact fragments [19].

The following topographic structures are associated with craters or craterlike features [9]:

(1) Walled Plains - Walled plains are found only in lunar uplands. These large depressions are characterized by little or no rim deposits above the surrounding area and relatively smooth floors. Diameters of these features vary from 70 to 300 km.

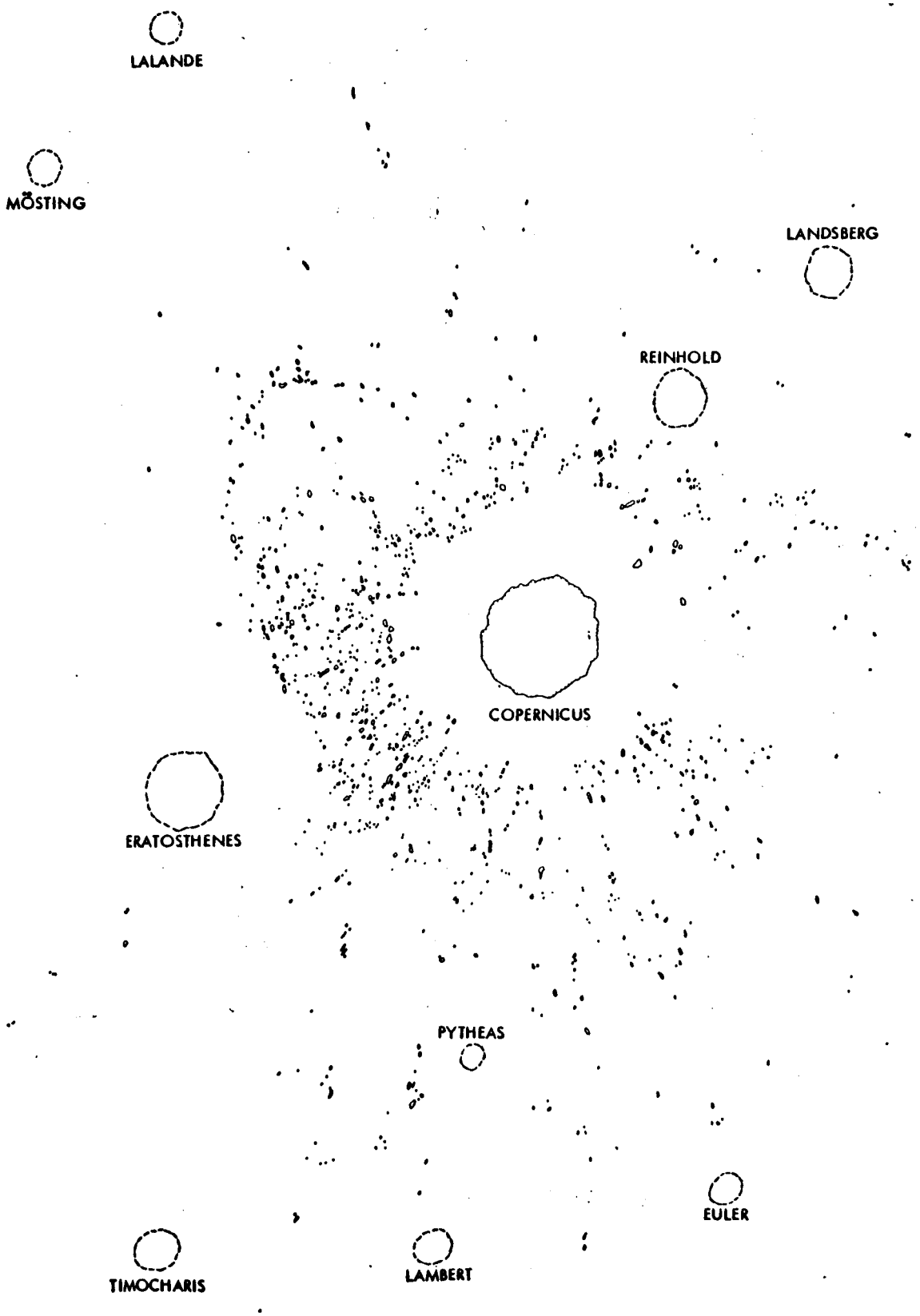

FIGURE 10: SECONDARY OR SATELLITE IMPACT CRATERS IN THE COPERNICAN RAY SYSTEM (Ref. 19)

(2) Ringed Plains - Ringed plains are smaller than walled plains, with continuous wall-like, vertical outcrops of lunar rocks and no rims. Floors are low-lying and flat and may be partially filled. These features range from 10 to 70 km in diameter.

(3) Craterlets - Craterlets are smaller than craters (range from 2-10 km in diameter) and lack central peaks.

(4) Crater Pits - Crater pits are circular depressions ranging downward from a few kilometers in diameter and without rims.

(5) Chain Craters - Chain craters are a group of craters of approximately the same size lying along a well defined line.

(6) Central Peaks - Central peaks are irregular peaks or hilly structures which occur in the centers of the larger craters. Their origins have been suggested as either volcanic or rebound.

(7) Others - Other features are small volcano-like structures having steep conical shapes capped by a vent-like opening and large "ghost" craters almost completely filled with deposits which occur on some of the Maria.

2. Structures and Landforms Produced by Crustal Movements

One of the most important facts concerning the lunar surface is the lack of evidence of rock deformation by folding of the surface formations. For example, most of the lunar crater shapes are still circular, but had they been located on the earth over the entire period of geologic history, these circular forms would have been greatly contorted and twisted. Distortion of rocks on the earth is common not only in the well known mobile belts, such as the geosynclinal areas, but also in the so-called stable areas such as the Canadian Shield. The fact that there has been little folding on the moon's surface stands as one of the most easily discernible differences between the earth and the moon.

However, the moon is not entirely devoid of evidence of structural movement. Gilbert in 1893 [26] observed a radiating system of linear topographic features surrounding Mare Imbrium which he named the "Imbrium Sculpture" (Figure 11).

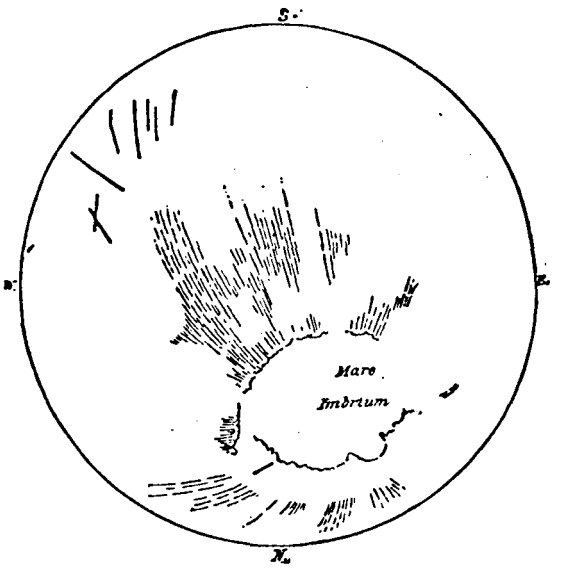

FIGURE 11. GILBERT'S SKETCH MAP OF THE IMBRIUM SCULPTURE (26)

Gilbert also believed that the circular Maria were the largest class of impact craters and that the "Imbrium Sculpture" was caused by fragments of ejected materials scouring deep grooves in the lunar crust. Shoemaker's interpretation is that the impacting meteorite produced giant shock waves radiating outward from the point of impact which fractured the moon's crust and created the "Imbrium Sculpture." This sculpture can be seen to good advantage in several of the photographs in Section VII (Figures 26, 28, 30, and 31). In addition, the following structural features have been observed on the lunar surface:

a. Wrinkle Ridges

These features are commonly located near the Maria margins where they exhibit broadly concentric patterns parallel to the bounding walls of the Maria. Upon close examination, they exhibit an en echelon pattern similar to a particular type of fault pattern seen on earth. The wrinkle, or pressure, ridges may correspond to anticlinal and synclinal folding caused by "compressive force imparted to the crust of a lava flow by the viscous drag of slowly moving subcrustal lava" [20].

b. Normal Faults

The Straight Wall has previously been mentioned as an outstanding example of a lunar normal, or gravity, fault. By definition, a normal fault is one in which the hanging wall moves down relative to the footwall (Figure 12).

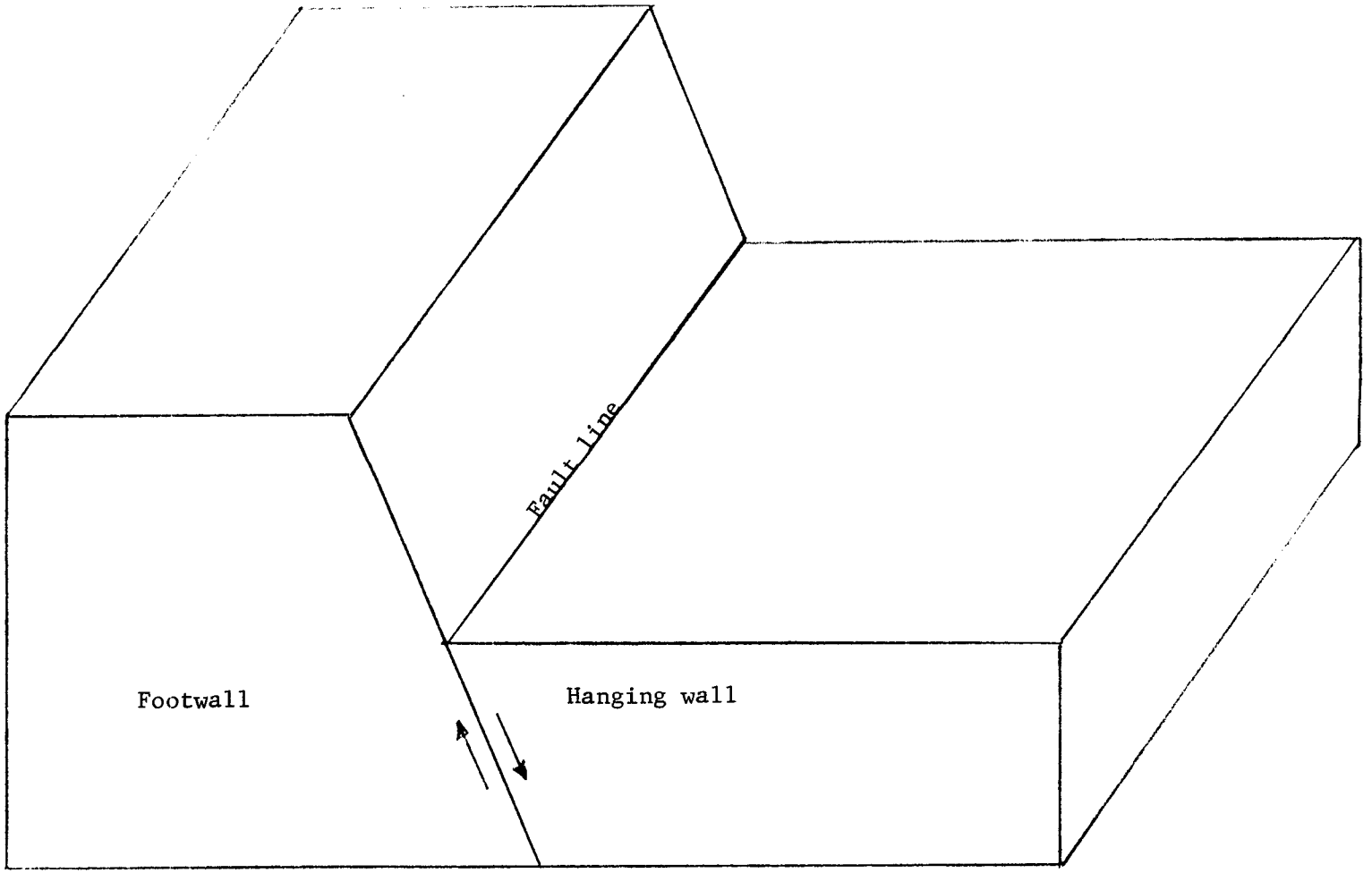

FIGURE 12: A NORMAL LUNAR FAULT (THE STRAIGHT WALL IS AN EXAMPLE OF THIS TYPE OF FAULT)

c. Rilles

These features are long narrow structural valleys developed on the surface of the Maria (Figure 13). They have been compared to rift valleys on earth such as the Rhine Graben or the Dead Sea Graben [21]. A possible analogy between the rift valleys of Iceland, known as gja and lunar rilles has been suggested [18].

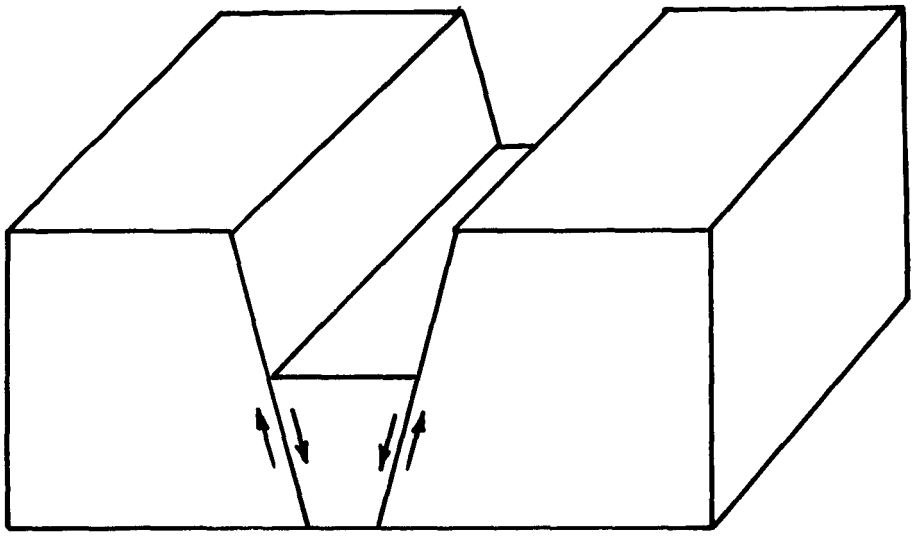

FIGURE 13. A GRABEN (A POSSIBLE ANALOGUE TO A LUNAR RILLE)

d. Joints or Fractures

These structures are defined as fractures which exhibit no appreciable vertical or horizontal movement. Apparently, the moon has a very old fracture system, laid out in a fairly well defined grid pattern. It has been suggested that these joints or fractures were induced by strong earth tides during the moon's primeval history. Presumably, these early tides exerted much greater force on the lunar crust than the present tides. During the time of the early tides, the earth and the moon were much closer together than they are now. The tidal forces increase as the inverse third power of the distance from the earth to the moon [22].

3. Structures and Landforms Caused by Igneous Activity

Some authors argue that strong tidal forces offer the best mechanism to account for large scale melting and igneous activity on the moon [20]. The argument is that deep fracturing of the lunar crust would cause an internal release of pressure in the rigid crust which would have resulted in large-scale melting at depth. Since the melting points of most silicate minerals are increased by adding pressure to the system, these minerals, under pressure, are stable at temperatures in excess of the melting points of the same minerals at atmospheric pressure. The sudden release of pressure, caused by impact produced or tidal fractures, could place many silicate minerals in a temperature-pressure environment which would result in their melting. It seems clear that there has been extensive igneous activity on the lunar surface, particularly in the Maria. Whether it was caused by tidal forces or large impacts, as suggested by Urey [17], is conjectural.

The following features are believed to be primarily produced by igneous activity:

a. Domes - See Section 3(b).

b. Maars and Chain Craters

The term Maar actually comes from the German and is applied to the small lakes that occupy volcanic craters in Germany [18]. In the geologic sense, a Maar is a circular-to-elliptical volcanic crater which ranges from 70 to 1500 meters in diameter, and from about 10 to 200 meters in depth.

The rim material of a Maar is composed of bedded ejecta made up of both surficial material and intrusive igneous rocks. Outer slopes of the rim are mostly smooth and at a low angle to the horizontal, but at the crest of the rim, slopes up to 30 degrees are attained. Apparently, the eruption of a Maar is concurrent with the generation of steam; the rapid transformation of water to gas is accompanied by an explosion [23].

It has been noticed that Maars tend to occur in chains, and this alignment is interpreted as due to magma welling upward in several places along a deep fracture. In this connection, it is important to note the presence of chain craters on the moon since these features may have an origin similar to the Maars. The similarities to lunar rilles exhibited by certain chain craters on the moon suggest that there may be a genetic relationship between these two features [18].

c. Calderas

By analogy with earth volcanic features, some authors have argued that lunar craters resemble volcanic features known as calderas [20]. To further this argument, central peaks which occur in many lunar craters are cited as evidence for the caldera origin.

A caldera has been defined as "a large basin-shaped volcanic depression, more or less circular or cirque-like in form, the diameter of which is many times greater than that of the included volcanic vent or vents" [23]. There are two main types of calderas, those due to explosive eruption and those due to collapse.

Figures 14 and 15 show the sequence of development believed to have occurred with both types of caldera. If the concept of the explosive caldera is invoked, then the ray material surrounding the crater would consist of pyroclastic volcanic ash deposits.

A slightly different interpretation of the ray material is that it is dust material laid down by a nuée ardente [24], a "highly heated mass of gas charged lava, ejected from a vent at the summit of a volcano where it continues its course as an avalanche, flowing swiftly, however slight the incline by virtue of its extreme mobility" [23].

d. Ring Dikes

A ring dike is a circular basin-type structure which resembles a lunar walled plain. The geological process responsible for this structure involves the subsidence of a nearly circular block of rock into an underlying magma chamber which forces magma up around the sides of the block.

A map and cross section of a ring dike in New Hampshire is shown in Figure 16 [25]. These circular structures vary in diameter from 1.28 km to over 14.5 km. The prominent rim structure exhibited by the ring dike is due to the process of differential erosion. This process simply means that certain rocks weather and erode faster than others, and that the material making up the rim has more resistance to erosion and weathering than the adjacent maerial.

On the moon in the near absence of weathering and erosion, the formation of a ring dike, if it did occur, would probably not advance far past the C or D stage on Figure 16, and the final result might be a walled plain (Figure 17).

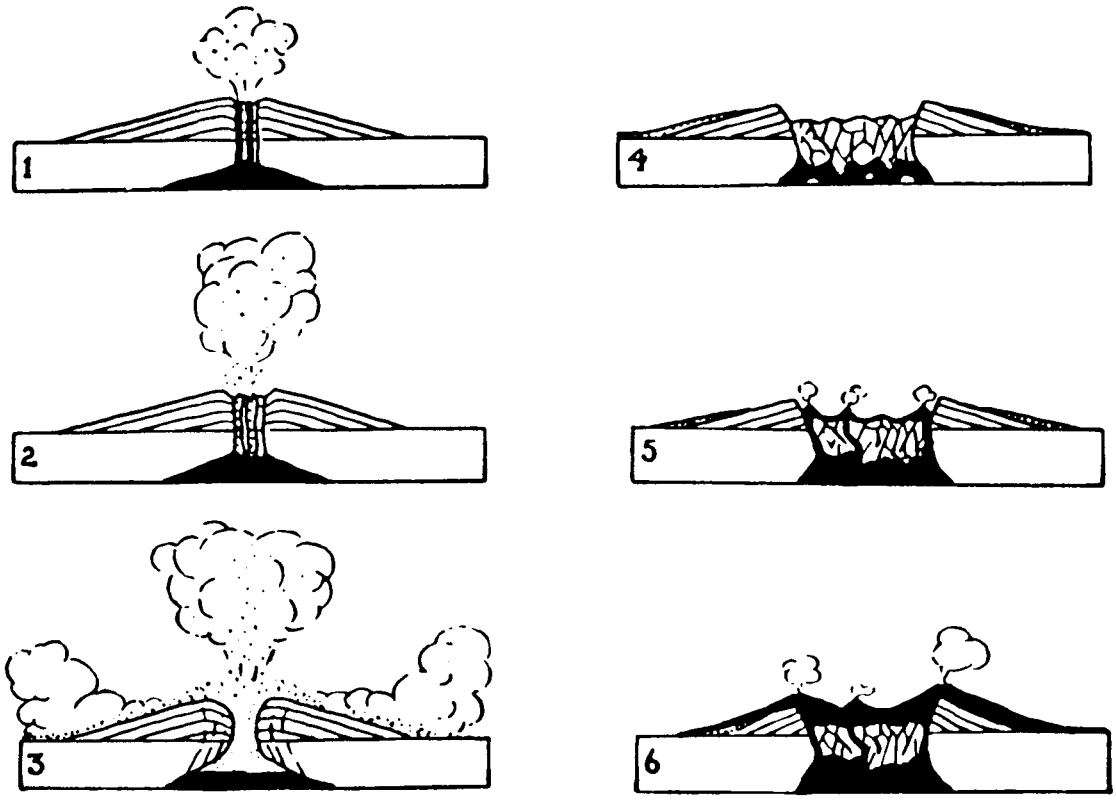

FIGURE 14: EVOLUTION OF A CALDERA OF THE KRAKATOA TYPE (Ref. 21)

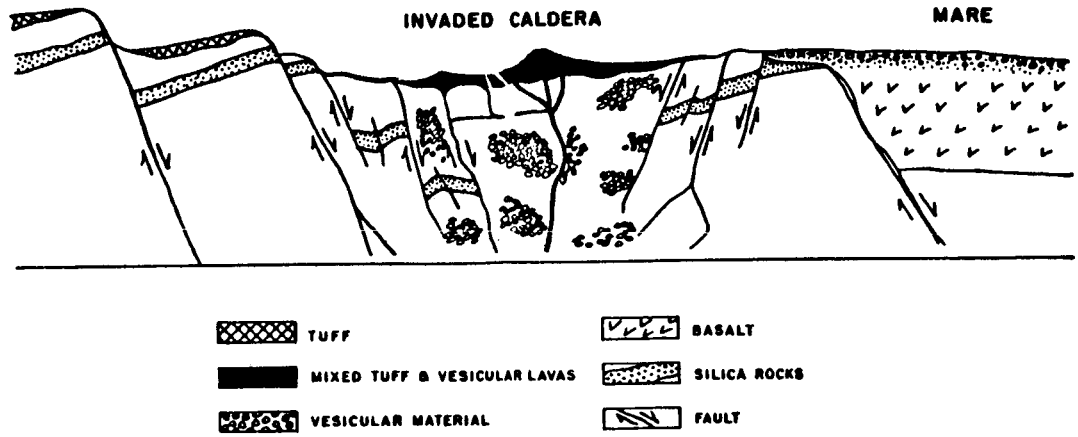

FIGURE 15: A CALDERA OF SUBSIDENCE (Ref. 13)

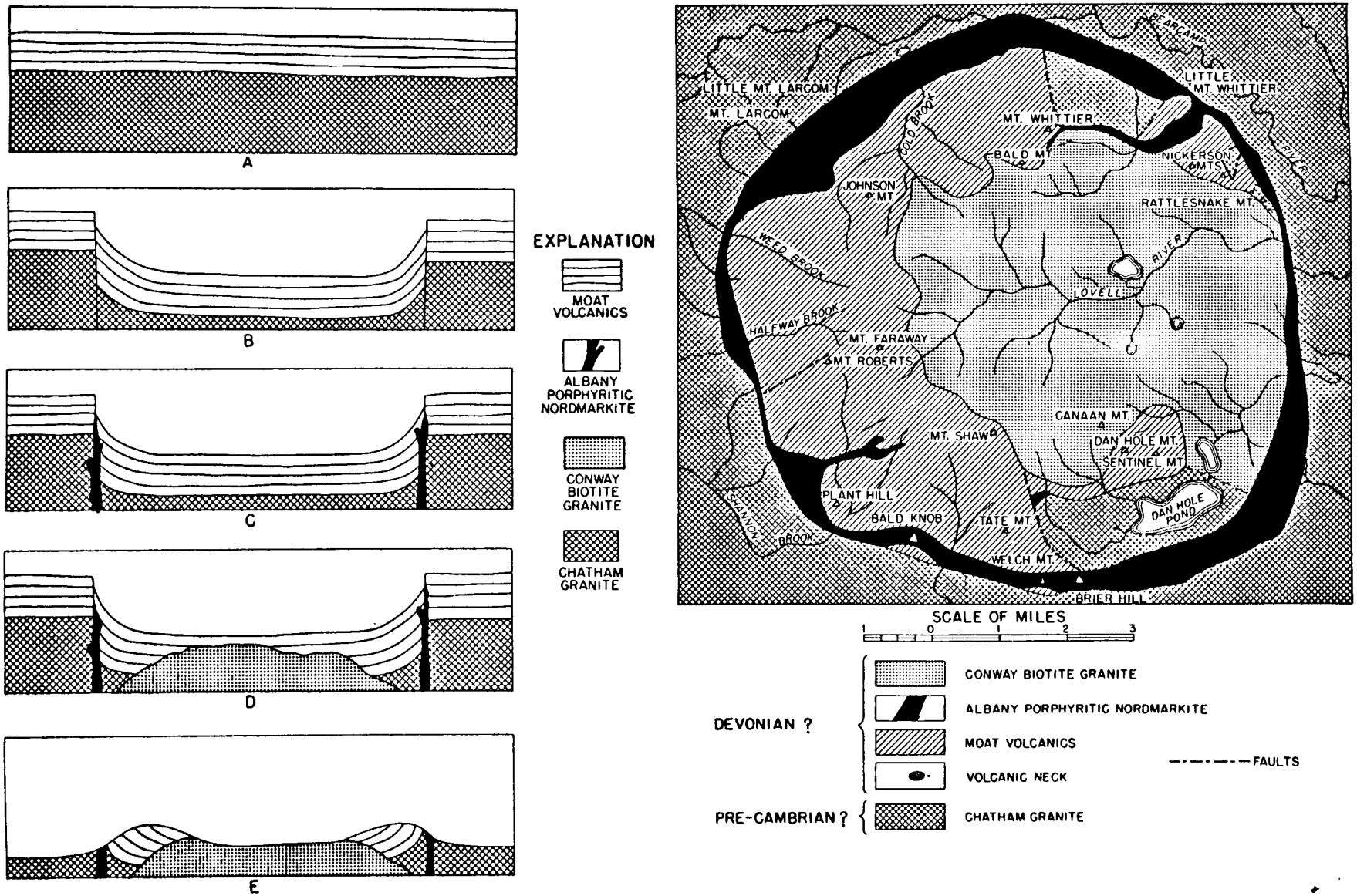

FIGURE 16: STAGES IN THE DEVELOPMENT OF A RING DIKE IN NEW HAMPSHIRE AND GEOLOGIC MAP OF THE RING DIKE

(Courtesy of John Wiley & Sons, N.Y.)

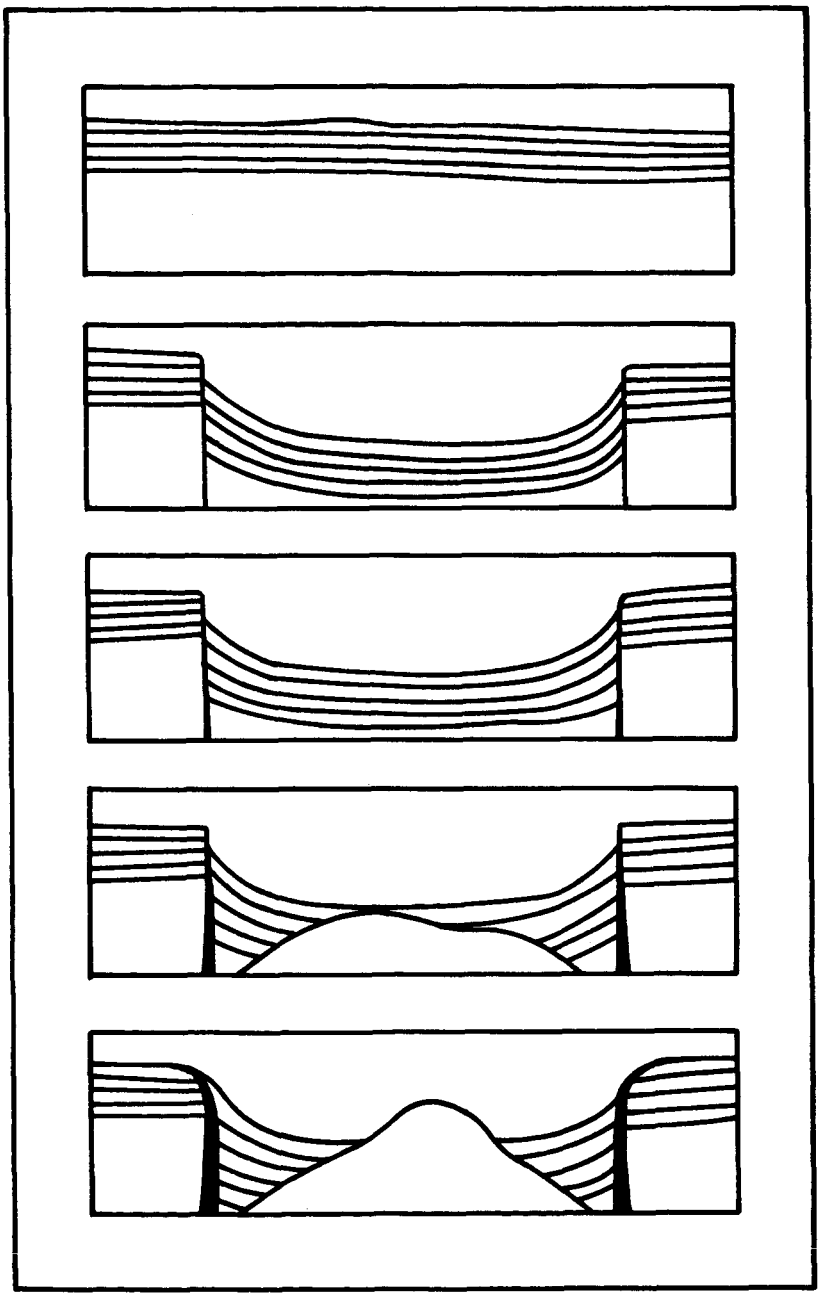

FIGURE 17. STAGES IN THE DEVELOPMENT OF A WALLED PLAIN WITH CENTRAL MOUNTAINS BY THE PROCESS OF CAULDRON SUBSIDENCE

e. Comparison of Lunar and Terrestrial Crater Morphologies

It is instructive to compare the morphologies of various lunar structures with some of their possible terrestrial analogues. Consider, for example, the subject of crater shapes or basin-like topographic structures on earth compared to those on the moon. It was observed by Gilbert in 1893 [26] that there are marked differences between earth impact and volcanic structures, and, by analogy, he was able to assign, tentatively, an impact origin to those lunar features which exhibit essentially identical morphological characteristics to earth impact structures. Likewise, Gilbert assigned a volcanic origin to lunar structures exhibiting a high degree of morphologic similarity to earth volcanic structures. However, he concluded that the earth volcanic structure of primary interest was the Maar-type volcano to which he attributed the origin of lunar chain craters.

As shown on Figure 18, Gilbert noted, in general, that the floors of both terrestrial impact craters and lunar craters of probable impact origin lie below the ground level (G.L.) of the surrounding terrain. With craters exhibiting central mountains Gilbert noted that the central mountains of lunar craters, in nearly all cases, lie below the outer rim, but in terrestrial caldera craters, the central mountains sometimes rise above the outer rim.

4. Structures and Landforms Produced by Erosion

a. Processes of Erosion

Processes of deposition and erosion result in a general leveling of the lunar surface. However, in the near absence of a lunar atmosphere, the process of slope reduction has gone on at a greatly reduced rate compared to the earth. In addition, the moon's low gravity does not encourage the downslope movement of material by slumping or mass movements to the same extent as earth gravity. The leveling process is also greatly retarded by the near absence of liquid water.

In spite of these difficulties, there is photographic evidence that, under the influence of lunar gravity, and probably triggered by moonquakes set off by impact-generated shock waves, lunar surface leveling has occurred on a large scale. On a smaller scale, it has been theorized that bombardment by micrometeorites and meteorites would have an overall erosive effect over a long period of time.

Bensko [9] has regarded the process of erosion so important as to categorize his Mesoselenic era as primarily a time in which "erosional agents such as micrometeorites and radiation" were particularly effective, and that eventually debris derived from erosional

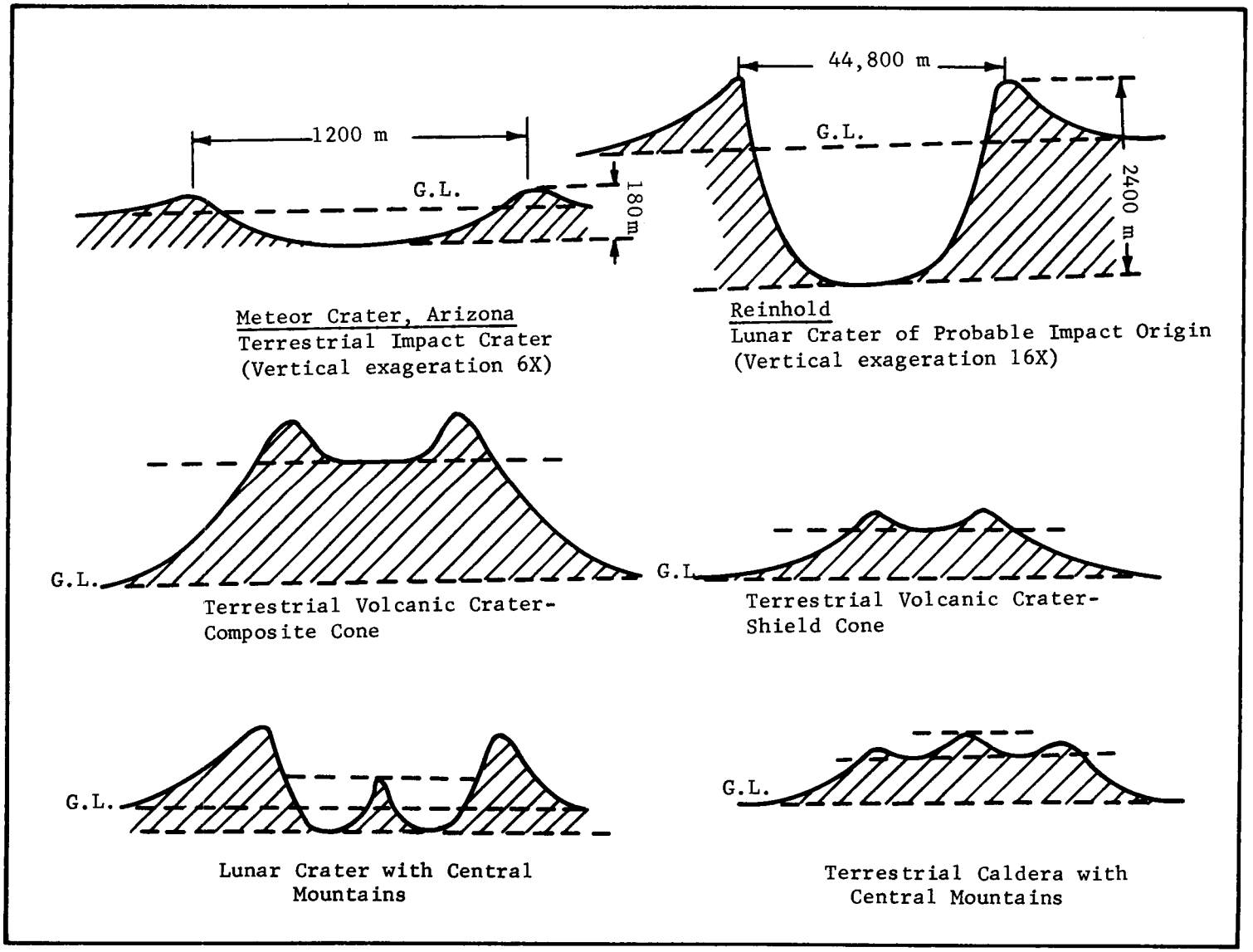

FIGURE 18. COMPARISONS OF LUNAR AND TERRESTRIAL CRATER MORPHOLOGIES

processes "became concentrated in the bases of craters, clefts, and any locally low areas on the moon's surface." According to this concept, the chief lunar erosional agents in addition to gravity are micrometeoroids and radiation.

b. Slumping and Mass Movements

A consideration of the crater Copernicus indicates that large slump blocks occur within the inner rim of the crater. This effect is probably due to downslope mass movement of fairly cohesive blocks of material along curved planes, similar to the slumpage process on earth. This phenomenon occurs when a load which exceeds the internal shear strength of the material is applied to a granular material on a steep slope. Such a load could be simulated by shock waves being transmitted through the material. Since slumping usually takes place in a number of discrete steps, the surface is terraced as in the example of Copernicus (Figure 29).

Mass movements can occur anywhere on the lunar surface where the required conditions of loose materials situated on a high slope are met. Thus, mass movements of material should be prevalent, not only on the inner rims of craters, but also on the sides of rilles, fault scarps, and along ridges.

c. Other Types of Mass Movement

Other types of mass movement of lunar rock material that can be expected include talus deposits, rock fans and pediment-type deposits. In this connection, there is an analogy between lunar erosional processes and those which occur in deserts on earth. Here again, the lunar process will not be nearly as complete as the analogous earth process due to the absence of running water and wind, but the processes of comminution by missile bombardment coupled with lunar gravitational forces acting on steep slopes over a long period of time will inevitably develop these analogous features.

B. Small-Scale Lunar Features

For purposes of establishing lunar design criteria, the small-scale features may be more important then the large-scale features which have just been discussed. However, in most cases, the small-scale features are derived from the large-scale features and the various processes responsible for the development of these large-scale lunar features, e.g., impact, volcanic activity, erosion, etc., will largely control the nature and arrangement of the small-scale features. For this reason, the theories for the development of lunar large-scale features were fully explained before attempting to discuss the various small-scale configurations.

In the sections to follow, various types of small-scale features will be discussed, e.g., those due to ejecta origin and volcanic origin, and features which have been postulated on the basis of their optical and thermal properties. Finally, the engineering parameters dealing with the various small-scale features will be discussed.

1. Features Derived from Impact Origin

Obviously, the ejecta,whether caused by meteoritic impact or explosive volcanoes, result in the widespread deposition of angular fragments on the surface. The size distribution may be logarithmic and range from clay-sized powders (.004 mm) to angular boulders (256 mm). Regardless of the size distribution, marked angularity and poor size-sorting of this material can be expected. The absence of an atmosphere and the weathering process is of great importance since the material will not have been greatly modified after it reached its final resting place. It is possible that the angularity of the mineral grains making up material such as ejecta blanket deposits surrounding the craters, for example, Kepler and Copernicus, will allow interlocking of grains and consequently relatively high bearing strength. This would result in angles of repose of the sand-sized fraction (12 mm to .06 mm), in excess of 34° (value for terrestrial sand deposits). The overall design effects produced by high slopes associated with this type of deposit may be negated, however, should there be a sufficiently high surface density of angular boulder-sized fragments (754 mm). For example, if the ejecta blanket material is sufficiently poorly sorted, the major engineering parameter of interest to vehicle designers will likely be surface roughness caused by protuberances. A reasonable assumption based on the behavior of ejecta around earth impact craters is that roughness will constitute a more serious problem than the bearing strength of the impact deposits.

Research performed by Bensko and Cortez of MSFC [27] sheds some light on the size of boulders associated with lunar craters. The authors contend that there is a similarity of sizes for all impact craters' debris regardless of whether it was formed on the earth or the moon. The essential difference is that the earth impact crater debris may exhibit better sorting of particles due to the presence of an atmosphere. The important similarity between terrestrial and lunar features is that the maximum block size of earth crater debris indicates an upper limit for the sizes of lunar fragments. Based on a curve of crater size versus block size, a crater the size of Meteor Crater in Arizona (1180 m in diameter), can produce blocks approximately 10-15 meters in diameter (Figure 19). Larger impact craters will produce proportionally larger blocks and smaller craters, smaller blocks.

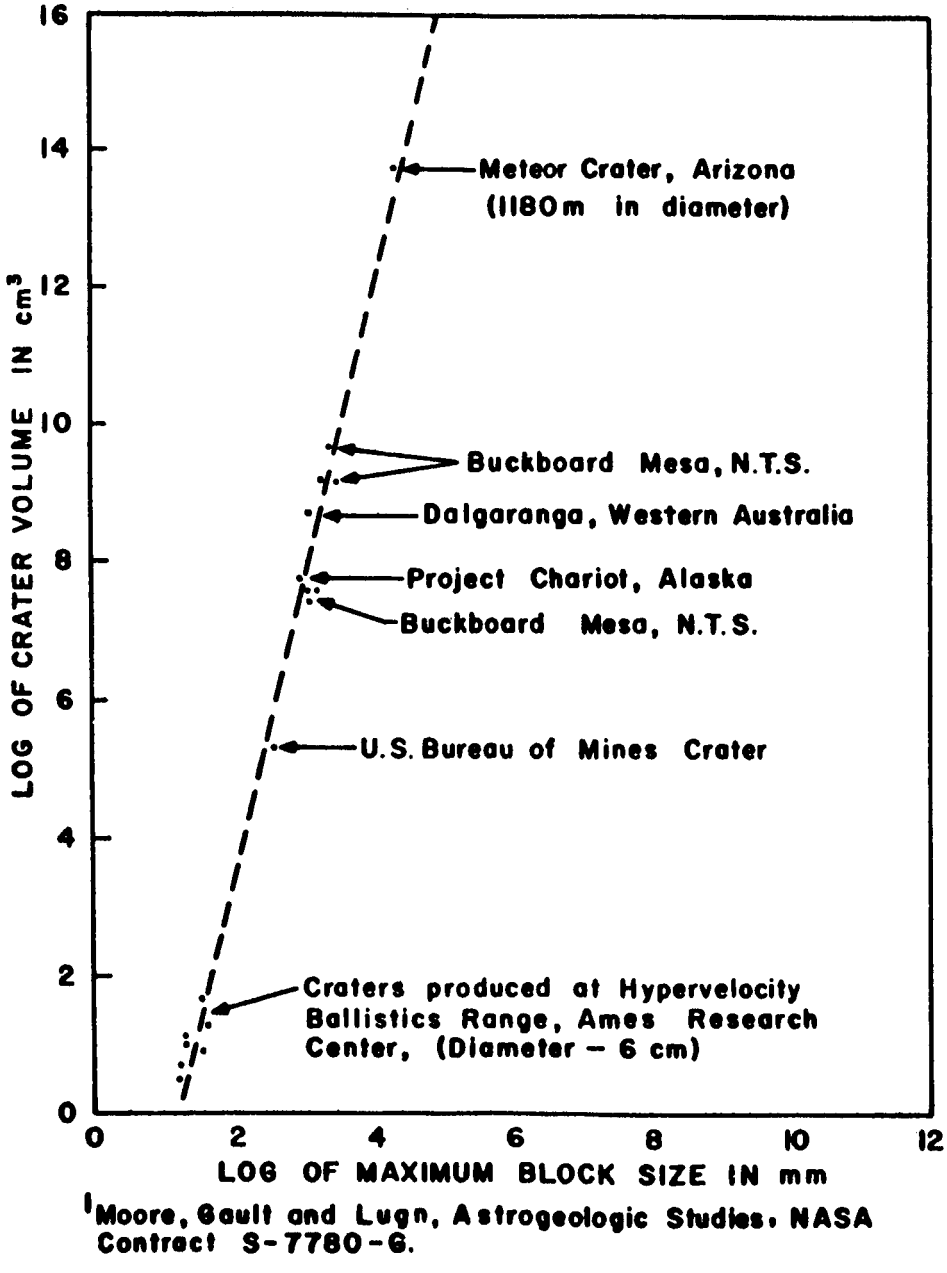

FIGURE 19: RELATIONSHIP BETWEEN CRATER VOLUME AND MAXIMUM BLOCK SIZE OF CRATER DEBRIS (Ref. 27)

Regarding other possible small-scale features associated with lunar ejecta phenomena, one should be aware of the emplacement of secondary or satellite craters caused by the bombardment of blocks ejected from a large impact crater. Studies made by Shoemaker [18, 19] indicate that the fragments capable of forming secondary craters which are visible at telescopic resolution are ejected at angles of 14 to 22 degrees (Figure 9). A map of areas exhibiting the zone of secondary craters around Copernicus is provided in Figure 10. A cursory glance at this map indicates that, for the purposes of establishing traverses for optimum mobility, regions of secondary crater formation must be considered from the standpoint of small-scale roughness. These regions will contain concentrations of smaller secondary craters both above and below the limit of optical resolution. The secondary craters shown on Figure 10 lie in a broad concentric belt surrounding Copernicus. Significantly, the area between the secondary craters and the main impact crater is relatively undisturbed at the visible scale, and it can be inferred that this area is covered by material of smaller grain size (ejecta blanket deposits). Perhaps areas such as this will provide better surface conditions for planning traverses around the large craters such as Copernicus.

Finally, Salisbury [13] points out that, according to the meteorite theory, the subsurface structure should consist "of highly fractured basement rock overlain by discontinuous layers of rubble, rock flour, and meteoroid material" and that "this subsurface structure should exhibit very little collapse hazard."

2. Features Derived from Volcanic Origin

Almost without exception, the students of lunar topography agree that the Maria are covered by thick deposits built up by separate lava sheets. This lava may have resulted from pressure released by large meteorite impacts which occurred during a critical phase of the moon's cooling history [28]. Probably the surface of the Maria consists of one or both of the major textures exhibited by earth lava flows with some modifications due to the lower gravity and the absence of atmosphere on the moon. The terrestrial-type examples of lava flows are aa and pahoehoe. Aa, the Hawaiian term for basaltic lava flows, is typified by a rough, jagged, spinose, clinkery surface, while pahoehoe is typified by a smooth, billowy, or ropy surface [23]. Modifications to these types of lava flows resulting from lower lunar gravity and vacuum may include deeper nucleation and slower rise of bubbles resulting in a highly vesicular lava which may present a collapse hazard. Tentative results of a study by Dobar [29] of Bendix indicate that on the moon vesicular igneous rocks such as pumice and scoria are likely to be more common than the dense basalt of earth terrains. Salisbury [13] estimates that the maximum depth of a vesicular layer would probably be 13 m with

average dimensions being about one-half the maxima. Fudali [15] indicates that, according to the volcanic theory of Maria formation, the surface will have a range of textures from smooth, if it is formed from pahoehoe or welded tuffs, to rough, if it is aa-type lava. Other small-scale irregularities in lava flows are wavy and highly fractured surfaces which resemble pressure cracks in ice flows. These fractured surfaces are caused by viscous flow. Also, the Maria surfaces will have been further modified by meteoroid bombardment, the result of which should be the production of craters and small-scale relief of rubble.

It has recently been suggested [30] that the erosive action of gas-filled clouds from lunar volcanoes heavily laden with ash and cinders (nuées ardentes) may be responsible for eroding Shröeter's Valley (Figure 32). If this interpretation were correct, pyroclastic deposits of volcanic ash, tuff, etc., may be found widely distributed in adjacent low areas and might be interbedded with the lava flows. A similar theory has been suggested by Green to explain the ray systems associated with the younger craters [24].

3. Features Based on Thermal and Optical Measurements

Many scientists have studied the moon's surface by observing its thermal and optical radiation. Moreover, one might add studies using radar measuring devices. This work has been concerned with the moon's spectral distribution, reflectivity (albedo), and optical scattering and polarization properties. It is not within the scope of this paper to discuss these studies in detail, but rather to discuss some of their conclusions, particularly regarding the lunar surface conditions.

a. Thermal Properties

Thermal inertia is defined by the expression $(K\rho c)^{1/2}$, where K is the thermal conductivity, ρ the density, and c the specific heat of the surface material [31]. With the lunar surface materials, the value of K ranges from 3×10^{-5} to 3×10^{-6} cal/cm^2 sec. Some typical values for thermal conductivities of terrestrial materials are as follows: copper, K = 0.9 cal/cm^2 sec; rock, K = 5×10^{-3} cal/cm^2 sec; pumice, K = 3×10^{-4} cal/cm^2 sec; and powder in vacuum, K = 3 to 10×10^{-6} cal/cm^2 sec [2]. In these examples, it is interesting to note that thermal conductivities decrease as the amount of surface contact within the material decreases. This relationship is apparently due to the decrease of conduction paths within a volume of dust, compared to an equal volume of solid rock. In addition, the presence of vacuum tends to decrease the already low thermal conductivity exhibited by granulated substances. Since dust or powdery materials in vacuum have about the

same low thermal conductivities as the lunar surface, a dust-layer model surface has been suggested by some researchers. However, other possible surface model configurations also have the same low thermal conductivity. These will be mentioned later in this report.

Thermal inertia is a measure of resistance to heat flow in a material. The moon's surface has a very low thermal inertia, which indicates that it is a very good thermal insulator. The lunar surface temperatures vary from 389°K ± 5° at the maximum to 120°K ± 2° at the minimum. Sinton [32] observed a temperature drop from 374°K to < 200°K during a period of one hour during an eclipse. The temperature continued to decline slowly, thus indicating that the moon's surface has excellent insulation properties.

The properties of low thermal conductivity and thermal inertia seem to indicate that the surface temperatures would not extend very deeply into the moon's interior and would have a superficial "skin" effect. One study of lunar subsurface temperatures published by General Electric [2] shows that at a depth of 76.2 cm the subsurface temperatures are almost constant, varying slightly from a mean temperature of approximately 235°K regardless of lunar surface temperatures.

b. Optical Properties

(1) Polarization

Studies have been conducted to determine the effects of the lunar surface materials on the polarization of light [33]. Since the degree of polarization is related to the nature of the lunar surface, it has been hoped that this type of analysis may be used to determine lunar soil properties. By studying materials exhibiting similar polarization to that of the moon's surface in the laboratory, it seems possible that analogies can be drawn with known earth materials having similar polarization properties.

Lyot is quoted by Dollfus [33] as making a precise analysis of the polarization of moonlight. Lyot obtained a curve of polarization variations with phase angles and noted that the percentage of polarization varies from a minimum of -1 percent at 10 degrees from full moon to a maximum of 10 percent at 115 degrees from waxing moon.

Lyot studied the polarization properties of a number of terrestrial materials including quartz sands, clayey sands, and chalky sediments which he says do not have the same polarization as the moon's surface. This conclusion is not too surprising in view of the fact that these minerals are all characteristic of sedimentary environments. Experiments with volcanic lavas and angular rock fragments

of basic igneous rocks met with more success in simulating the lunar polarization properties. On the basis of this work, Dollfus writes that "we must conclude, therefore, that the lunar surface is covered with a very absorbing powder, having a constitution similar to that of volcanic ash" although the specific type of ash is not mentioned.

Niedz's report [2] on the lunar surface was somewhat less optimistic than Dollfus and concludes that it is possible to hope that terrestrial counterparts of lunar rocks may be found, but the state-of-the-art of polarization studies does not permit our discerning this property. Niedz concludes, however, based on the behavior of its polarized light, that the surface of the moon should consist of a fine-grained surface layer.

(2) Albedo

The albedo, or reflectivity, of the lunar surface is reported to be very low by comparison to earth terrains, ranging from a minimum of 0.051 to a maximum of 0.183 [31]. The average spherical albedo of the moon as a whole is 0.073 [2].

Attempts to correlate the moon's albedo with terrestrial counterparts indicate that only very dark substances such as basaltic lava and the fusion crust of meteorites have albedos approaching those of the moon. Granite has albedos which are too high for possible lunar surface materials except in the continental and mountainous regions in which the albedos are twice as high as the Maria.

Niedz [2] reports terrestrial igneous rocks where albedos match lunar albedos as follows:

> Lightest regions. (Continents and mountains) - basalts and stony meteorites.
>
> Medium lightness regions - lavas, dark tuffs, volcanic ash.
>
> Darkest region - basaltic lavas, dark volcanic ash, fusion crust of meteorites.

Niedz [2] cautions, however, that rock types exhibiting lunar albedos are numerous and that it is not yet considered justifiable to select the type of lunar rocks on the basis of this photometric property alone.

(3) Light-Scattering Properties

It has been pointed out in the literature [2] that the intensity of scattered light changes very rapidly before and after full moon. Full moon is approximately 11 times as bright as first or last quarter. This observation is quite unlike any smooth surface known, but it can be simulated by a vesicular surface covered by pits and irregularities on a centimeter to millimeter scale.

Another interesting observation concerning the light-scattering properties of the moon is that there is no limb-darkening and that each part of the moon's surface attains its maximum brightness at full moon, regardless of its relative position or angular distance from the center of the moon. This observation bears out the theory of a highly vesicular, rough microstructure of the surface materials [2].

(4) Color

According to Dugan [31] the moon's surface is essentially colorless. There is a relationship between brightness and color in which the brighter the feature, the redder its color. Mare regions are bluish areas.

If one attempts to correlate the coefficient of brightness and color of lunar rocks with possible earth analogues, the following types of terrestrial rocks all satisfy the lunar data: volcanic ash, coarse-grained basalt (diabase), red quartz porphyry, iron quartzite, and tuff [2].

4. Concepts of Possible Surface Configurations

Our knowledge of the actual small-scale surface structure is based largely on the data from the preceding sections. Attempts have been made to correlate thermal and optical properties with various theoretical models which actually exhibit all of the measured properties available. On the basis of this data, the following models have been suggested.

a. Whisker Model

This surface would consist of fine whisker crystals produced by the effects of sputtering due to proton bombardment [15].

b. Rock-Froth Model

This type of surface is produced by the outgassing of molten lava and the formation of a vesicular igneous rock not unlike

scoria or pumice. The actual texture of the froth would be quite variable and depend on the composition of the melt, cooling rate, viscosity, etc. [15].

c. Dust Model

This model presupposes micrometeorite erosion and the production of vast quantities of dust-sized (> 0.06 mm) particles derived from lunar surface rocks [15]. The rate of production of lunar dust layer may vary from a maximum of 75 meters/4.5 x 10^9 years based on an estimate of erosion rates by Whipple to 4.5 meters/4.5 x 10^9 years according to Orrok's estimate quoted by Fudali [6]. Significantly these estimates presuppose that all of the eroded material was immediately removed by transporting agents - which likely do not exist on the moon - and thus constitute maxima which probably range far above actual values. In fact, Öpik, recognizing this difficulty, is quoted by Fudali [6] as indicating that the total thickness of eroded dust is small and probably ranges from 20 to 100 cm.

d. Two-Layered Model

The moon's property of extremely low thermal conductivity based on infrared and optical emissions has led to the concept of a two-layered model consisting of an upper layer of dust, approximately 9 mm thick, and an underlying rock layer [34]. The properties of the upper layer are as follows:

K (thermal conductivity) = 2.8 x 10^{-6} cal/cm/sec/°C

Q (density) = 1.8 g/cm^3

c (spec. heat) = 0.2 cal/g

Under this layer is a vesicular rock layer of composition of basalt [39] having the following properties:

K (thermal conductivity) = 6.8 x 10^{-4} cal/cm/sec/°C

Q (density) = 2.08 g/cm^3

c (spec. heat) = 0.2 cal/g

e. Correlation of Small-Scale Data with Large Scale Data

It is gratifying to observe the broad similarities that are emerging from a consideration of the moon's small-scale and large-scale features. For example, thermal and optical properties of the moon point to a highly insulating material having a low thermal conductivity and low thermal inertia. The albedo, polarization, and color properties suggest the existence of basic igneous rocks such as basalt, or diabase, plus volcanic ash, and fusion crust of meteorites. Polarization, particularly, seems to indicate that the surface material contains a granular layer. By comparison, the large-scale features should be composed largely of basalt or vesicular lavas in the Maria and granulated, perhaps fused, meteoritic material in the continental areas. Broadly speaking, there is good general agreement between the interpretations applied to the large-scale features and those applied to the small-scale ones.

It seems significant that future studies dealing with lunar surface criteria should try to obtain correlations of this nature, for this appears to be a fruitful way to solve many of the remaining problems dealing with lunar technology. This type of endeavor will require an effort on the part of several types of scientific specialists working together to arrive at a common goal - a better understanding of the lunar surface environment - just as soil scientists, chemists, and bacteriologists may work together to solve a terrestrial soil problem.

VI. ENGINEERING PARAMETERS OF THE LUNAR SURFACE

Many subjects of value to engineers have been discussed on the previous pages. For example, knowledge of the large-scale features will be necessary for proper planning of traverses for a lunar mobile vehicle, and a knowledge of the small-scale features is required if a proper conceptual design of the optimum vehicle configuration is to be made. However, there exist several problems which are peculiar to vehicle engineering design or for site selection which will be discussed at this point. These problems are concerned with the bearing strengths, slopes, protuberances, and the relative roughness of the lunar surface.

A. Bearing Strength

The bearing strength of the lunar surface is dependent upon the lunar surface model that is selected, e.g., froth, whisker, dust, etc. If a "worst-case" model is selected, it would consist of a thick deposit of loosely packed dust. With the "worst-case" model, the bearing points will penetrate no further than 3 - 5 cm (1 - 2 inches) under a load of 6.89×10^4 newtons/m^2 (10 psi) [15].

A whisker surface layer would have a negligible bearing strength, but it would be so thin as to present no bearing strength problem. Rock froths should have static bearing strengths [15] ranging from 1.38×10^6 newtons/m^2 (200 psi) to 8.27×10^7 newtons/m^2 (12,000 psi).

For the "worst-case" model cited above, this is a very conservative model and does not allow for any mitigating effects such as cold-welding in vacuum or fusion resulting from micrometeorite and cosmic radiation bombardment. Recent studies by Wehner et al. [5] seem to indicate that bombardment by the solar wind would not only darken a granular material, but it would also cement the grains together into a brittle, fibrous crust by sputtering. Under these circumstances, one would expect to find an increase in bearing strength over a loose dust model.

B. Slopes

1. Regional

Maximum regional slopes on the Maria surface average from 2 degrees to 3 degrees. Slopes on inner rims of craters may run as high as 35 degrees to 40 degrees [15]. Average slopes in the continental regions (including mountainous regions) rarely exceed 10 degrees. In the inner rims of craters the following relationships hold (Reference 2 quoting Baldwin):

CRATER DIAMETER	328 m	3,280 m	32,800 m
Average Slope of Inner Rim	30°	24°	16°
Maximum Slope of Inner Rim	70°	46°	28°

Bronner [12] points out the following relationships concerning lunar regional slopes.

a. Mountain Slopes

Lunar mountains have slopes which are concave upward and in which the upper portion is steeper than the lower portion.

b. Outer Slopes of Craters

The above relationship holds for the outer slopes of larger craters and the inner slopes of smaller craters.

c. Mare Borders

Some of the Mare borders display the characteristic steep slopes of escarpments.

d. Inner Slopes of Craters

The inner slopes of numerous craters are terraced due to the downslope movements of slump blocks. These terraces which are relatively horizontal may have fore slopes of from 20 degrees to 45 degrees.

2. Local Slopes and Protuberances

If one accepts the theory of meteoroid bombardment with resulting debris-ejecta deposits, a large portion of the moon's surface is covered by angular fragments of ejecta which exhibit a wide size-distribution. Slopes may reach 40 degrees in the case of large angular blocks or lava structures. The average blocky fragment should be about one meter in diameter. In addition, small craters ranging from less than one inch to several hundred meters in diameter may be numerous.

C. Rough Versus Smooth Maria

Fudali [6] contrasts the major arguments for smooth versus rough Maria in an attempt to show that neither view has the preponderance of scientific merit in its favor. Basically, the view for a smooth Maria emphasizes the extremely old ages (4.5×10^9 years) placed on the Maria by Shoemaker et al. [10], which provide an extremely long period for micrometeoroid bombardment and leveling. The contrasting view for a rough Maria emphasizes the effect of ejecta from cratering processes and minimizes the effects of micrometeoroids' erosive capabilities.

VII. LUNAR PHOTOGRAPHIC ATLAS

This section presents selected photographs from G. P. Kuiper's Lunar Photographic Atlas, which have been reproduced by courtesy of the University of Chicago Press. They have been compiled by Dr. Kuiper from the best photographs available from the world's leading observatories including Wilson, Lick, McDonald, Yerkes, and Pic-du-Midi. It is hoped

that they will be instructive, not only in providing data on lunar geography and lunar formations, but more importantly, in illustrating the morphologies of the various large-scale lunar features. Most of the structures and landforms discussed in the preceding sections have been noted on the photographs and keyed into the text. It is hoped that the reader will use these photographs as he reads the text to obtain a realistic viewpoint of the lunar surface, its structural and topographic features, and their scale and physical appearance.

The photographs are oriented with south at the top just as they are viewed telescopically. This arrangement places west on the right-hand side of the page.

LUNAR PHOTOGRAPHIC ATLAS

FIGURE 20. FIRST QUARTER

(Courtesy University of Chicago Press)

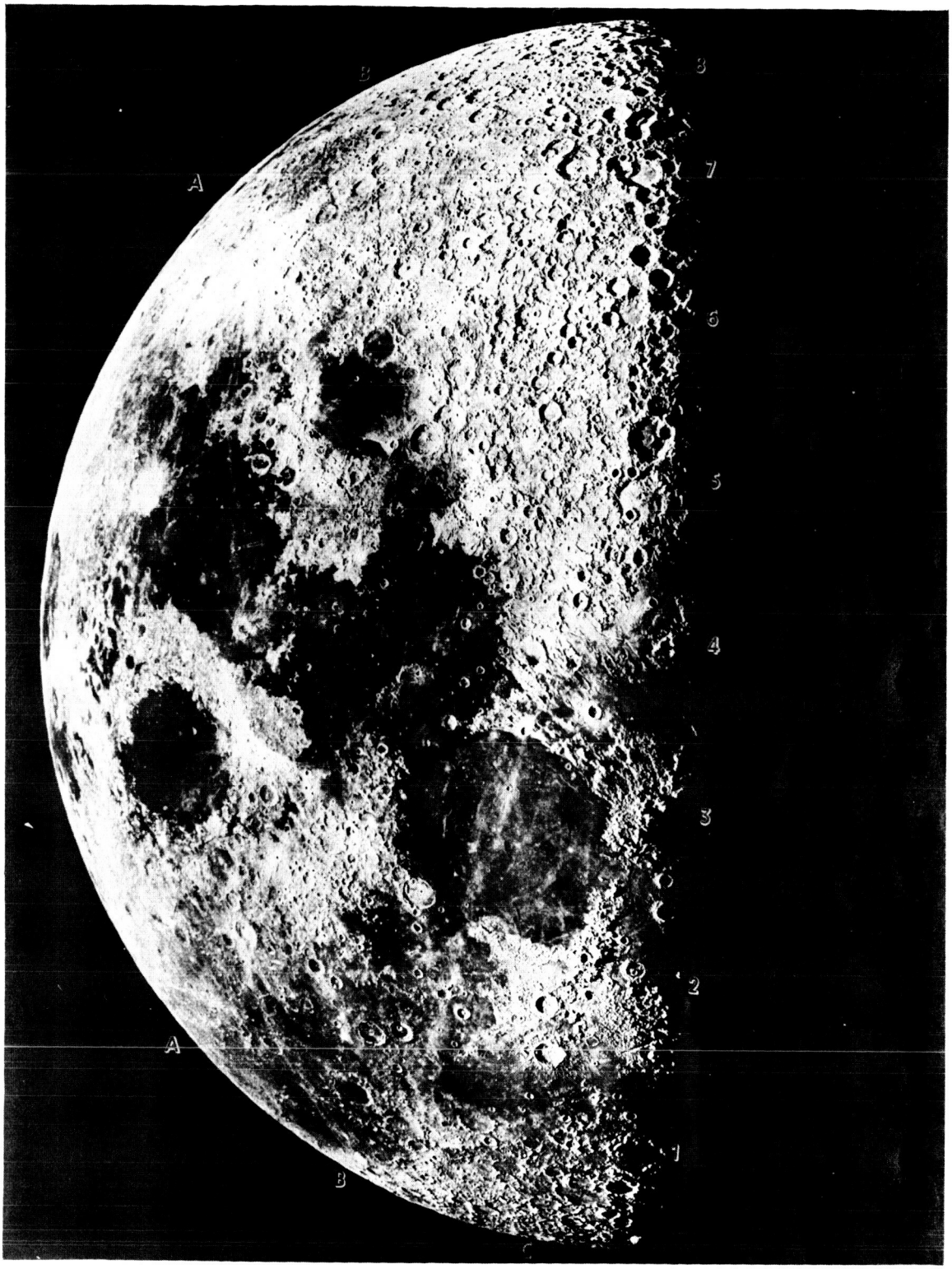
B
A
A
B
8
7
6
5
4
3
2
1

FIGURE 21. LAST QUARTER

(Courtesy University of Chicago Press)

8
7
6
5
4
3
2
1
E
F
F
E

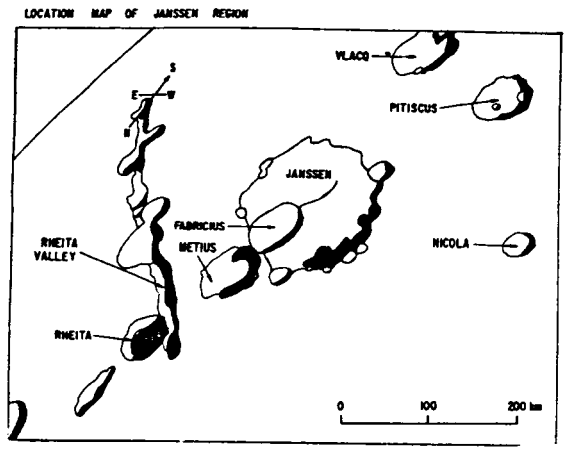

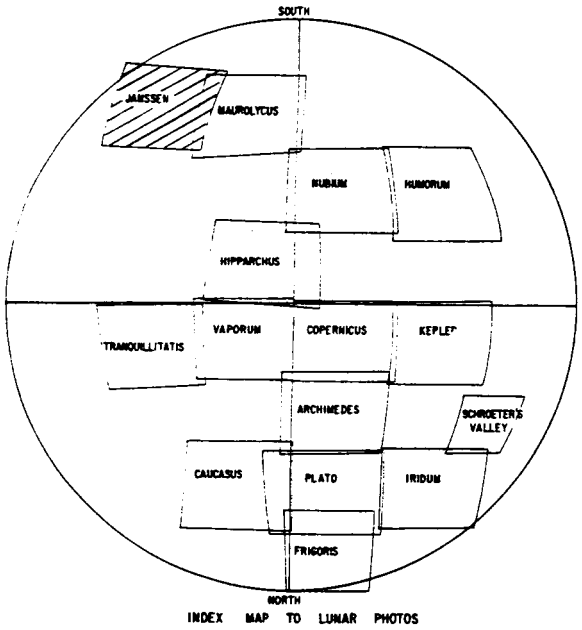

INDEX MAP TO LUNAR PHOTOS

FIGURE 22. JANSSEN REGION

(Courtesy University of Chicago Press)

The large crater, Janssen, in the center of this photograph is approximately 250 km in diameter. The area is covered by craters including subsequent craters within Janssen itself. In the central part of Janssen is a curved fault line.

In the NW part of the photograph, trending SE by NW is the Rheita Valley. This valley has been interpreted as a rille.

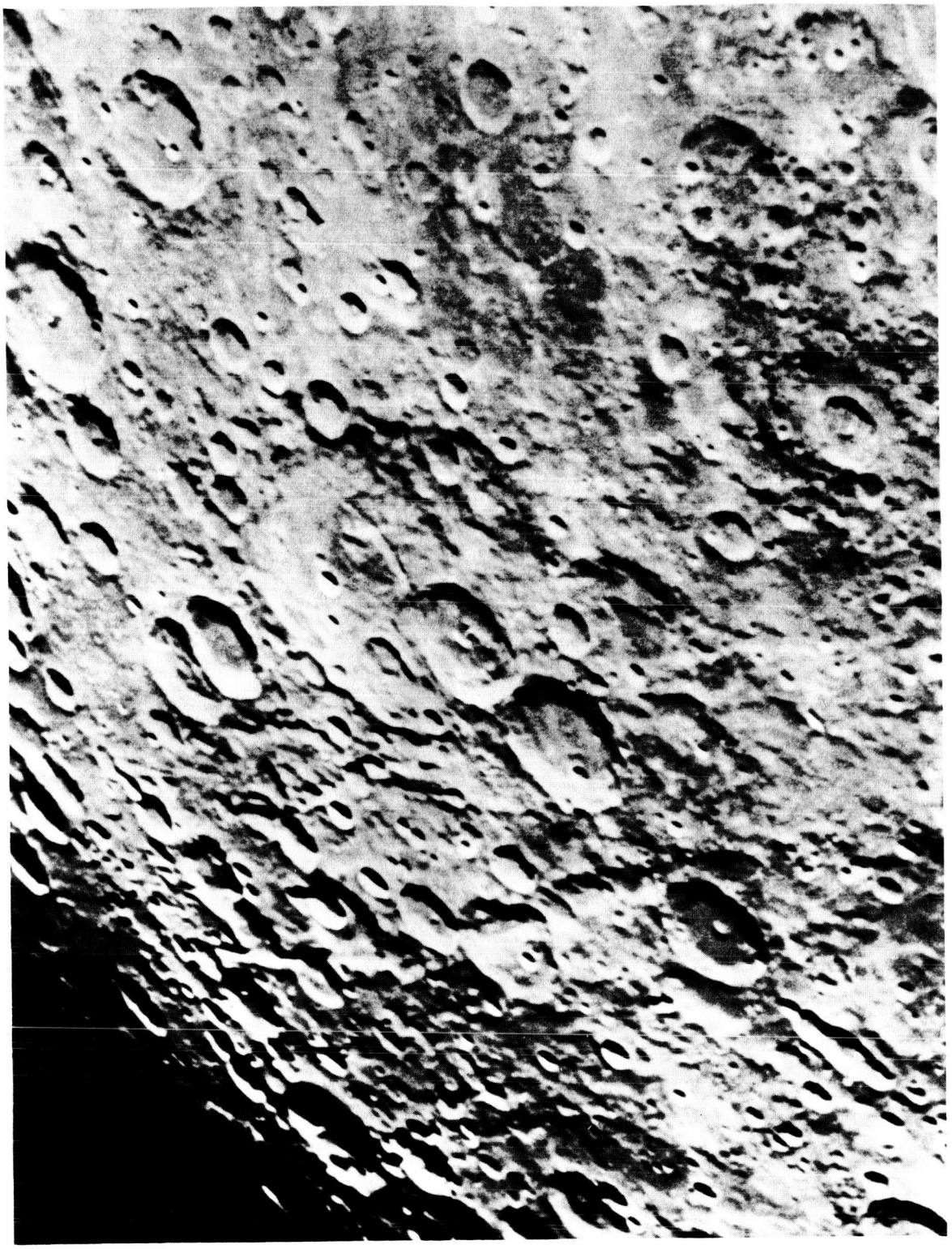

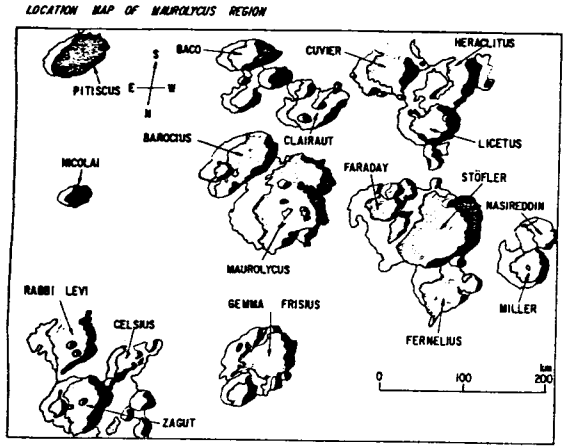

FIGURE 23. MAUROLYCUS REGION

(Courtesy of University of Chicago Press)

This region, located in the lunar highlands, has extensive areas covered by craters. There are many examples of craters within craters, e.g., Stöfler and Maurolycus. The east side of Stöfler exhibits overlapping craters of four different ages as indicated by the truncated rims exhibited by each successively younger crater. Many of the craters in this area are interpreted as walled plains or ringed plains since they exhibit little or no rim material.

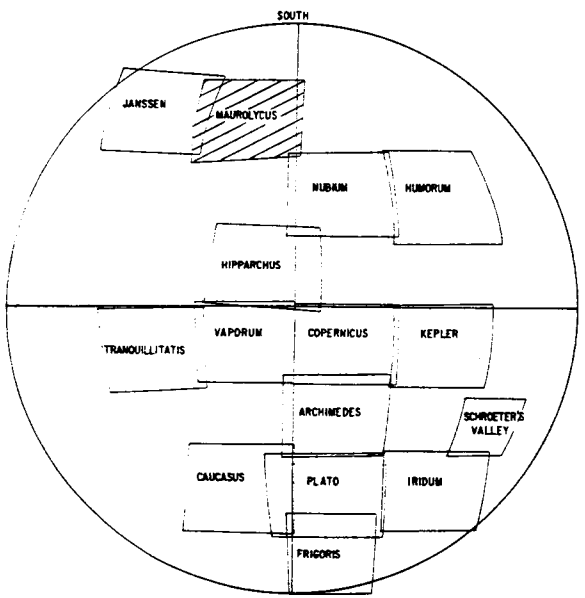

INDEX MAP TO LUNAR PHOTOS

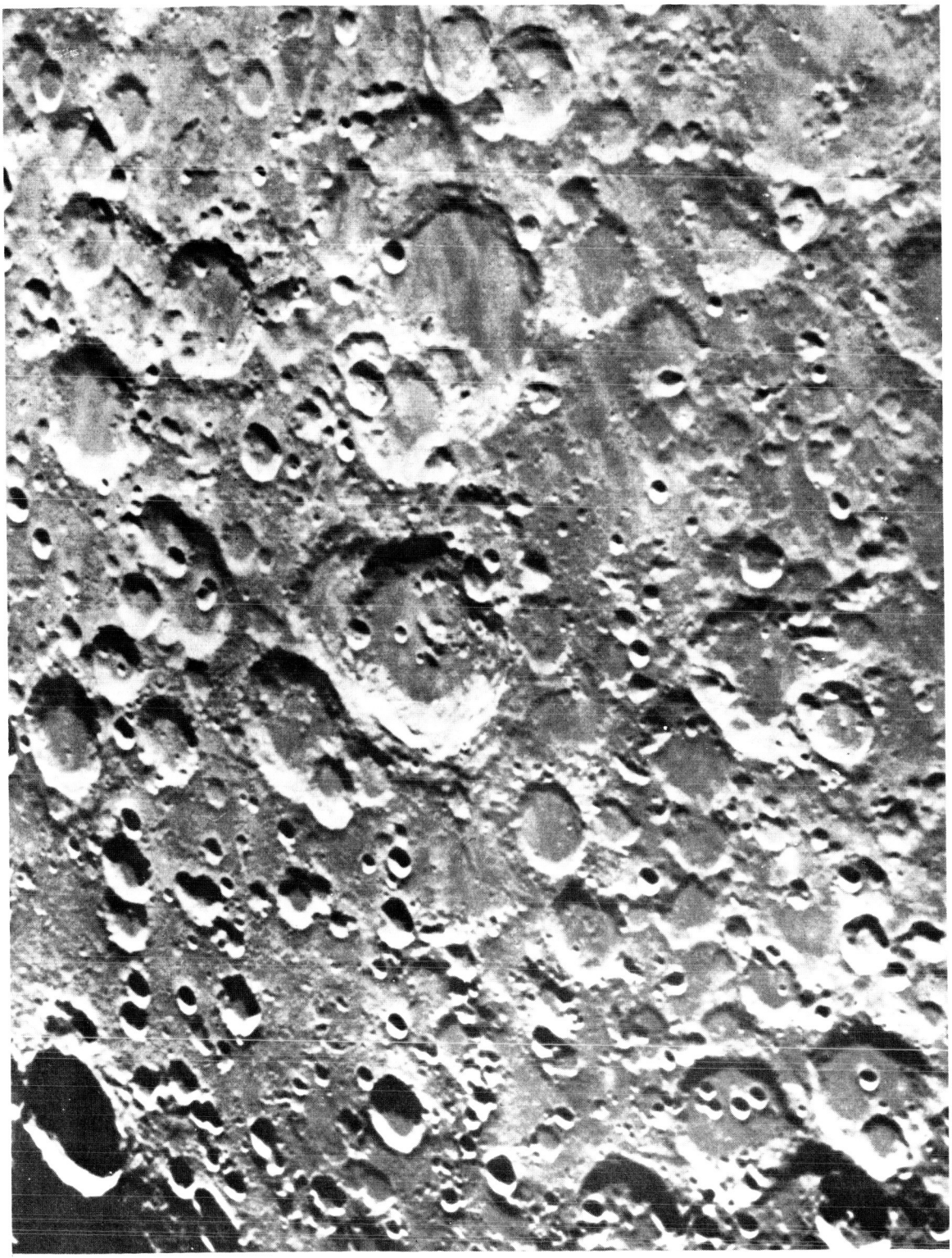

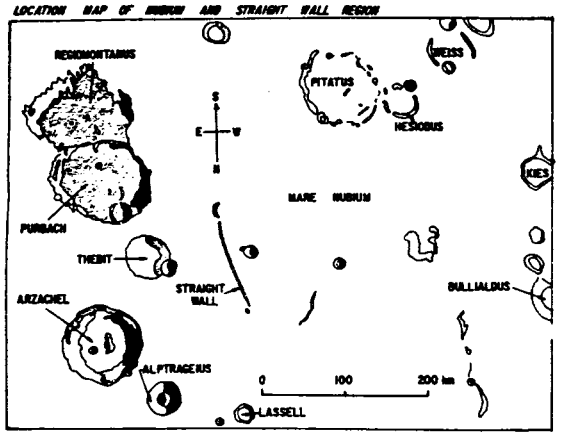

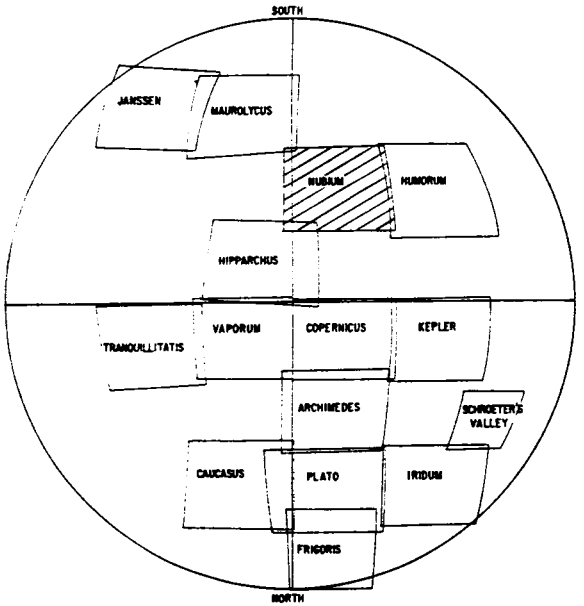

INDEX MAP TO LUNAR PHOTOS

FIGURE 24. MARE NUBIUM AND STRAIGHT WALL REGION

(Courtesy of University of Chicago Press)

Lava appears to have invaded the lunar highlands to the south and east of Mare Nubium. The craters, Pitatus and Kies, are partially flooded. Regiomontanus and Purbach are large, flat-bottomed, walled plains, whereas Arzachel has a well-defined rim, terrace deposits, and central mountains. There is a conical, volcano-like structure located in the north part of Regiomontanus.

The Straight Wall is the outstanding example of normal fault on the moon's surface. It is 125 km long and has a vertical displacement of several hundred meters. The fault plane dips at approximately 41° to the west. There is an interesting crater consisting of an outer rim concentrically bounding a smaller inner rim near the SW flank of the crater Hesiodus.

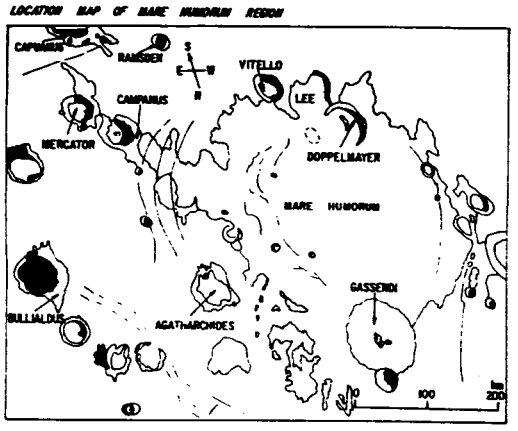

FIGURE 25. MARE HUMORUM REGION

(Courtesy University of Chicago Press)

Mare Humorum is a circular Mare. It is believed that the floor of the Mare is covered by a pock-marked lava surface which extends into the adjacent borderlands on the south, west, and north sides. The craters, Doppelmayer and Gassendi, have been partially flooded by lava and are known as "ghost" craters. There are numerous wrinkle ridges on the Mare surface. Some linear ridges extending NW from the crater Bullialdus suggest possible downslope movement of material. The radial markings around the south side of Bullialdus are indicative of a ray pattern. A set of three arcuate faults marks the eastern margin of the Mare.

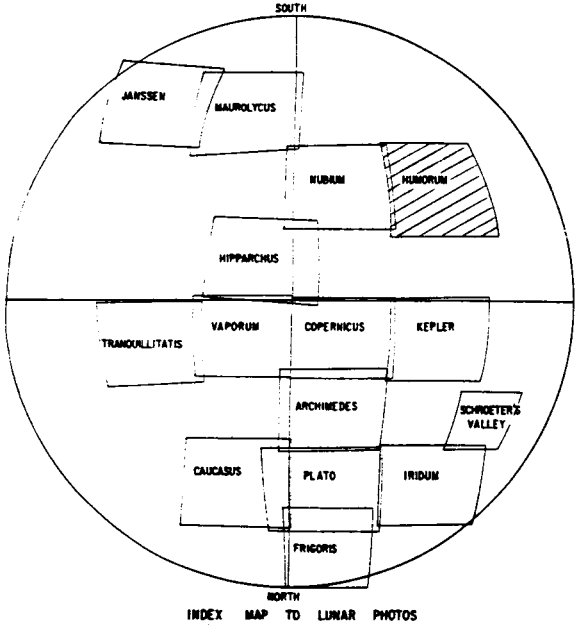

INDEX MAP TO LUNAR PHOTOS

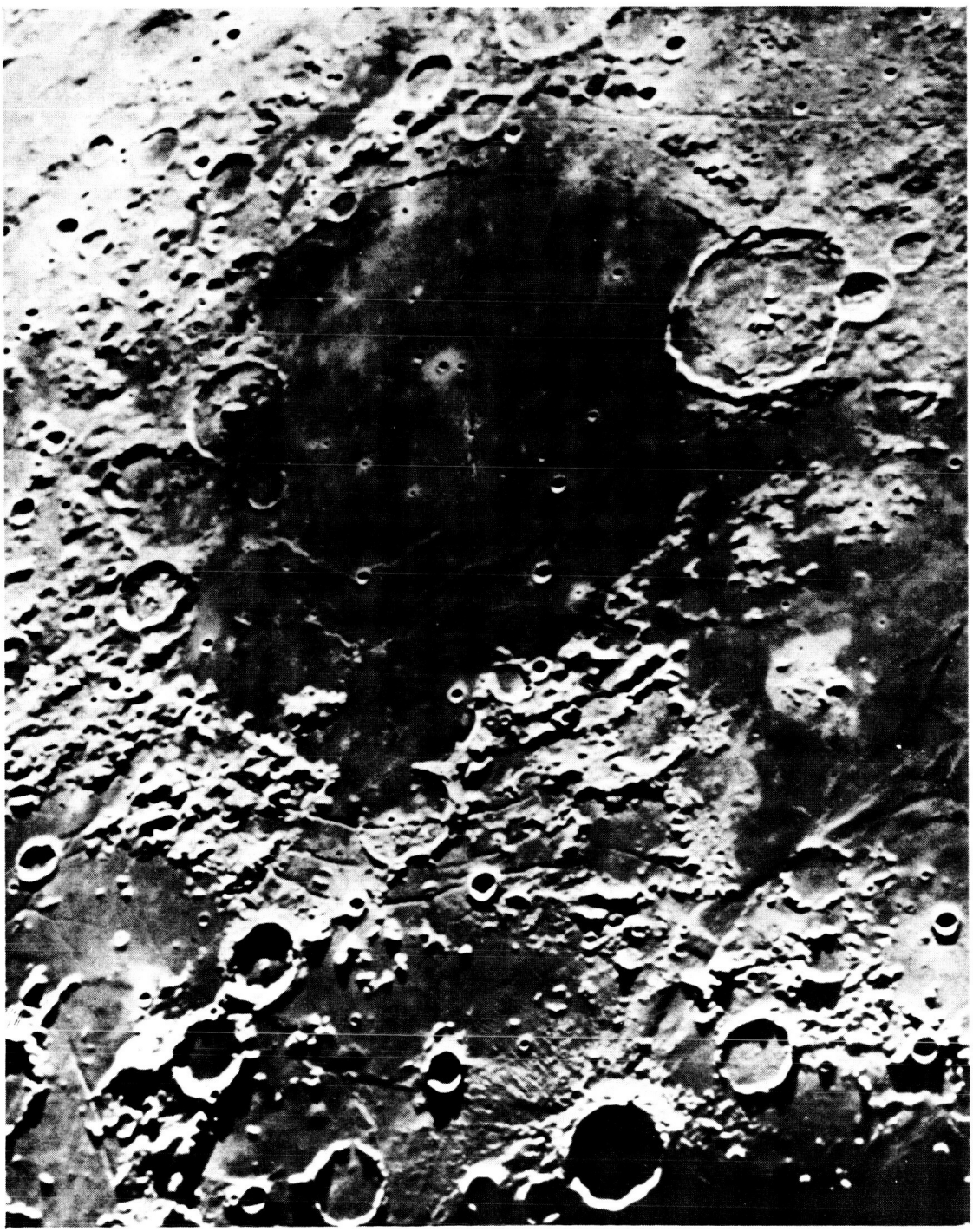

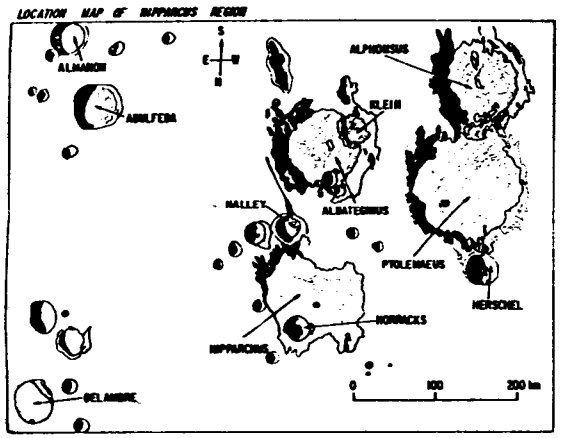

FIGURE 26. HIPPARCHUS REGION

(Courtesy University of Chicago Press)

The major craters on this photograph, Hipparchus, Albategnius, Ptolemaeus, and Alphonsus, all appear to have been flooded by lava and have relatively flat floors. Northeast of Ptolemaeus and Alphonsus, there is a strong structural alignment with a NW/SE orientation. This structural alignment was identified as the "Imbrium Sculpture" of Gilbert [26]. Shoemaker [18] suggests that the alignment was produced by shock waves originating from the impact-created explosion which formed Mare Imbrium.

The crater Alphonsus is the one from which Kozyrev observed gaseous emissions [3].

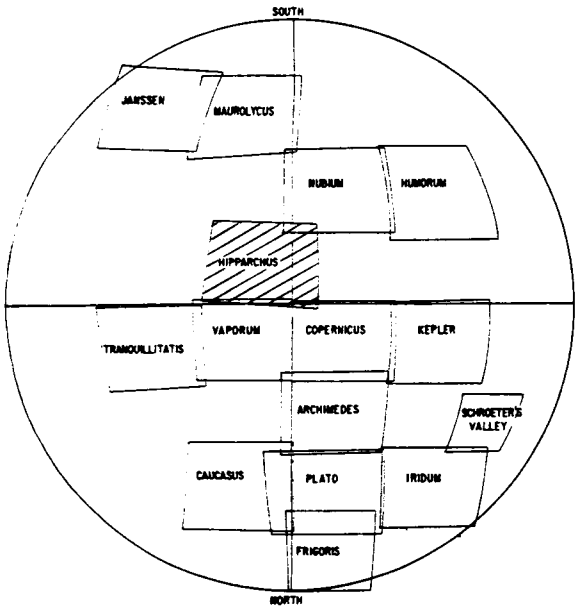

INDEX MAP TO LUNAR PHOTOS

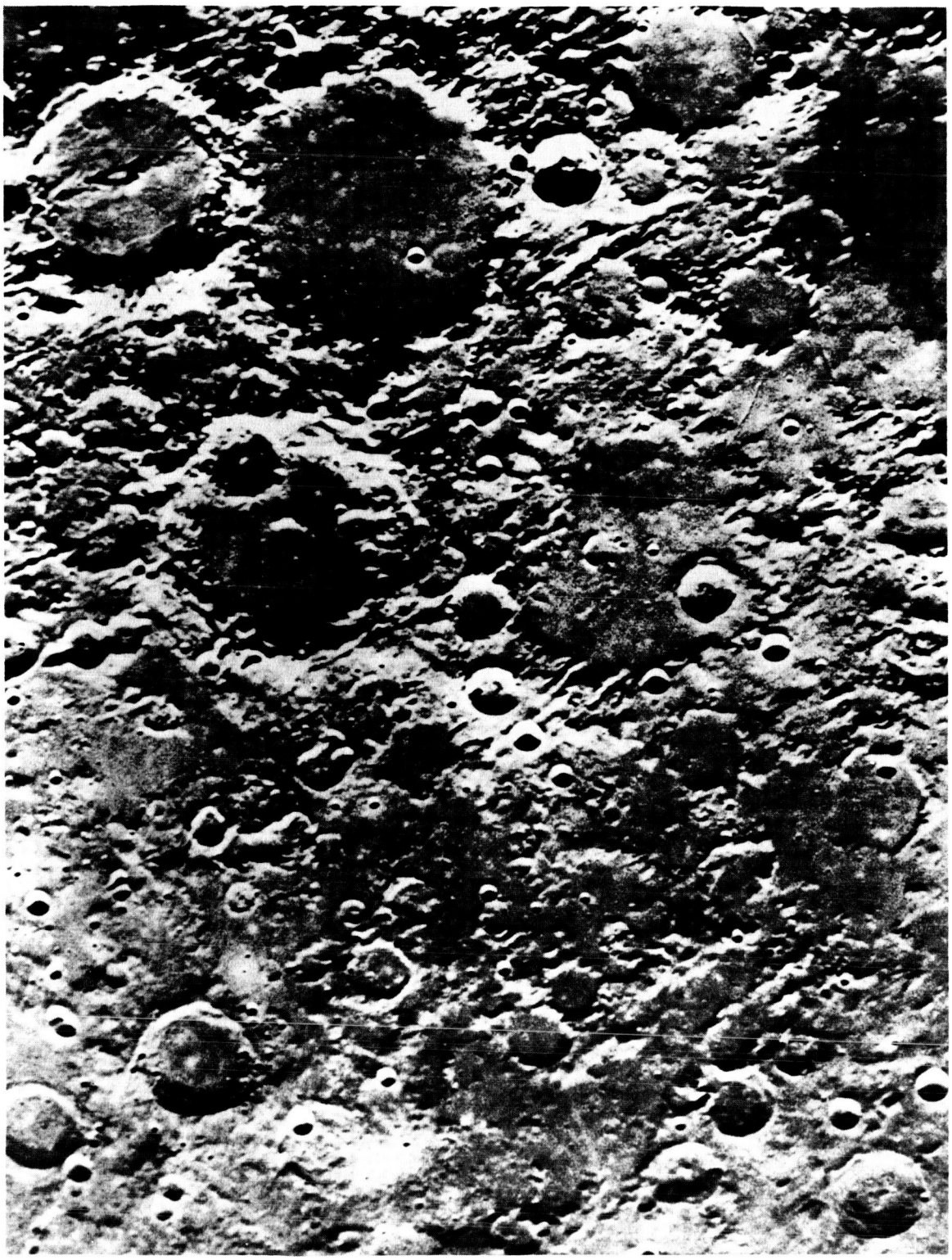

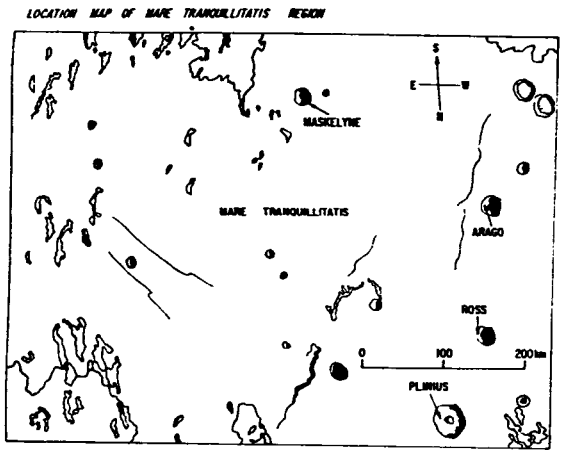

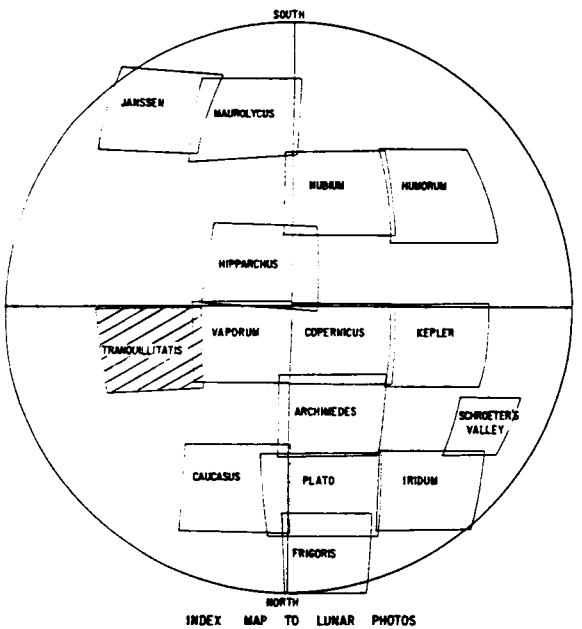

INDEX MAP TO LUNAR PHOTOS

FIGURE 27. MARE TRANQUILLLITATIS REGION

(Courtesy University of Chicago Press)

This photograph shows the easternhalf of one of the larger Maria. Like all the Maria, this one is believed to be filled with lava and exhibits a pock-marked surface. The area has some good examples of both pre-Mare and post-Mare craters. The post-Mare are those such as Plinus, Arago, and Maskelyne which have not been filled with lava. The pre-Mare craters are the "ghost" craters or those with crescent-shaped rims in the SW part of the region. The presence of pre-Mare craters suggests that the Mare lavas were relatively shallow in the eastern half of this region.

The two SE trending linear features in the east half of the region are interpreted as rilles which may be related to subsurface structures.

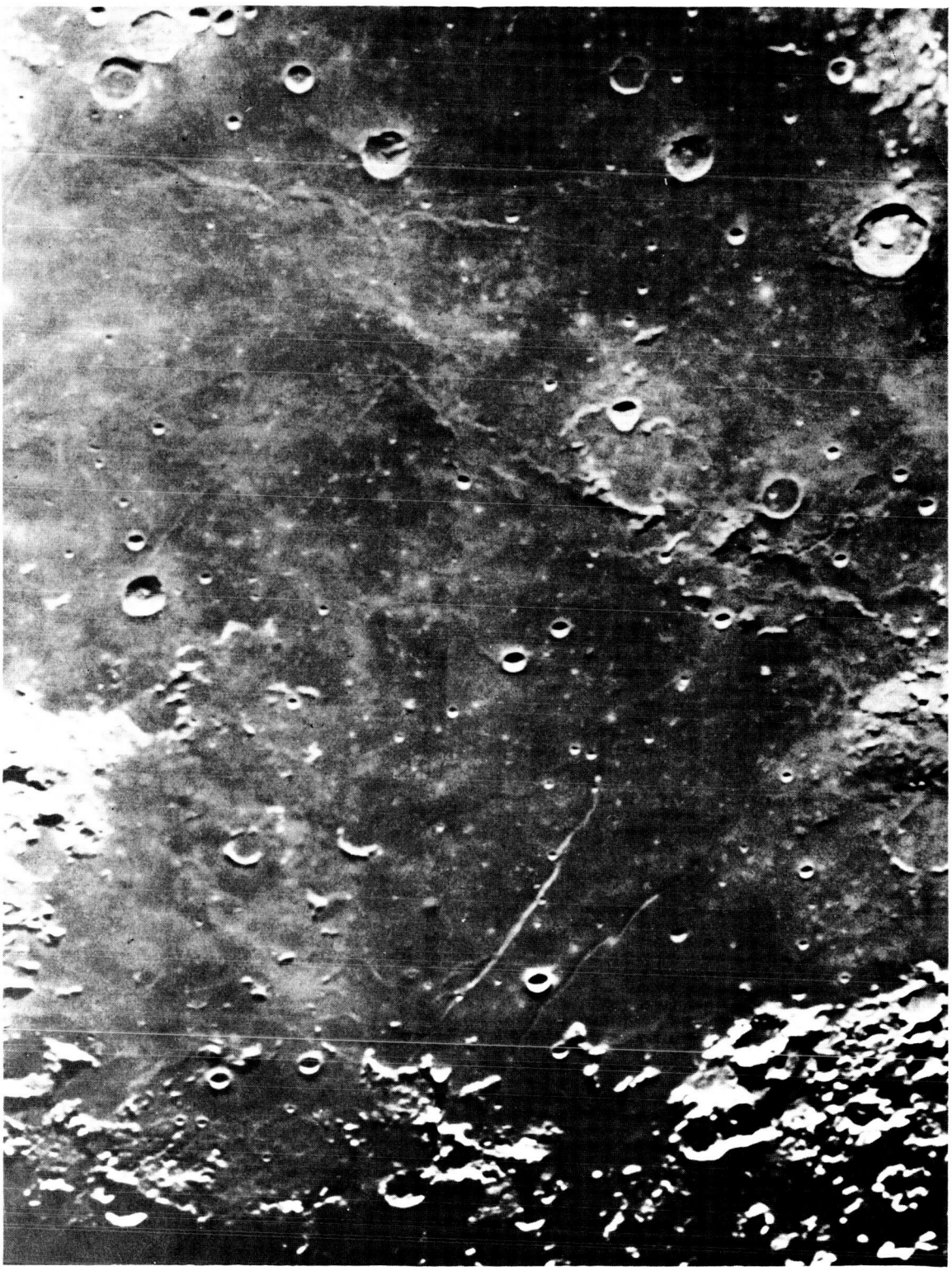

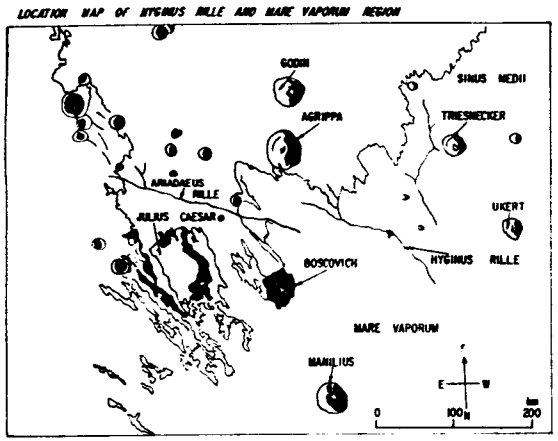

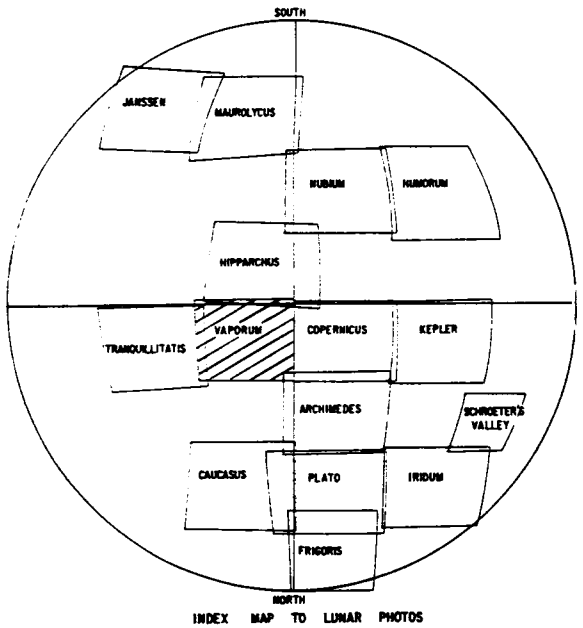

INDEX MAP TO LUNAR PHOTOS

FIGURE 28. HYGINUS RILLE AND MARE VAPORUM REGION

(Courtesy University of Chicago Press)

This photograph shows both the Hyginus Rille and the Ariadaeus Rille. These rilles have as their closest earth analogues the graben structure. The strong SE alignment exhibited by the rocks in the rugged highland area around Julius Caesar is the "Imbrium Sculpture" identified by Gilbert. Northeast of the crater Triesnecker, there is a polygonal fracture pattern which is situated on the lava flows of Mare Vaporum.

The rim materials of Julius Caesar and Boscovich are affected by the lineations of the "Imbrium Sculpture," but the craters Agrippa and Godin are post-Imbrian.

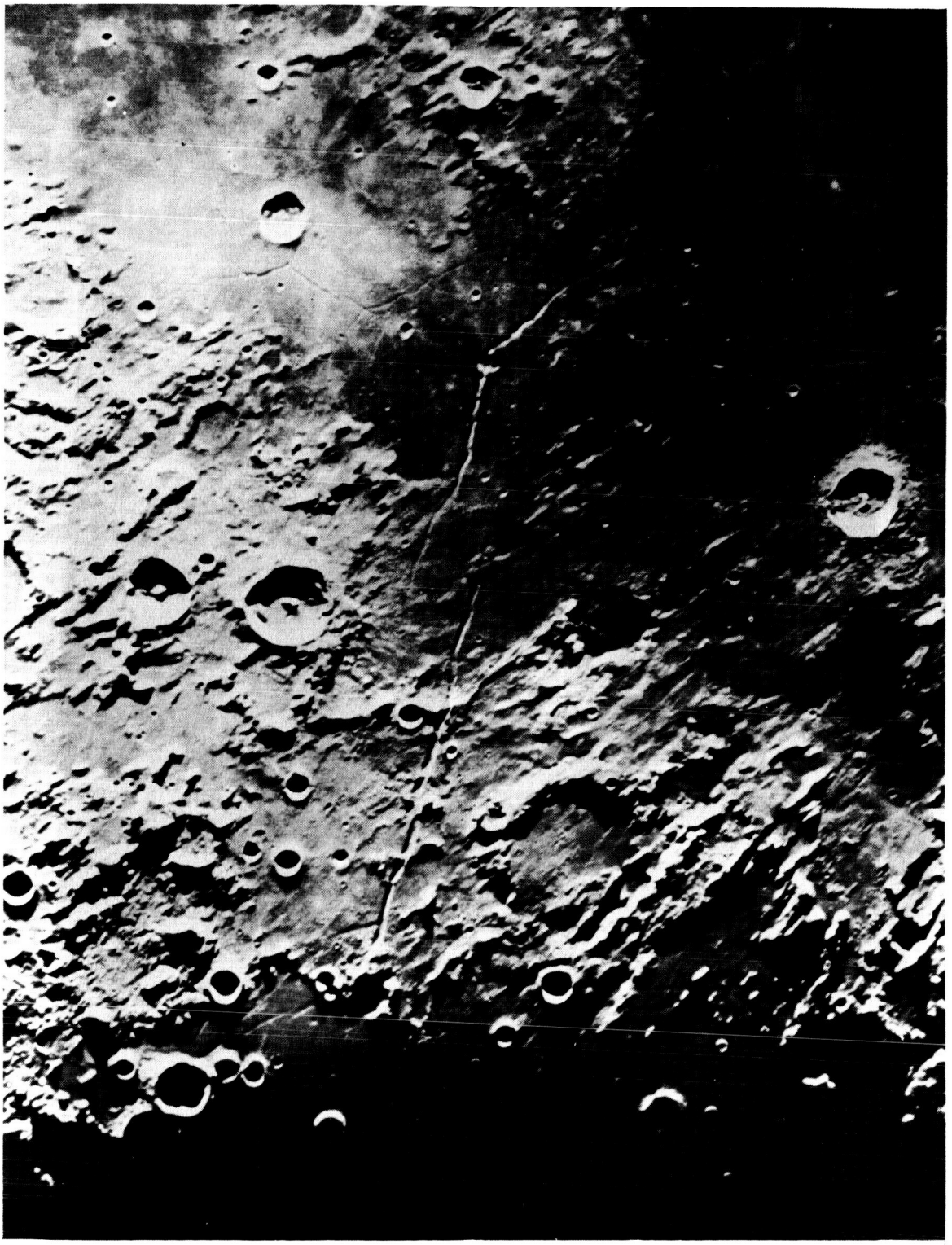

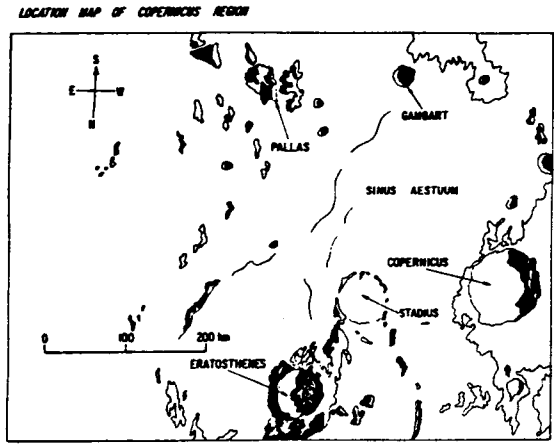

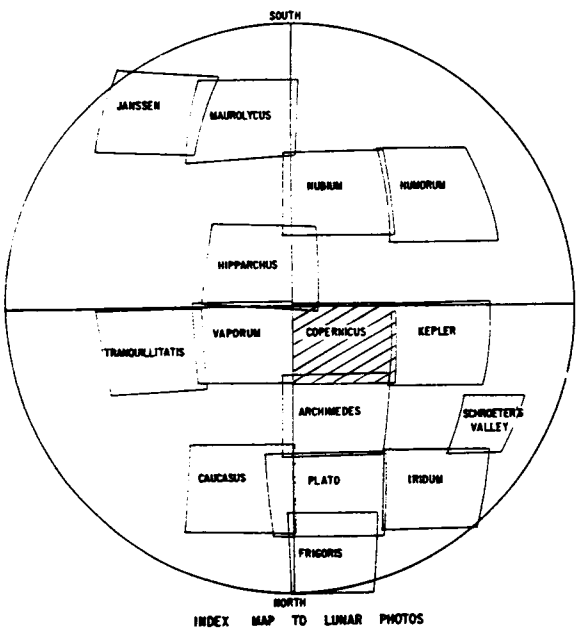

INDEX MAP TO LUNAR PHOTOS

FIGURE 29. COPERNICUS REGION

(Courtesy University of Chicago Press)

The large ray crater, Copernicus, is an impact crater [18] which has been designated the type section for the Copernican System. Similarly, Eratosthenses is the type section for the Eratosthenian System. Dark Procellarian lavas with wrinkle ridges form the floor in this region. Stadius is a partially buried crater of pre-Imbrian age. The rilles and chain craters around Stadius are probably Procellarian or Eratosthenian in age.

Copernicus has well-defined scarps and massive slump blocks within the inner rim, and the crater itself is dominantly polygonal in shape. The crater floor is composed of breccia.

A belt of large secondary impact craters centers about half way between Copernicus and Eratosthenes and is approximately 110 kilometers wide. The belt lying adjacent to the crater rim extending out 50 kilometers to the belt of secondary craters is inferred to be composed of a deposit of ejecta blanket material which contains fewer large secondary craters than the zone of secondary concentration. However, this latter area is probably covered by thousands of smaller craters below the limit of optical resolution.

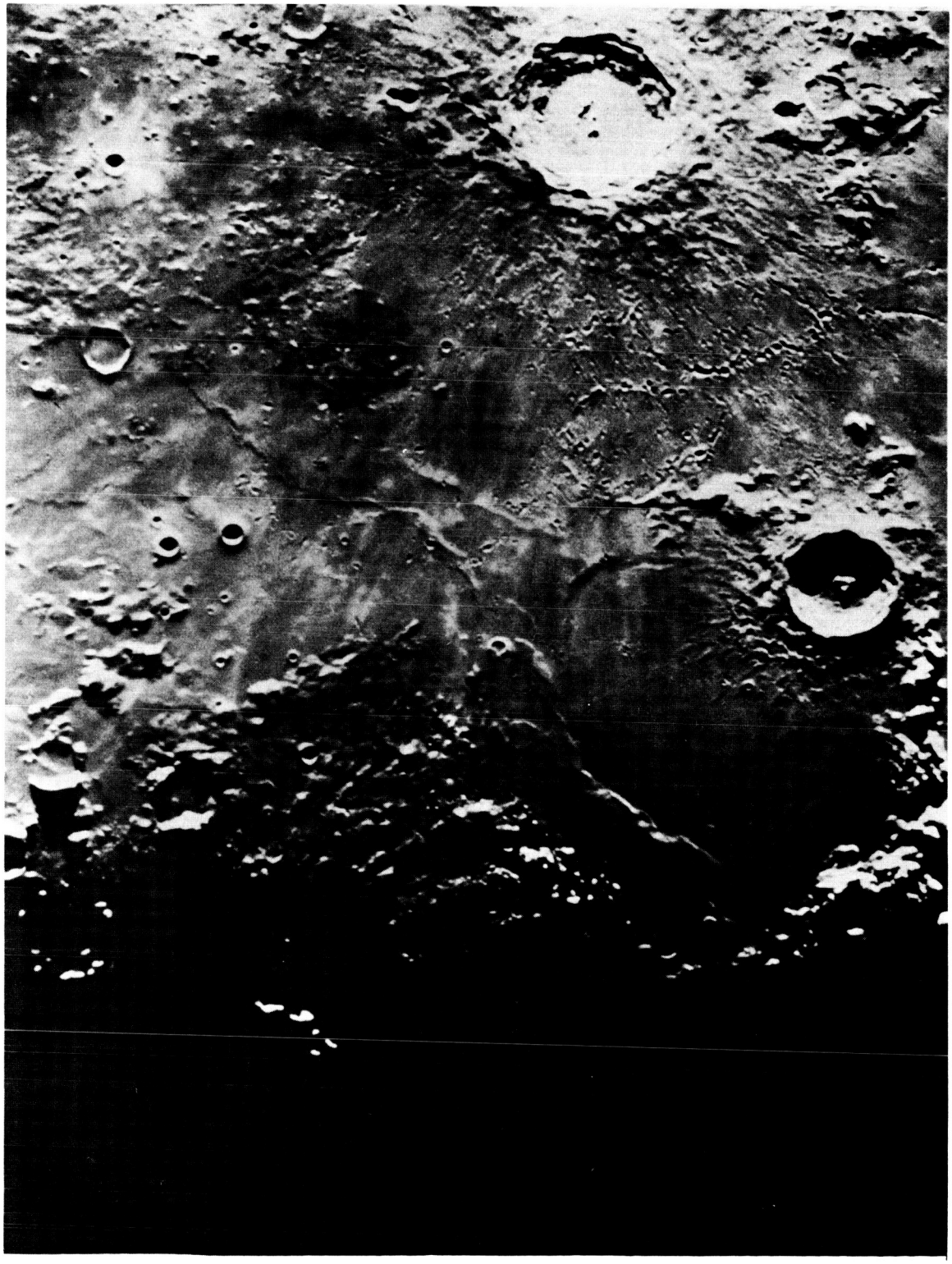

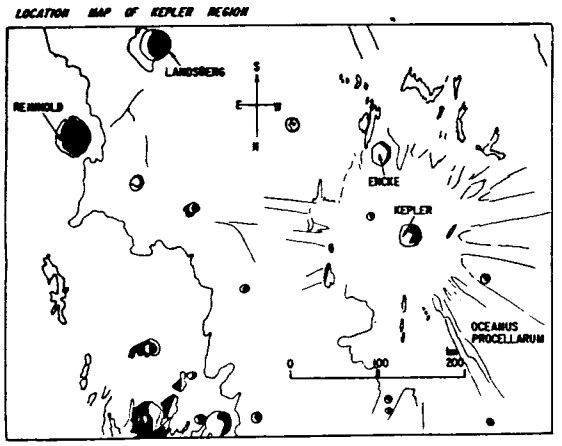

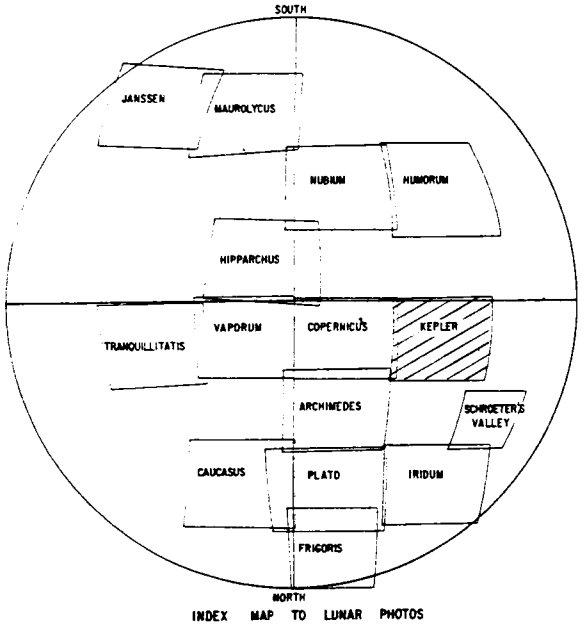

INDEX MAP TO LUNAR PHOTOS

FIGURE 30. KEPLER REGION

(Courtesy University of Chicago Press)

The outstanding ray system of Kepler indicates that this is a crater of Copernican age. It has been interpreted by most students of lunar geology as of impact origin. Lunar domes which may be due to the upwelling of magmas underlying the Oceanus Procellarum are situated in the central part of the photograph. Other significant features in this region include the north-south oriented mountain structures surrounding Kepler in the NE part of the photograph. This structure is supposedly of combined impact-tectonic origin and is the "Imbrium Sculpture" of Gilbert [26]. A comparison of this photograph with the geologic map of the Kepler region (Figure 5) shows that the rocks of several ages are included on the photograph. The crater Encke has a roughly polygonal shape which may indicate a pre-existing joint pattern.

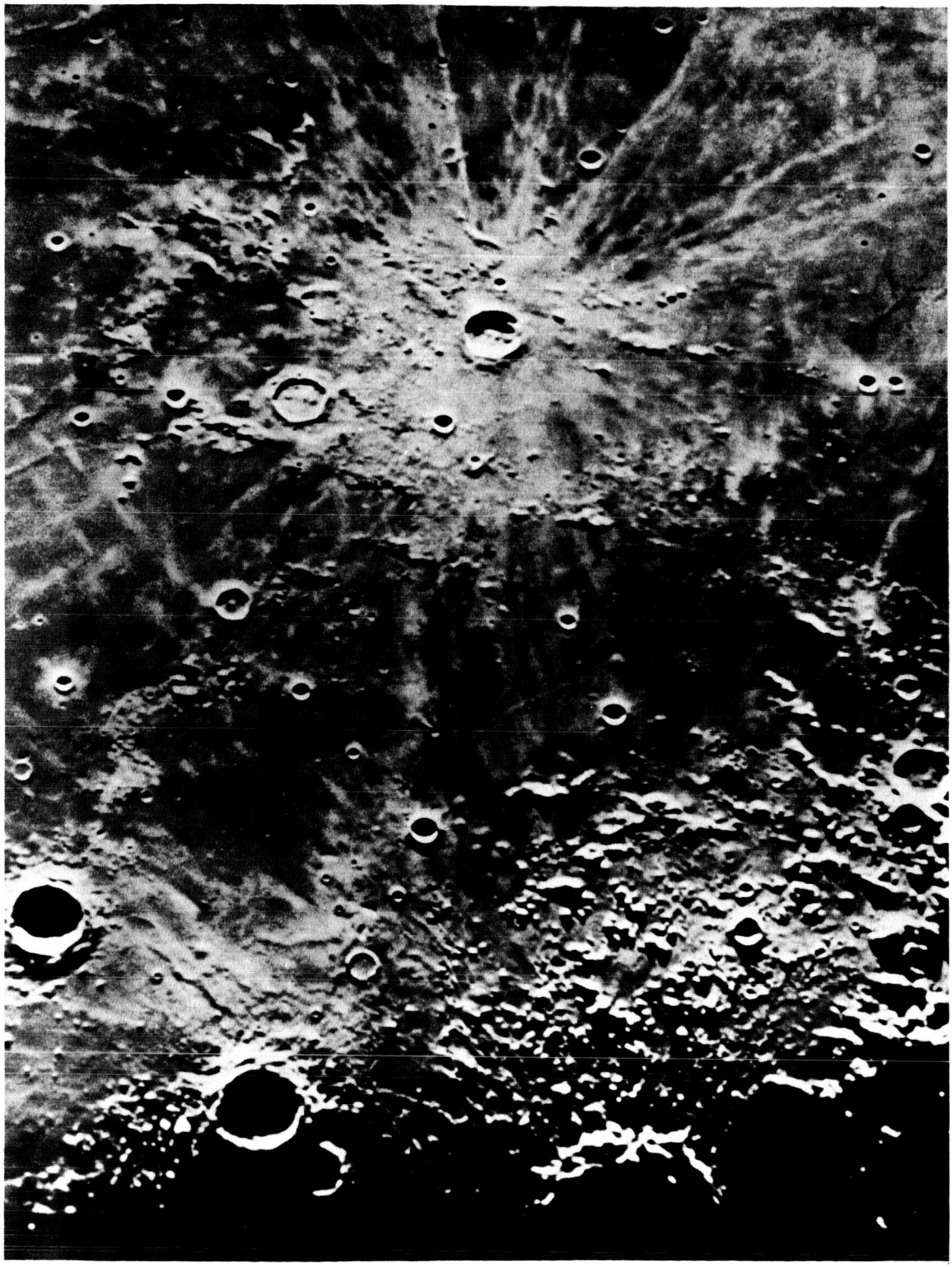

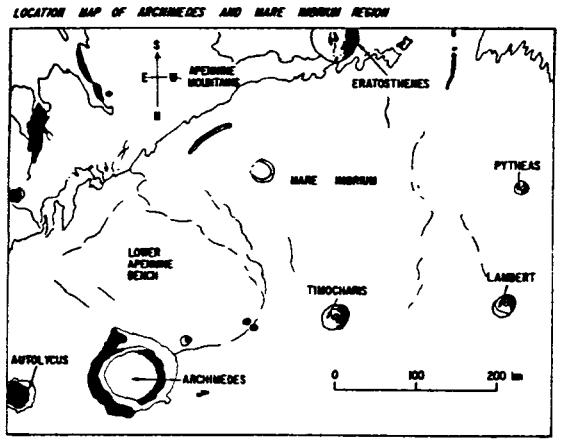

FIGURE 31. ARCHIMEDES REGION

(Courtesy University of Chicago Press)

The southwestern part of the photo shows the Imbrium Sculpture [26]. The boundary between Mare Imbrium and this region is very abrupt, suggesting that great vertical movement has occurred. The Apennine Mountains extend 4000 to 5000 meters above the plain of Mare Imbrium. Directly in front of and parallel to this large NE-SW trending escarpment is a low ridge of hills. This ridge appears to be composed of a linear trend of conical-shaped structures indicative of a fissure eruption and a resultant chain of volcanoes. In the SW part of the photo is a chain of craters. This chain is broken at its southern end, but it continues on again where it goes off the photo. Rilles may be observed in the area to the south and west of the crater Archimedes. Several good examples of wrinkle ridges can be observed in the Mare itself.

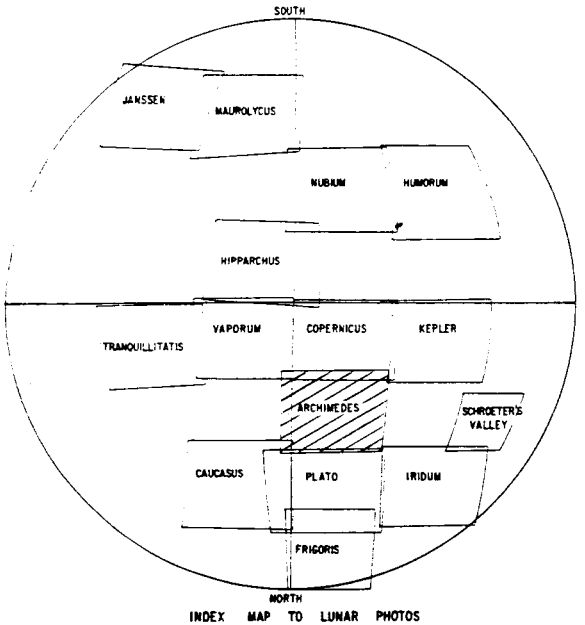

INDEX MAP TO LUNAR PHOTOS

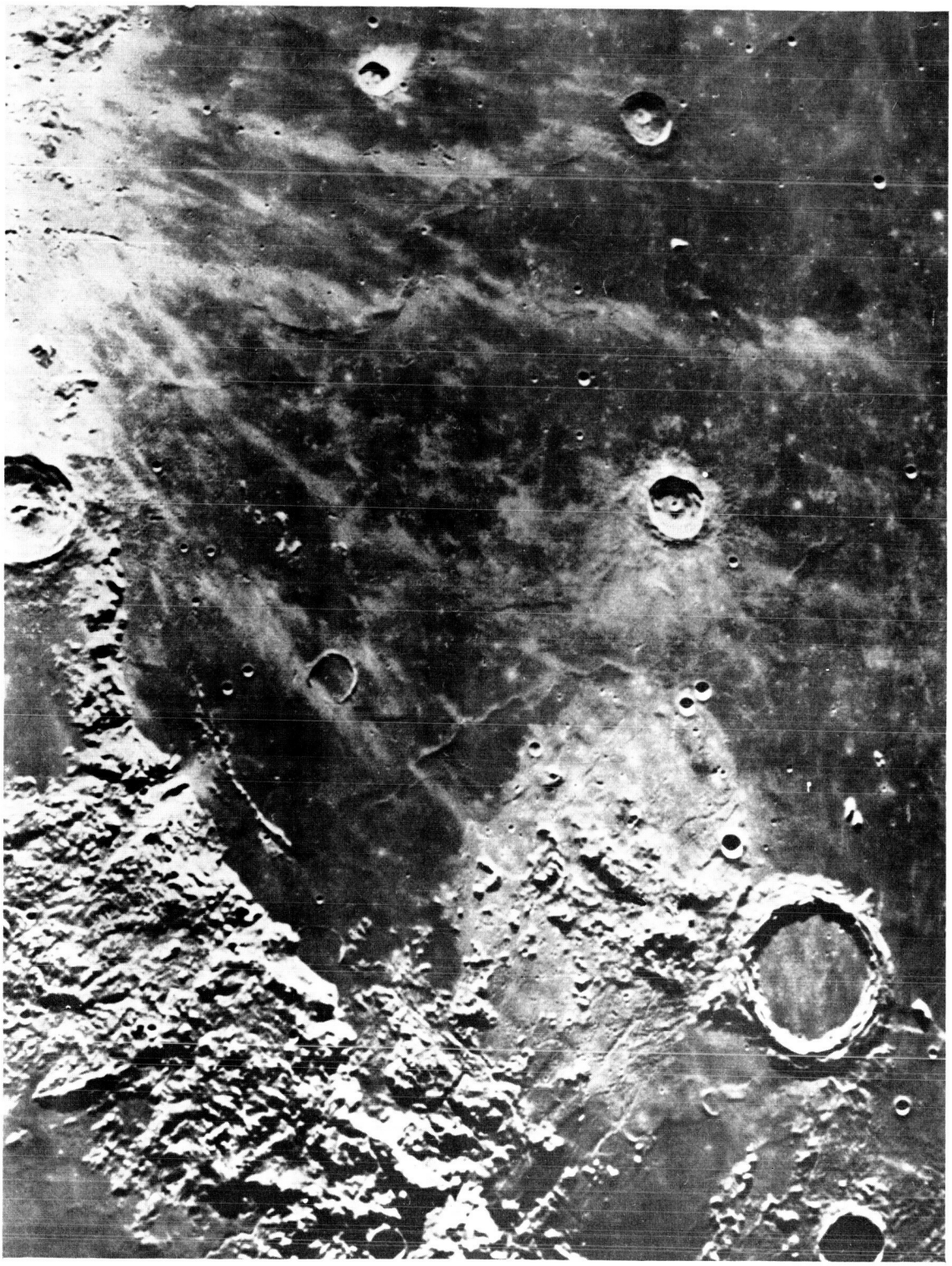

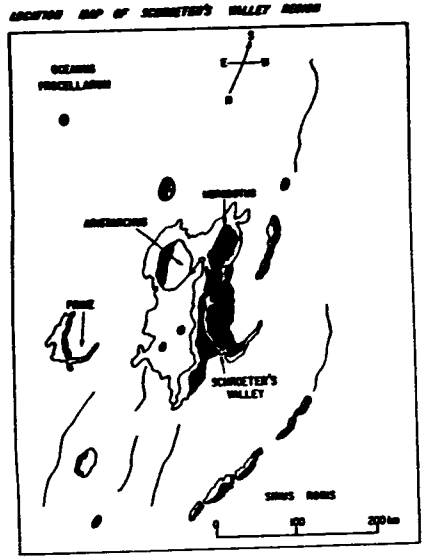

FIGURE 32. SCHRÖETER'S VALLEY REGION

(Courtesy University of Chicago Press)

This photograph shows Schröeter's Valley near the terminator. The large crater at the head of the valley, Herodotus, has been descriptively called the "Cobra's head." Aristarchus is the large crater directly to the east of Herodotus from which visible red glows have been observed. These craters and Schröeter's Valley are all situated on the dark lavas of the Oceanus Procellarum.

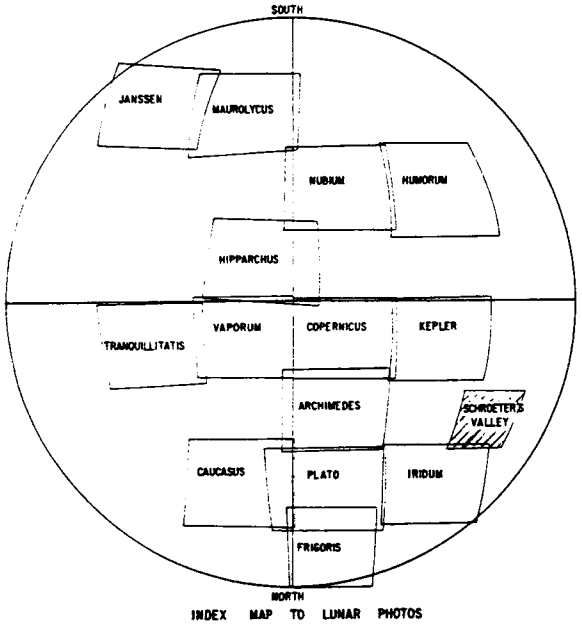

INDEX MAP TO LUNAR PHOTOS

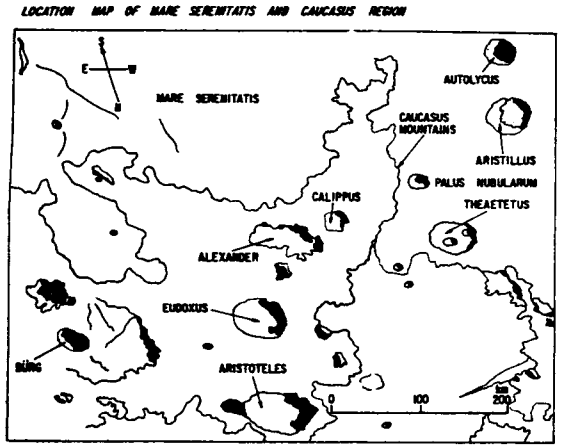

FIGURE 33. MARE SERENITATIS AND CAUCASUS REGION

(Courtesy University of Chicago Press)

The Caucasus Mountains form a peninsula which extends southward between Mare Serenitatis and Mare Imbrium. Both of these Maria are circular. There are several important craters in this photograph including Autolycus and Aristillus which are situated on Mare Imbrium, and Eudoxus and Aristoteles which are in the area of the Caucasus Mountains. The crater, Burg, is situated within Lacus Mortis. Theatetus is a ghost crater which contains two smaller craters.

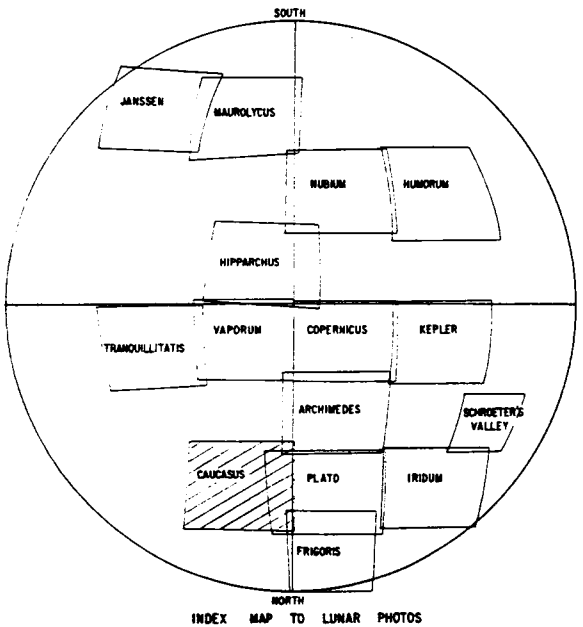

INDEX MAP TO LUNAR PHOTOS

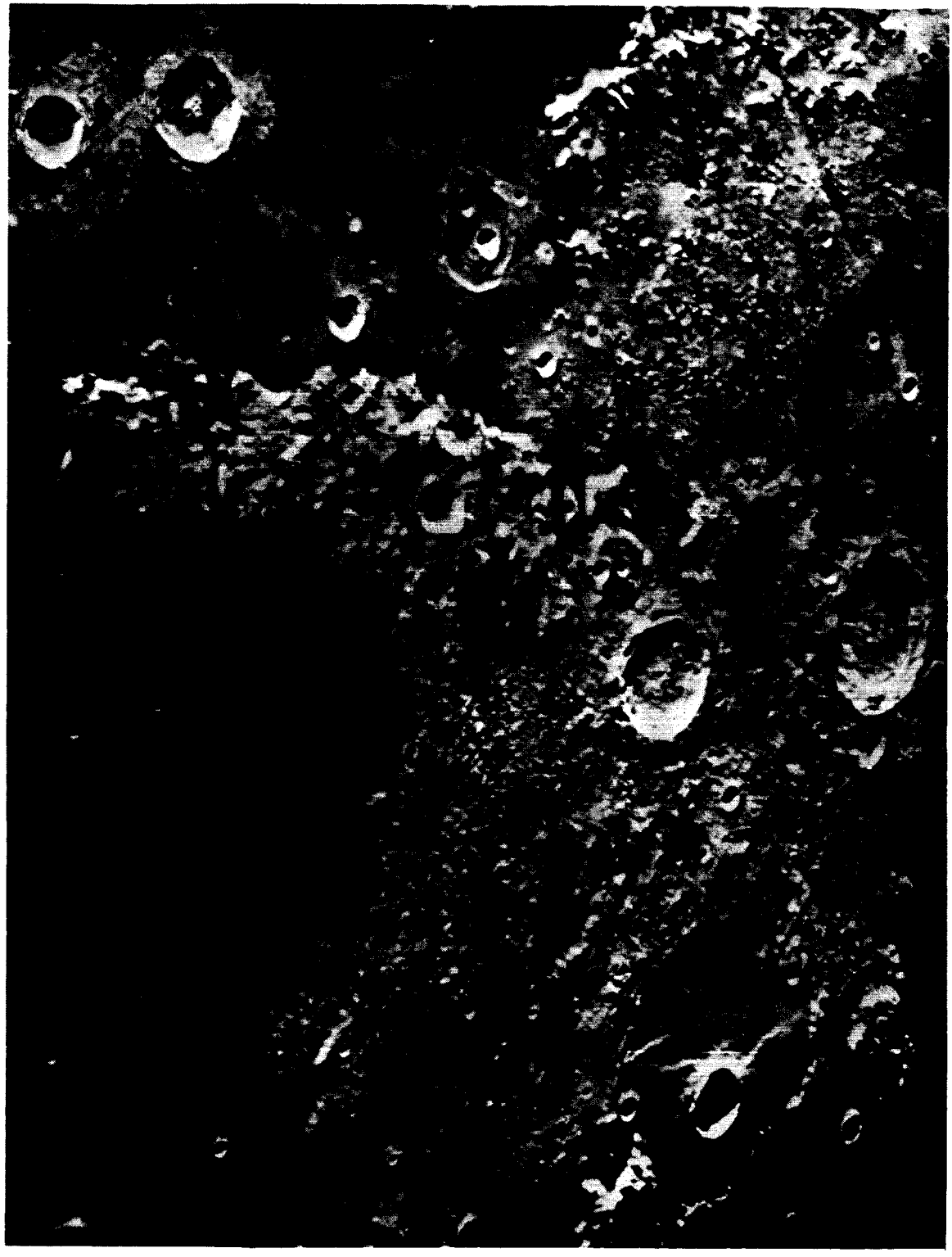

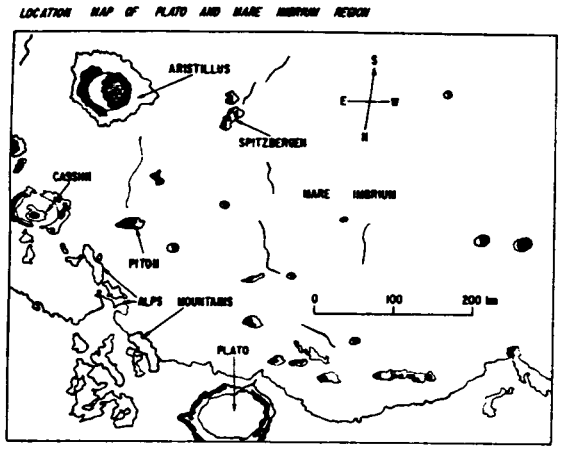

FIGURE 34. PLATO AND MARE IMBRIUM REGION

(Courtesy University of Chicago Press)

This region is located at the north end of Mare Imbrium. It has a number of mountains within the Mare itself, notably Spitzbergen and Piton. These mountains mark the inner limit of the Imbrium explosion according to Urey [17]. Extensive flooding by Imbrium lavas has covered the floor of a much larger area than the Imbrium explosion "crater" and the mountains are now isolated as islands in a sea of congealed lava. Plato is filled with lava indicating that it is pre-Imbrian in age. There is a large triangular shaped slump block at the east side of Plato which indicates that the material making up the rim of Plato is fairly cohesive. Aristillus is post-Imbrian, and its rays extend across the floor of Mare Imbrium.

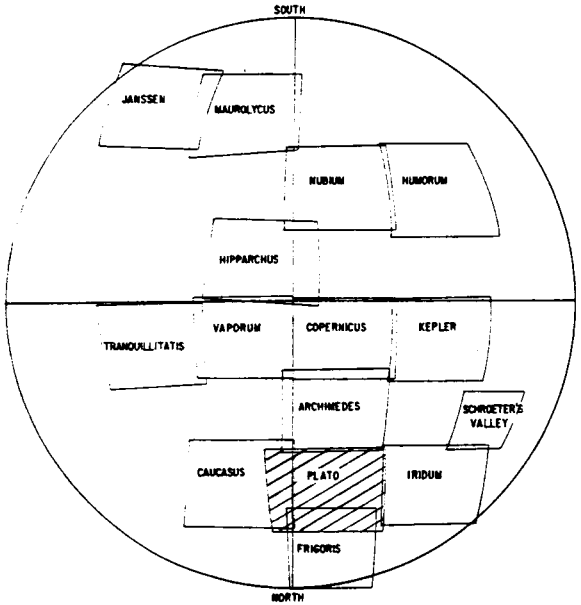

INDEX MAP TO LUNAR PHOTOS

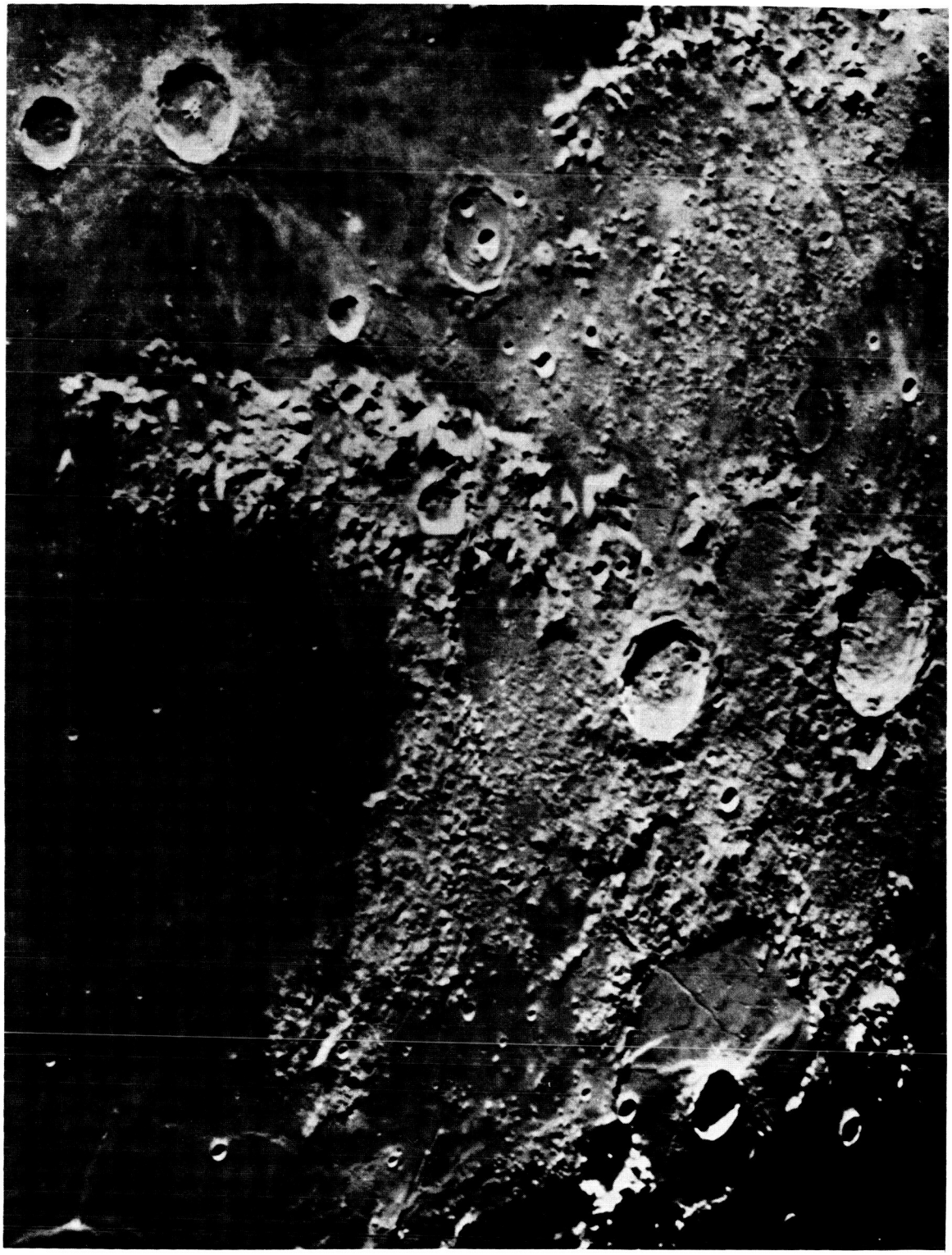

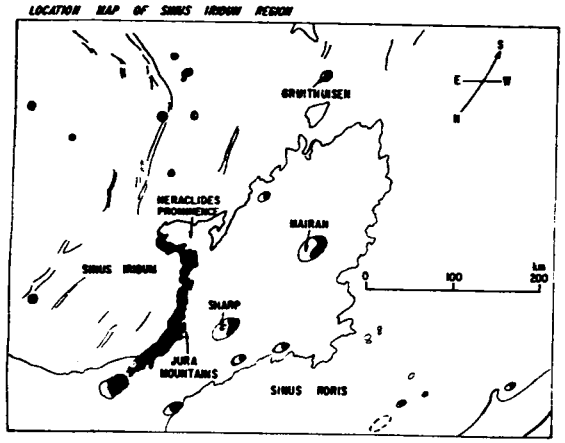

FIGURE 35. SINUS IRIDUM REGION

(Courtesy University of Chicago Press)

The large escarpment of Sinus Iridum is one of the most prominent features on the lunar surface. It indicates that a large vertical displacement has occurred and its nearly semi-circular shape has led some writers [17] to suggest that this escarpment is the outline of an asteroidal-sized meteorite responsible for the creation of Mare Imbrium and the bounding Imbrium Sculpture. Notable features on this photo also include wrinkle ridges, flooding of embayments in adjacent highland areas, and pock-marked highlands such as the Jura Mountains.

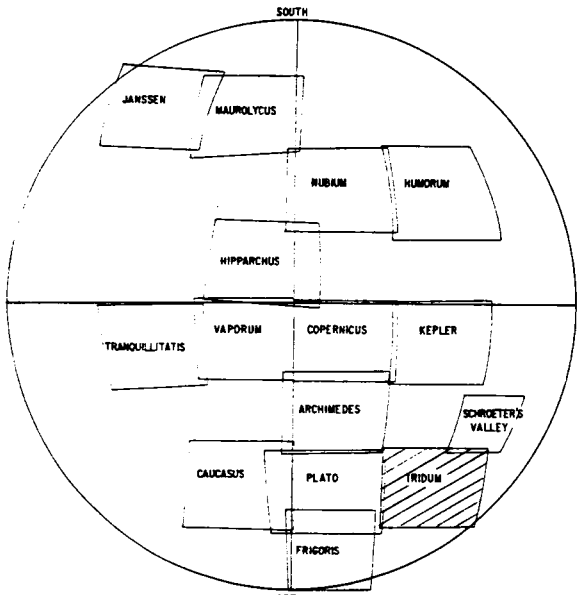

INDEX MAP TO LUNAR PHOTOS

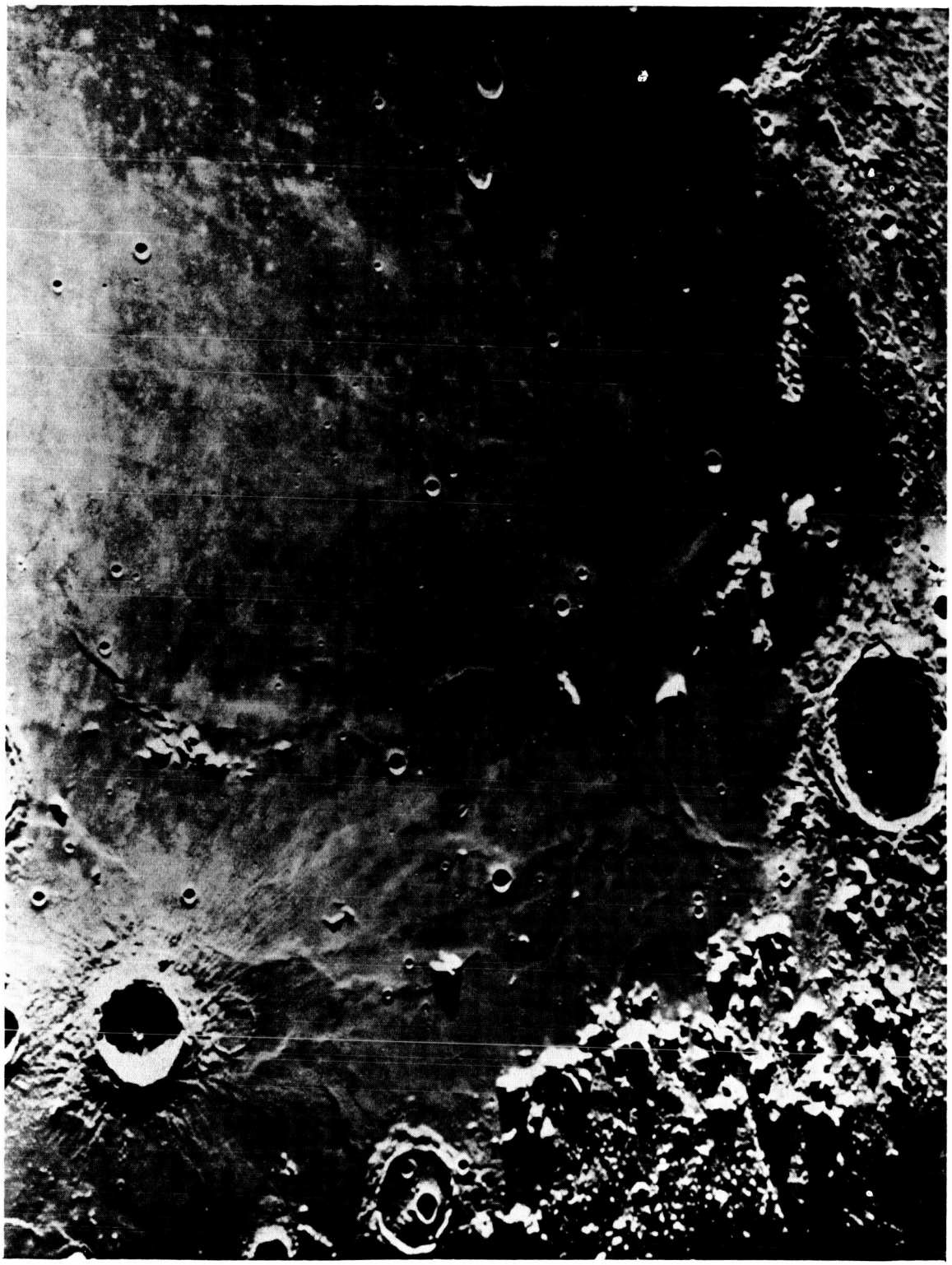

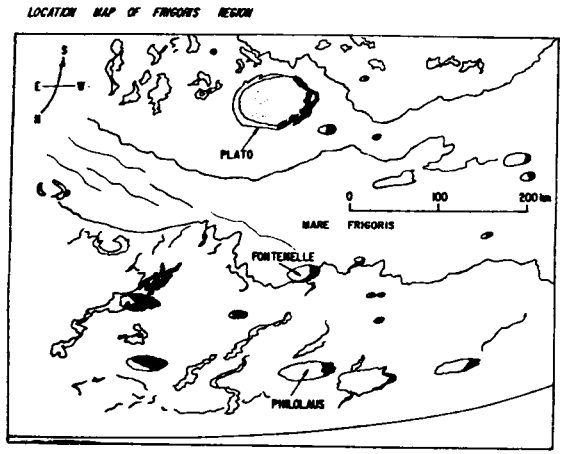

FIGURE 36. MARE FRIGORIS REGION

(Courtesy University of Chicago Press)

This region forms the extreme north part of the moon. Mare Frigoris is an east-west trending, elongated Mare. It exhibits some good examples of wrinkle ridges on the east part of the photograph. The area to the north is an ancient pock-marked surface of craters on lunar highlands. The Mare seems to merge imperceptibly into the adjacent highlands on the north and south.

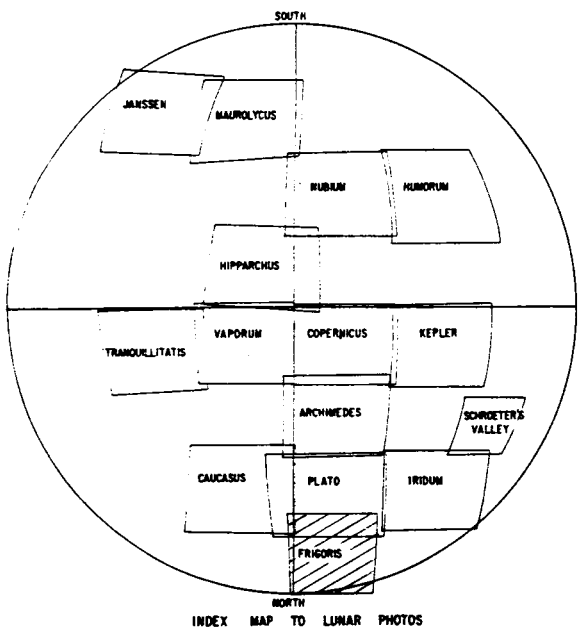

INDEX MAP TO LUNAR PHOTOS

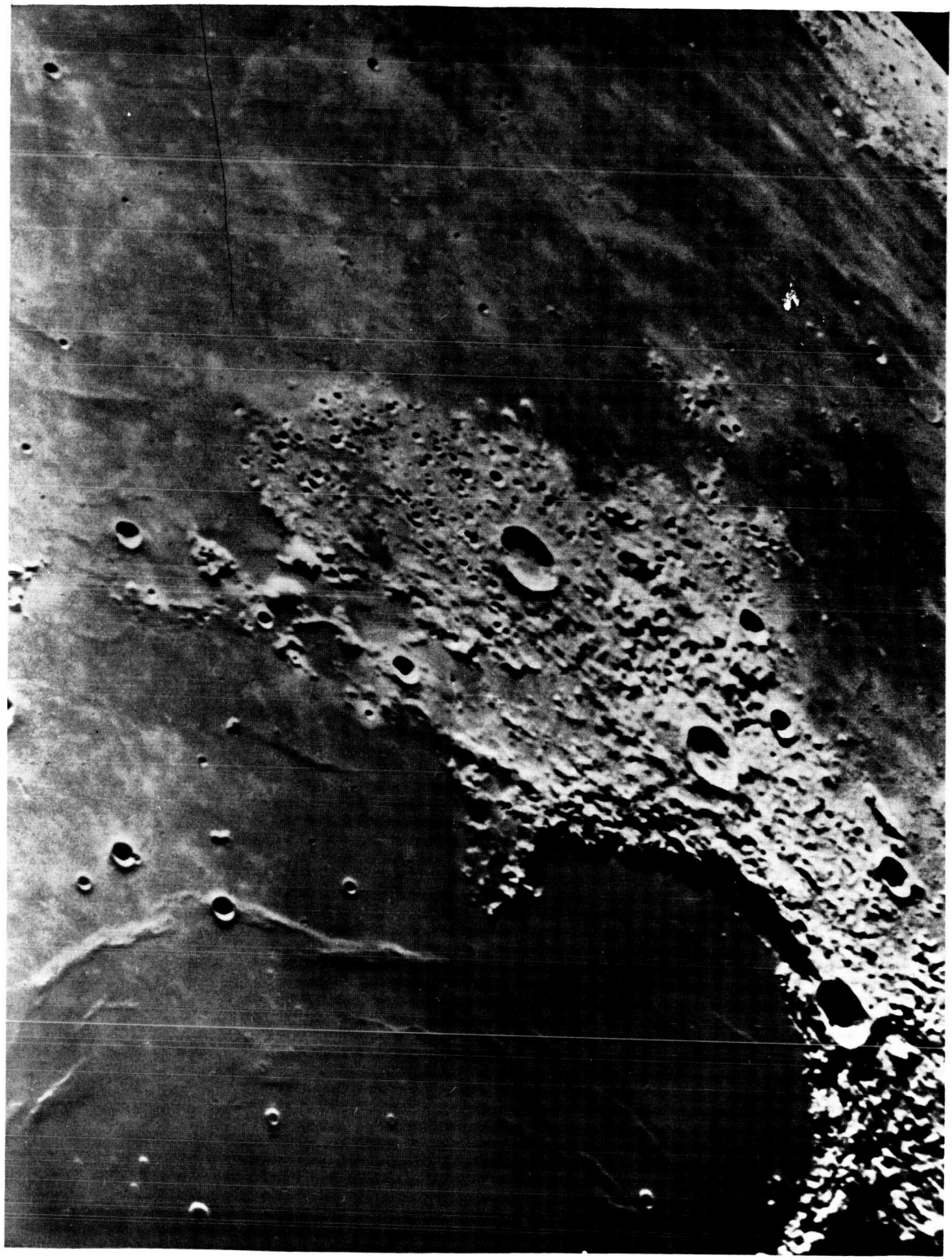

VIII. RANGER VII'S LUNAR PHOTOGRAPHIC MISSION

The successful photographic mission of Ranger VII on July 31, 1964, provided 4,316 photographs of the lunar surface. Several of these photographs are included in Figures 39 through 45 and a location map of the fields of view of these photographs is included in Figure 38. At the time of this writing, the Astrogeology Branch of the U. S. Geological Survey, Flagstaff, Arizona, is making detailed analyses of these photographs and will make the official interpretation for future vehicle design. The results published in this report are tentative and are based on press releases made by Drs. Eugene Shoemaker of the Astrogeology Branch, and Gerard Kuiper of the Lunar and Planetary Laboratory of the University of Arizona [36, 37].

Tentative results of the Ranger VII photographs indicate that the small-scale roughness of the lunar surface does not constitute a serious problem for a mobile vehicle. Probably the Maria will contain crater pits ranging down to 0.5 m in diameter, but craters will cover only between 1 to 10 percent of the Maria surface.

There are two types of craters on the Maria, primary and secondary.

A. Primary Craters

In the Ranger VII impact area, the primary craters were the least frequent type. It is believed that primary impact craters were formed by high-velocity projectiles which were traveling at velocities in excess of 2.4 km/sec. which is the escape velocity of the moon. It is probable that most of the primary craters were formed from extralunar objects which impacted the moon's surface.

Primary craters are distinguished from secondary craters by their steeper slopes and larger depth/diameter ratio.

B. Secondary Craters

These craters are much more numerous in the Ranger VII impact area and are believed to be caused by secondary ejecta which bombarded the lunar surface and which was derived from the large primary crater Copernicus (Figure 29). The ejecta which formed these secondary craters was traveling at speeds less than 2.4 km/sec. Kuiper [37] indicates that typically this ejecta was traveling at 0.8 km/sec.

Secondary craters have a soft, rounded appearance, low slopes, and a smaller depth/diameter ratio than primary craters.

C. Implications of Surface Hardness

The Ranger VII photographic mission was not designed to provide quantitative data on the surface hardness or bearing strengths of the lunar surface. Any attempts to infer the hardness of the lunar surface from these photographs is an interpretation and should not be considered definitive at this time. Present interpretations on surface hardness based on the Ranger VII photographs range from one which states that the moon's surface might have a few centimeters of loose, unconsolidated dust overlaying a solid substrate to one at the other extreme which states that the moon's surface is covered by unknown thicknesses of unconsolidated dust of low bearing strength. The argument for a reasonably hard surface is based on these observations: (1) the surface layer is capable of preserving both primary and secondary craters; (2) primary craters have high slopes; and (3) a rock fragment is observed in a crater on one of the photographs (Figure 44). The arguments for an abnormally soft surface are as follows: (1) the surface is covered mostly by soft rounded craters having low slopes; (2) there is a notable lack of rock fragments which might indicate that they are buried by dust; and (3) there is an absence of fractures, fissures, etc., which should be relatively abundant on a lava surface.

Presently, neither of these arguments can be proven or disproven. It is significant, however, that the data on surface roughness which were obtained by Ranger VII indicated that our fears of a surface littered by protuberances and obstacles may be largely discounted, at least in the intra-crater areas of the Maria. There remains the bearing strength problem, but the conservative model adopted by the LEM vehicle designers still seems adequate for even loose-dust surface.

D. Other Findings by Ranger Photographs

The Ranger VII photographs confirm the widely-held theory that the lunar micro-relief is reflected in its macro-relief. Shoemaker [37] points out that "even though the craters increased in number very rapidly, the pictures no longer looked as rough." This observation tends to confirm an observation made by Bensko and Cortez [27] prior to the Ranger photos when they concluded "that the surface does not become infinitely rougher by cratering."

One of the most significant findings of the Ranger photographs concerns the nature of the lunar rays. Previously, it was thought that the rays were due to a light-colored dust covering the lunar surface which was derived from the large primary craters, e.g., Copernicus. Since many of the older lunar craters did not have well-defined ray systems associated with them, it was assumed that the ray material was darkened by radiation, just as radiation darkens glass on earth. Ranger VII indicates that the

rays are actually concentrations of secondary impact craters and have extremely rough micro-relief and would not provide likely landing sites. This interpretation of rays would seem to preclude radiation-darkening of ray material as an explanation for their absence. Instead, it would seem that a more reasonable explanation is that they are absent because of the superposition of younger material over them. Salisbury [38] has provided a good illustration of the superposition of lunar craters and associated debris by younger material (Figure 37).

It seems reasonable to assume at this time that, if the ray material of the Ranger VII photograph is too rough for a landing site, then the surface roughness will increase sharply in the direction of the parent ray crater which in this case is thought to be Copernicus. This conclusion, though tentative, could have far-reaching implications for possible lunar traverses by a mobile vehicle. It would seem advisable to consider follow-up missions to confirm the results of Ranger VII by photographing a very clean Maria and another to determine the nature of the surface near Copernicus.

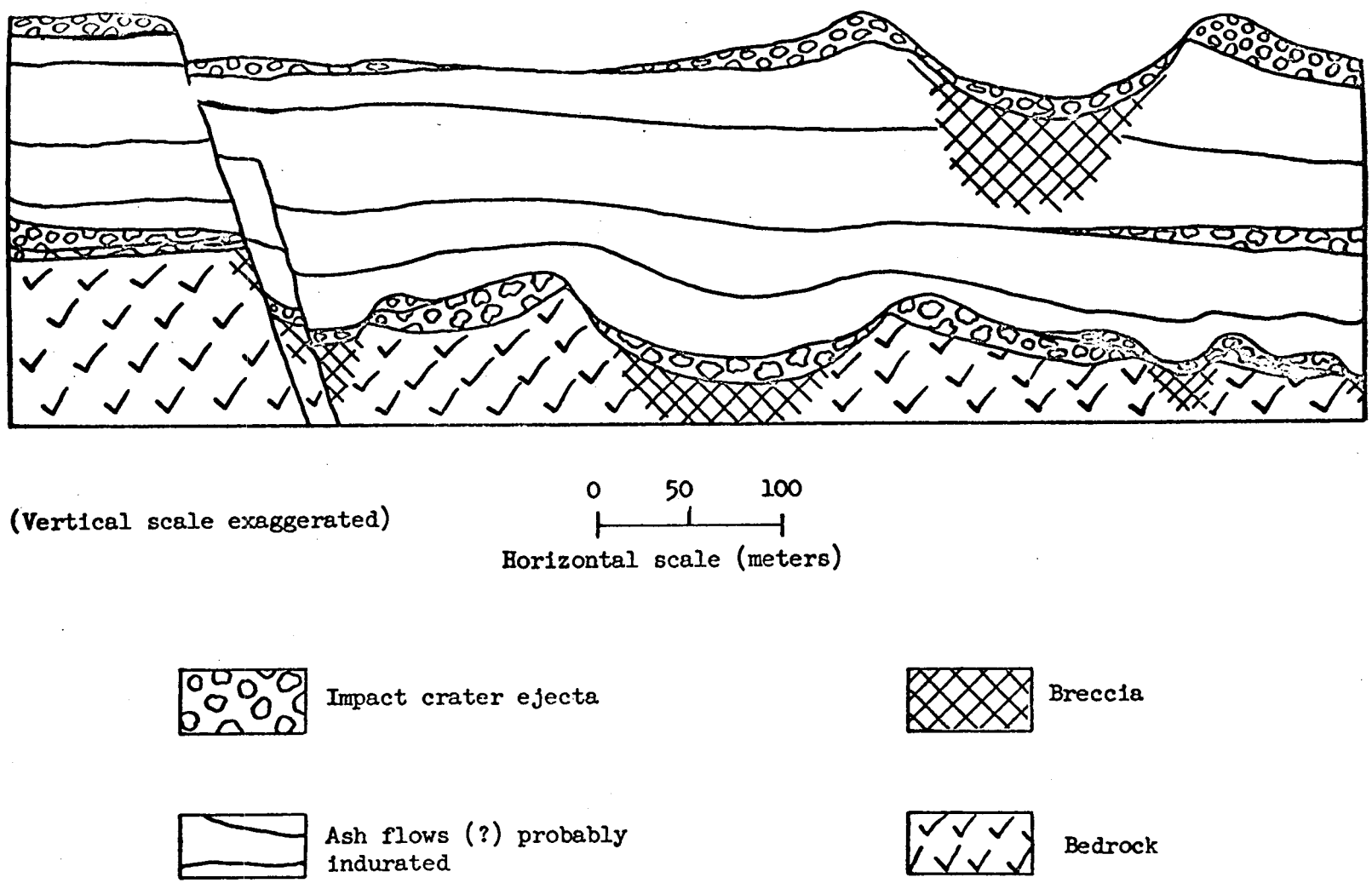

FIGURE 37: SALISBURY'S CONCEPT OF LUNAR SUBSURFACE CONDITIONS AND SUPERPOSITION OF YOUNGER MATERIAL ON OLDER MATERIAL (Ref. 39)

FIGURE 38. INDEX MAP OF RANGER VII IMPACT AREA

This index map is a reduced section of the map, Monte Riphaeus LAC 76, April 1964, produced by the Air Force Aeronautical Chart and Information Center, St. Louis, Missouri. The areas outlined on this map refer to Figures 40 through 44.

TABLE IV

Corresponding Areas on Index Map	Figure Number	Altitude		Side of Photograph	
		km	Miles	km	Miles
	39	672.3	480	324	180
1	40	378.1	235	181.8	113
2	41	136.8	85	76.8	48
3	42	54.7	34	25.7	16
4	43	17.7	11	6.4	4
5	44	4.8	3	2.67	1.66
6 & 7*	45 Lower	.912	3000 ft	30.4 m	100 ft
	45 Upper	.304	1000 ft	30.4 x 18.2 m	100 ft x 60 ft

* Areas 6 and 7 correspond to the final Ranger VII photographs.

PARRY
BONPLAND
GUERICKE
OPELT
DARNEY
1
2
3
4
5

FIGURE 39. PHOTOGRAPH TAKEN BY THE RANGER VII SPACECRAFT AT AN ALTITUDE OF 672.3 KM (480 mi)

Viewed with the clock at the upper left-hand corner, north is at top of picture. This photo duplicates closely resolution obtained by earth-based photography. The large flat bottomed crater in the lower margin between the réseau marks is Lubiniezky. The approximate point of impact of Ranger VII is indicated by ✕.

The area inside the white lines corresponds to Area 1 in Figure 38.

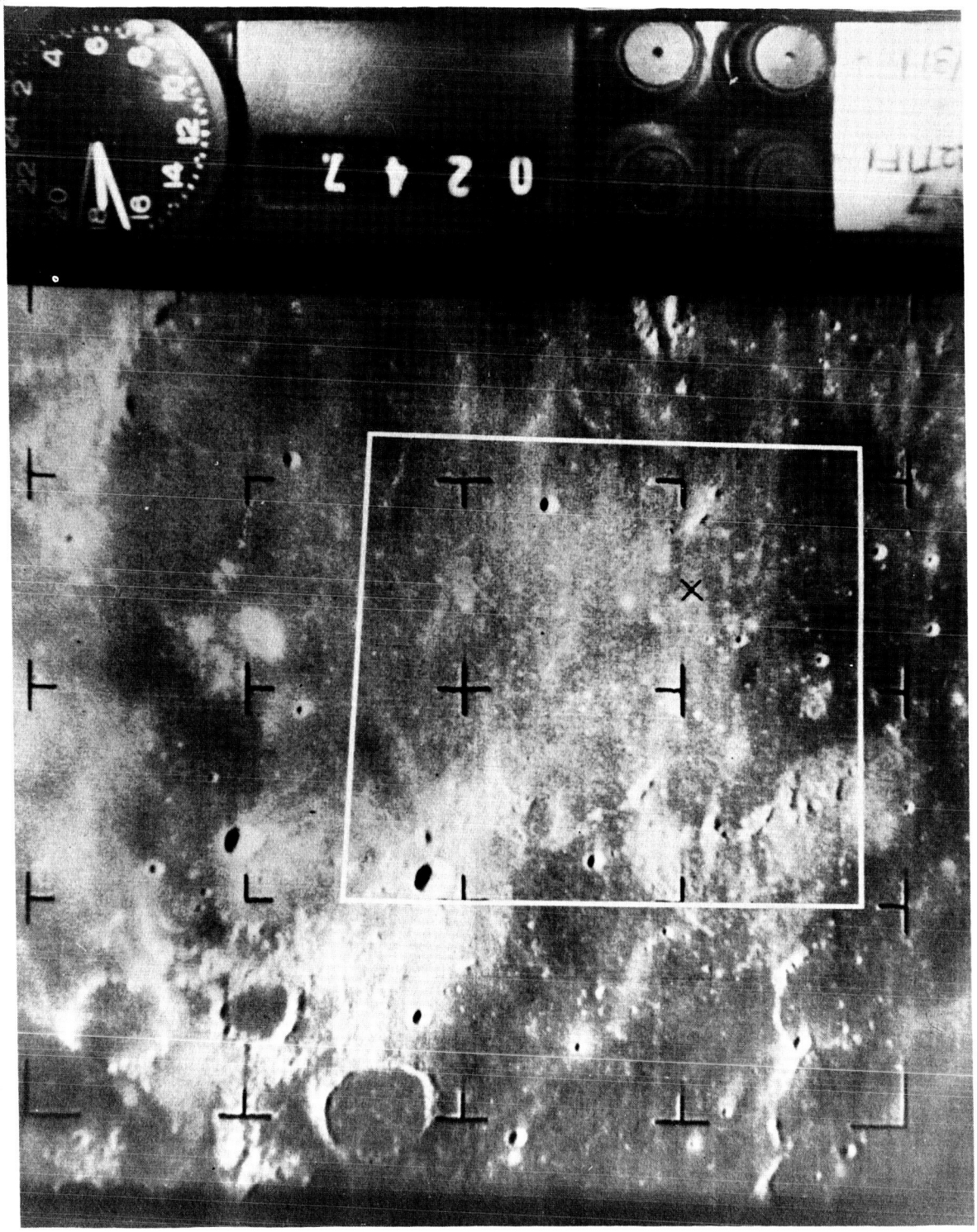

FIGURE 40. PHOTOGRAPH TAKEN BY THE RANGER VII SPACECRAFT AT AN ALTITUDE OF 378.1 KM (235 mi)

Viewed with the clock at the upper left-hand corner, north is at the top of the photograph. Each side of the photograph is about 181.8 km (113 mi). The entire photograph corresponds to Area 1 on Figure 38.

The predominant feature in the lower left-hand corner is the crater Darney, 15.28 km (9.5 mi) in diameter. The small indistinct white spots in Figure 39 now appear as small craters. These craters are approximately 304.78 meters (1,000 ft) in diameter.

The area inside the white lines corresponds to the entire photograph shown on Figure 41.

FIGURE 41. PHOTOGRAPH TAKEN BY THE RANGER VII SPACECRAFT AT AN ALTITUDE OF 136.8 km (85 mi)

Viewed with the clock at the upper left-hand corner, north is at the top of the photograph. The entire photograph corresponds approximately to area 2 on Figure 38. Each side of the photograph shown is about 76.8 km (48 mi).

The largest crater in the photo is Bonpland H, approximately 3.8 km (2.3 mi) in diameter. Note the intense amount of cratering in the area inside the white lines. This pattern is interpreted to be the result of some of the ray material from the impact crater Copernicus.

The area inside the white lines corresponds to the entire photograph shown in Figure 42.

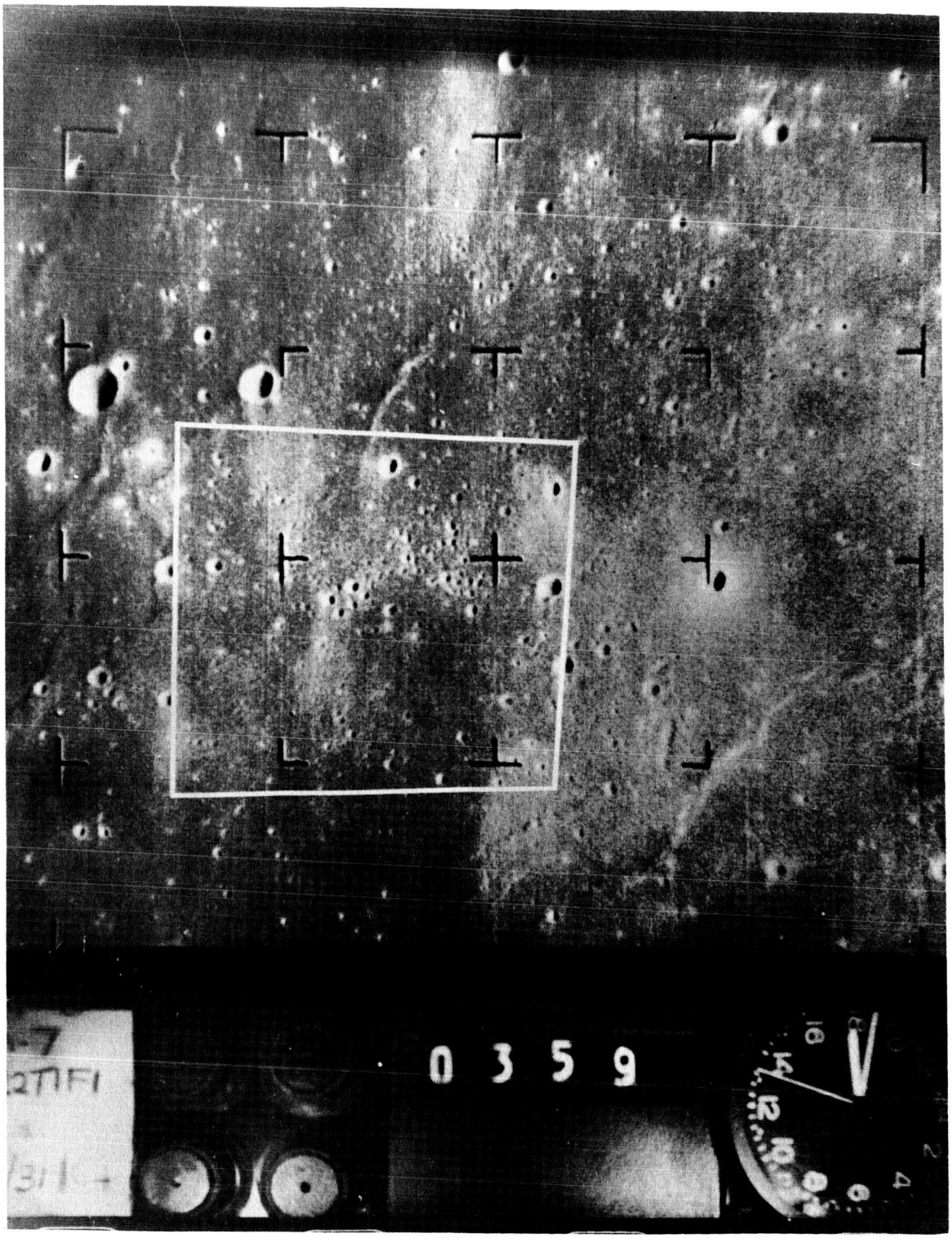
0359

FIGURE 42. PHOTOGRAPH TAKEN BY THE RANGER VII SPACECRAFT AT AN ALTITUDE OF 54.7 KM (34 mi)

Viewed with the clock in the upper left-hand corner, north is at the top of the photograph. Each side of the photograph shown is about 25.7 km (16 mi). The entire photograph corresponds approximately to area 3 on Figure 38.

The craters of the Copernicus ray group seen in the preceding photograph are shown in greater detail. The smallest craters are approximately 45.72 meters (150 feet) in diameter.

The area inside the white lines corresponds to the entire photograph shown on Figure 43.

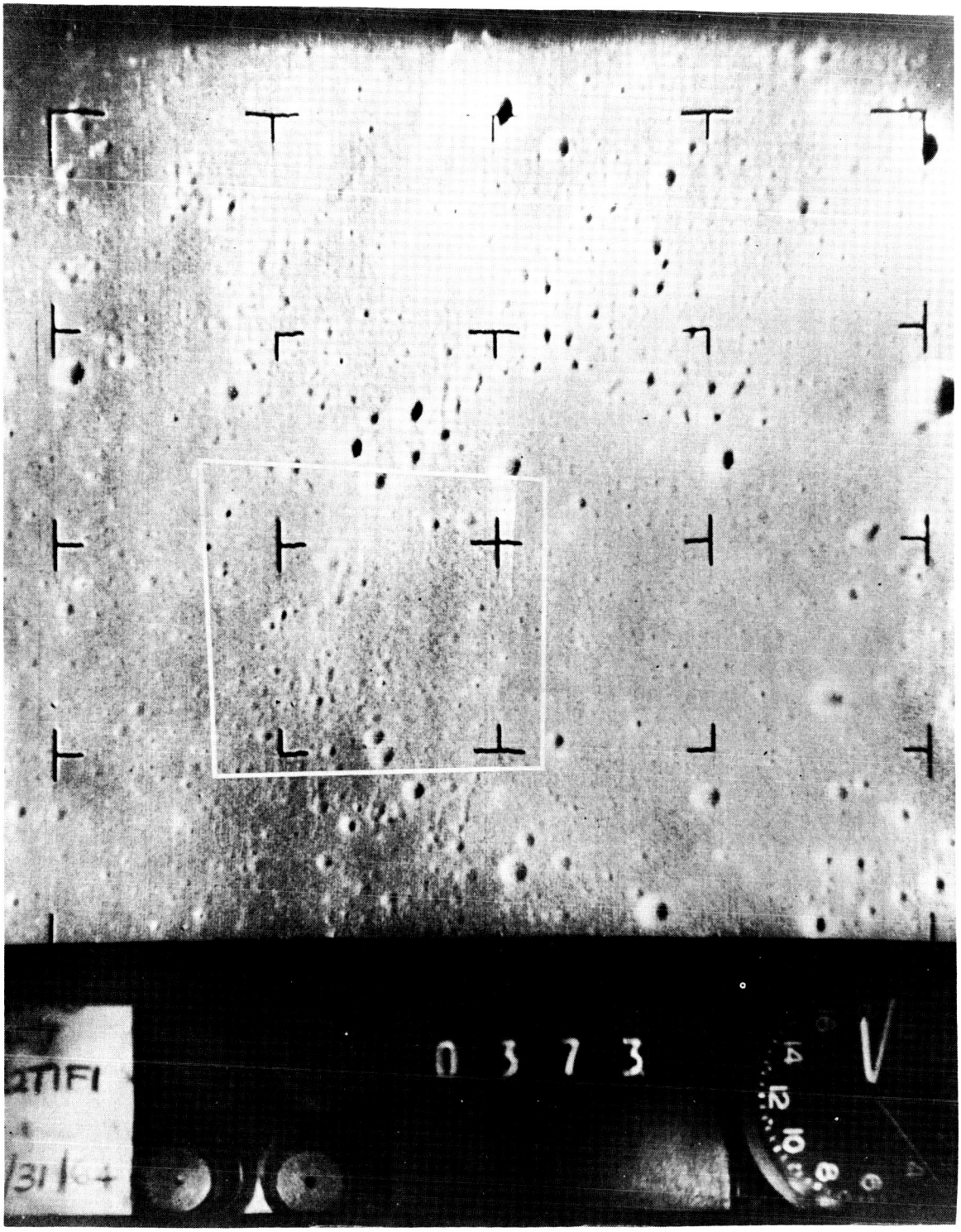
0373

FIGURE 43. PHOTOGRAPH TAKEN BY RANGER VII SPACECRAFT AT AN ALTITUDE OF 17.7 KM (11 mi)

Viewed with the clock in the upper left-hand corner, north is at the top of the photograph. Each side of the photograph shown is about 6.4 km (4 mi). The entire photograph corresponds approximately to area 4 on Figure 38.

Craters as small as 13.7 meters (45 ft) can be recognized.

The area inside the white lines corresponds to the entire photograph shown on Figure 44.

FIGURE 44. PHOTOGRAPH TAKEN BY RANGER VII SPACECRAFT AT AN ALTITUDE OF 4.8 KM (3 mi)

Each side of area shown is about 2.67 km (1.66 mi). This area corresponds to area 5 on Figure 38.

Crater, upper left, with two rock masses protruding into sunlight is about 91.2 m (300 ft) across. The resolution obtained in this photograph shows craters about 9.14 meters (30 ft) in diameter.

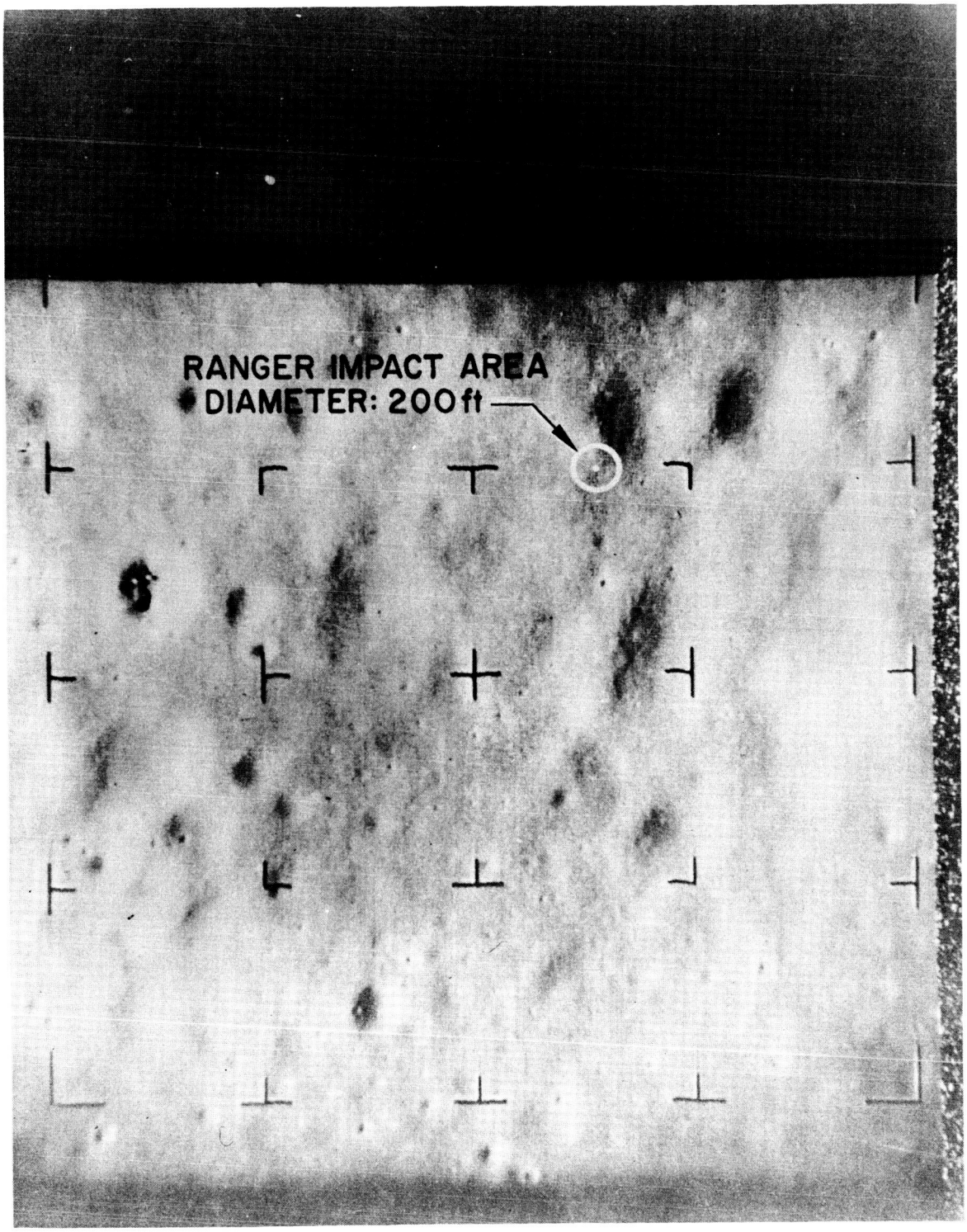
RANGER IMPACT AREA
DIAMETER: 200ft

FIGURE 45. FINAL PHOTOGRAPHS OF RANGER VII SPACECRAFT AT ALTITUDES OF 912 m (3000 ft) and 304 m (1000 ft)

The lower complete picture was taken at an altitude of about 912 m (3000 ft) above the lunar surface and encloses an area approximately 100 ft on each side.

Viewed with the partial picture and line of receiver noise at the top, north is at the top in both pictures. The top partial picture was the last taken at an altitude of 304 m (1000 ft) above the lunar surface and encloses an area about 30.4 m (100 ft) by 18.2 m (60 ft).

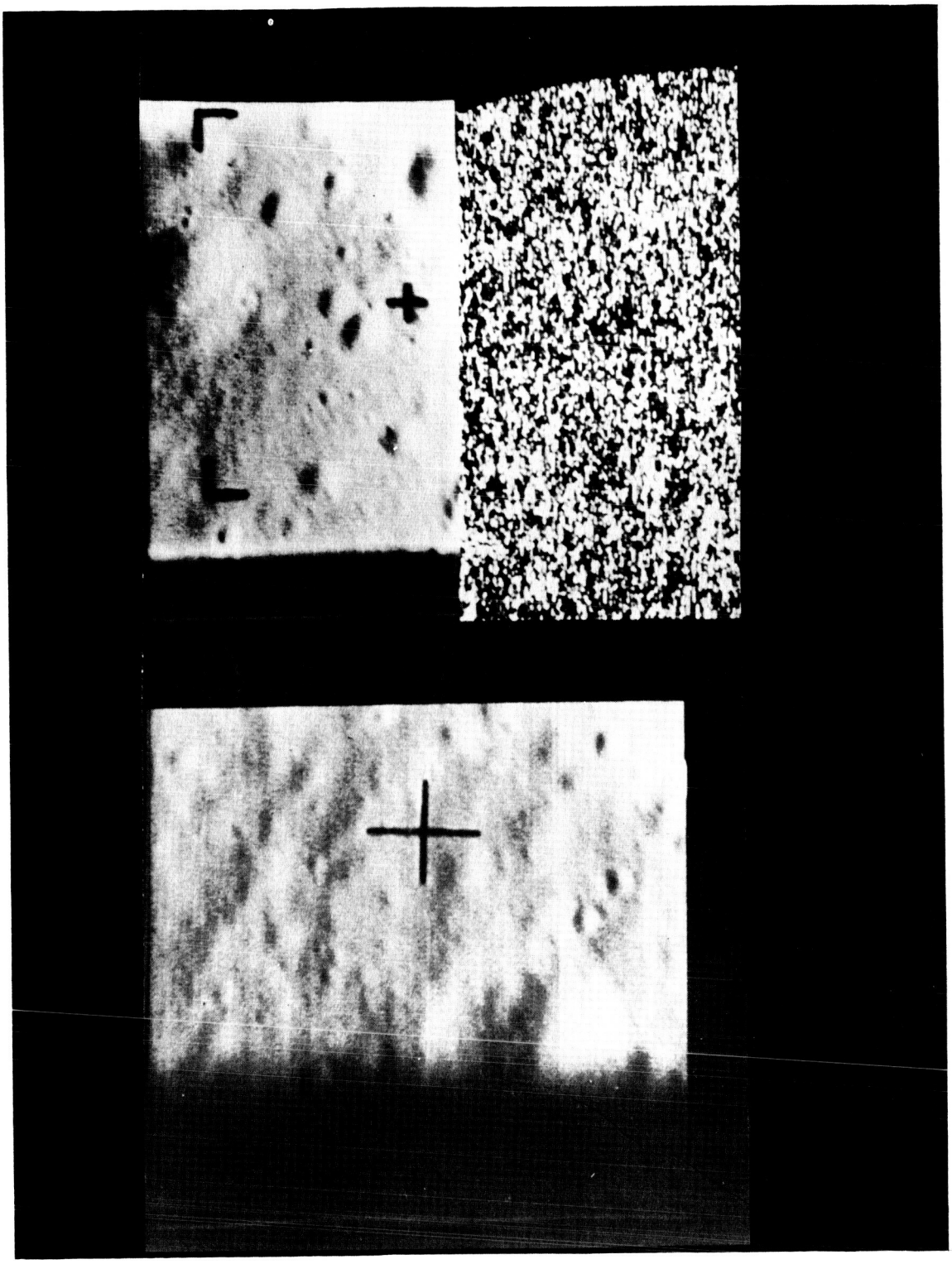

IX. CONCLUSIONS AND RECOMMENDATIONS

This report provides a geologic frame of reference which can be used as the fundamental basis for future lunar exploration programs. For optimum utilization, the lunar scientific experiments and instruments should be designed to operate within this framework. This report should be updated at appropriate intervals to insure inclusion of the latest interpretations of the lunar environment, contained in data from other NASA Centers, the Astrogeology Branch of the United States Geological Survey, and qualified government contractors. Additional supporting data will be provided by NASA's continuing lunar investigations in Ranger, Surveyor, and Lunar Orbiter programs.

Our knowledge about the lunar environment is limited to interpretations of maps, photographs, and analogous earth features and processes. Because of present limitations of earth-based photography, improved interpretations of small-scale features will require more high-resolution photographs such as provided by Ranger VII taken in various types of lunar terrain. Also, definitive interpretations of lunar surface hardness and composition, structure of the interior, and the relative significance of volcanic versus meteoritic processes, must await the data which may be provided by the Surveyor series.

GLOSSARY

ARCUATE	Curved or bowed.
BASALT	An extrusive rock composed primarily of calcic plagioclase, pyroxene, with or without olivine. Basalt constitutes one of the two major igneous rock clans (cf. granite).
BRECCIA	A rock made up of highly angular coarse fragments. There are friction or fault-breccias, talus-breccias and eruptive breccias.
CALDERA	A large basin-shaped volcanic depression, more or less circular or cirque-like in form, the diameter of which is many times greater than that of the included volcanic vent or vents, no matter what the steepness of the walls or form of the floor.
CLASTIC	A textural term applied to rocks composed of fragmental material derived from pre-existing rocks by a process of mechanical transportation.
DETRITAL	A synonym for clastic, e.g., minerals or rock fragments which were derived from pre-existing igneous, sedimentary or metamorphic rocks.
EJECTA	Material thrown out of a volcanic or impact meteorite crater by explosion.
EN ECHELON	Parallel structural features that are offset like the edges of shingles on a roof when viewed from the side.
ESCARPMENT, SCARP	The steep face of a ridge of high land; a cliff or relatively steep slope separating level or gently sloping tracts.
"FAIRY CASTLE" STRUCTURE	A type of small-scale surface structure of dust particles a few microns in diameter which has been proposed to satisfy the data on lunar photometric properties. The "fairy-castle" structure depends on electrostatic charges to hold the dust particles together.

FAULT	A fracture or fracture zone along which there has been displacement of the two sides relative to one another parallel to the fracture. The displacement may be a few centimeters to several thousand meters.
GEOSYNCLINE	A surface of regional extent subsiding through a long time while contained sedimentary and volcanic rocks are accumulating; great thickness of these rocks are almost invariably the evidence of the subsidence, but not a necessary requisite.
GRANITE	A plutonic rock consisting essentially of alkalic feldspar and quartz. Granite constitutes one of the two major igneous rock clans (cf. basalt).
LANDFORM	In geomorphology, the term landform is applied to each one of the multitudinous features that taken together make up the surface of the earth.
LUNATION	One complete phase of the moon lasting approximately 28 days.
MAGMA	Naturally occurring mobile rock material, generated within the earth and capable of intrusion and extrusion, from which igneous rocks are considered to have been derived by solidification.
OLIVINE	A mineral series, solid solutions of forsterite, Mg_2SiO_4, with fayalite, Fe_2SiO_4, the composition often expressed as mol percent of the constituents. An important rock-forming mineral, especially in the mafic and ultramafic rocks.
OUTCROP	That part of a stratum which appears at the surface; to crop out is to come to the surface of the ground.
PYROCLASTIC	A general term applied to detrital volcanic materials that have been explosively or aerially ejected from a volcanic vent. Also, a general term for rocks made up of these materials.
RILLE	Long narrow structural valleys developed on the lunar surface.

GLOSSARY (Continued)

SERPENTINE	$Mg_3Si_2O_5(OH)$. A common rock-forming mineral which forms by the hydrothermal alteration of olivine.
STRUCTURE	The sum total of the structural features of an area. Structures refer to such occurrences as faults, folds, unconformities, etc.

REFERENCES

1. Gault, Donald E., "Lunar Atmosphere," Environment Criteria for Spacecraft Design, Ames Research Center, October 8, 1963.

2. Niedz, F. J., "Survey of the Physical and Environmental Parameters of the Moon," Apollo Support Department, General Electric Company, Daytona Beach, Florida, February, 1963, NASw-410-20-13-10.

3. Alter, Dinsmore, "The Alphonsus Story," Proceedings of Lunar and Planetary Exploration Colloquim, Space and Information Systems Division, North American Aviation, Inc., Downey, California, January 1, 1959.

4. Shorthill, R. A., "Space Science Seminar Lecture," MSFC, June, 1964.

5. Wehner, G. K., D. L. Rosenberg, and J. E. Ken Knight, "Investigation of Sputtering Effects on the Moon's Surface," General Mills Electronics Division, Minneapolis, Minnesota, July 31, 1963.

6. Fudali, R. F., "Small-Scale Lunar Topography," Bellcomm, Inc., Washington, D. C., June 28, 1963.

7. Hackman, R. J. and A. C. Mason, "Engineer Special Study of the Surface of the Moon," Misc. Geol. Investigations, Map I-351, U.S.G.S., Washington, 1961.

8. Hackman, R. J., "Geologic Map and Sections of the Kepler Region of the Moon," Map J-355 (LAC-57), U.S.G.S., Washington, 1962.

9. Bensko, J., "Selenology," Fundamentals of Astronautical Engineering, McGraw-Hill Book Co., Inc., New York, 1961.

10. Shoemaker, E. M., R. J. Hackman, and R. E. Eggleton, "Interplanetary Correlation of Geologic Time," Advances in the Astronautical Sciences, Volume 8, Plenum Press, Inc., New York, 1962.

11. Salisbury, J. W., "Origin of Lunar Domes," Proceedings of Lunar and Planetary Exploration Colloquim, Space and Information Systems Division, North American Aviation, Inc., Downey, California, March 17, 1960.

12. Bronner, F. E., "Outline of Lunar Geography and Geology," Space Systems Operations, General Electric Company, Santa Barbara, Calif., July 1962, 62 SPC-8.

13. Salisbury, J. W., "The Lunar Environment," Space and Planetary Environments, Air Force Surveys in Geophysics, Shea L. Vally, ed., AFCRL-62-270, January, 1962.

14. Speed, R. C., J. E. Conel, R. L. Korach, A. A. Loomis, "Geological Exploration of the Moon and Planets," NASA SP-14, December, 1962.

15. Fudali, R. F., "Lunar Surface Characteristics," Bellcomm, Inc., Washington, D. C., June 25, 1963.

16. Shoemaker, E. M., "Exploration of the Moon's Surface," American Scientist, Vol. 50, pp. 99-130, 1962.

17. Urey, H. C., "Origin and History of the Moon," Physics and Astronomy of the Moon, Z. Kopal, ed., Academic Press, New York and London, 1962.

18. Shoemaker, E. M., "Interpretation of Lunar Craters," Physics and Astronomy of the Moon, Z. Kopal, ed., Academic Press, New York and London, 1962.

19. Shoemaker, E. M., "Ballistics of the Copernican Ray System," Proceedings of Lunar and Planetary Exploration Colloquim, Space and Information Systems Division, North American Aviation, Inc., Downey, California, March 17, 1960.

20. Green J., "The Geosciences Applied to Lunar Exploration," The Moon, Proceedings of Symposium No. 14, International Astronomical Union, Pulkova Observatory, Levingrad, U.S.S.R., Academic Press, New York, December 1960.

21. Green, J., "Geochemical Aspects of Lunar Degassing," Proceedings of Lunar and Planetary Exploration Colloquim, Space and Information Systems Division, North American Aviation, Inc., Downey, Calif., January 12, 1959, Vol. 1, No. 4.

22. Field, G., "Origin of the Moon," American Scientist, pp. 349-354, September 1963, (Autumn).

23. Glossary of Geology and Related Sciences, American Geological Institute, NAS-NRC Publication 501, Washington, D. C., 1957.

24. Green, Jack, lecture, MSFC, March 1964.

25. Thornbury, W. D., "Principles of Geomorphology," John Wiley & Sons, Inc., New York, January, 1956.

26. Gilbert, G. K., "The Moon's Face: A Study of the Origin of Its Features," Bull. Phil. Soc., Washington, Vol. 12, 1893.

27. Bensko, J., and J. L. Cortez, "Lunar Surface Considerations for the Logistics Vehicle Study," MTP-RP-63-2, April 24, 1963.

28. Kuiper, G. P., "The Moon," The Exploration of Space, ed. Robert Jastrow, Macmillan Co., New York.

29. Judge, John F., "Bendix Simulating Lunar Magma in Laboratory Tests," Missiles and Rockets, March 23, 1964.

30. Cameron, W. S., "An Interpretation of Schröeter's Valley and Other Lunar Sinuous Rills," Jour. of Geophysical Research, Vol. 69, No. 12, June 15, 1964.

31. Dugan, Duane W., "Lunar Surface Environment Criteria for Spacecraft Design," Ames Research Center, January 24, 1964.

32. Sinton, W. M., "Temperatures on the Lunar Surface," Physics and Astronomy of the Moon, ed. Z. Kopal, Academic Press, New York, 1962.

33. Dollfus, Andouin, "The Polarization of Moonlight," Physics and Astronomy of the Moon, ed. Z. Kopal, Academic Press, New York, 1962.

34. Jaeger, J. C., "Surface Temperature of the Moon," Australian Journal of Physics, Vol. 6, pp. 10-21, 1953.

35. Baldwin, Ralph B., The Measure of the Moon, The University of Chicago Press, Chicago, Illinois, 1963.

36. Watkins, Harold D., "Ranger Photos Boost Confidence in Apollo," Aviation Week and Space Technology, August 10, 1964, pp. 19-24.

37. "Ranger VII Proves Apollo Feasibility," Missile and Rockets, August 10, 1964, pp. 16-24.

38. Salisbury, J., "Models Used in Air Force Cambridge Research Laboratory Lunar Surface Studies," OART Coordinating Group on Lunar Technology Situation Report, May 7, 1964, pp. 41-46.

39. Wechsler, A. E. and P. E. Glaser, "Thermal Properties of Postulated Lunar Surface Materials," The Lunar Surface Layer, edited by J. E. Salisbury and P. E. Glaser, Academic Press, New York, 1964.

LUNAR ENVIRONMENT: AN INTERPRETATION OF THE SURFACE OF THE MOON AND ITS ATMOSPHERE

By John R. Rogers and Otha H. Vaughan, Jr.

The information in this report has been reviewed for security classification. Review of any information concerning Department of Defense or Atomic Energy Commission programs has been made by the MSFC Security Classification Officer. This report, in its entirety, has been determined to be unclassified.

This document has also been reviewed and approved for technical accuracy.

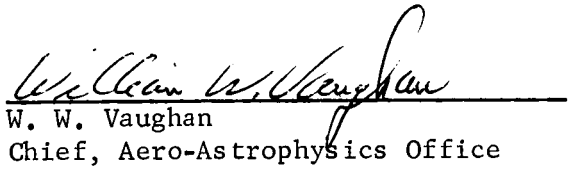

W. W. Vaughan
Chief, Aero-Astrophysics Office

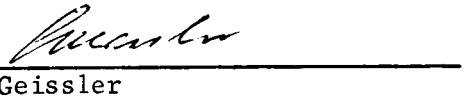

E. D. Geissler
Director, Aero-Astrodynamics Laboratory

DISTRIBUTION

INTERNAL

DIR
Dr. von Braun
Mr. F. L. Williams

AST-S
Dr. Lange

DEP-T
Dr. Rees

R-DIR
Mr. Weidner
Dr. McCall

R-FP
Dr. Koelle (3)
Dr. Ruppe
Mr. Hamby

R-SA
Mr. Dannenberg
Dr. Kuettner
Dr. Farish

R-AERO-DIR
Dr. Geissler
Mr. Jean

R-AERO-S
Mr. deFries (3)
Mr. Schaefer
Mr. Dale Ruth
Mr. Yarborough
Mr. Madewell
Mr. Bradford

R-AERO-D
Mr. Horn

R-AERO-F
Dr. Speer
Mr. Emanuel

R-AERO-G
Dr. Hoelker

R-AERO-P
Mr. McNair (2)

R-AERO-T
Mr. Murphree
Dr. Heybey
Dr. Sperling

R-AERO-Y
Mr. W. Vaughan (3)
Mr. Scoggins
Mr. O. E. Smith
Mr. Daniels
Mr. R. E. Smith
Mr. Dalton
Mr. O. H. Vaughan (150)

R-ASTR-DIR
Dr. Haeussermann

R-ASTR-A
Mr. Digesu (2)

R-P&VE-DIR
Mr. Cline

R-P&VE-A
Mr. Goerner (2)
Dr. Krause
Mr. Swanson

R-P&VE-AL
Mr. Johns
Mr. Vaccaro

R-P&VE-AB
Mr. Raines

R-P&VE-P
Mr. Paul

DISTRIBUTION (Cont'd)

INTERNAL (Cont'd)

R-P&VE-M
Dr. Lucas (2)

R-RP-DIR
Dr. Stuhlinger

R-RP-J
Mr. Downey (5)

R-RP-N
Dr. Hale (2)

R-RP-S
Dr. Mechtly

R-RP-T
Mr. Bensko (5)

RSIC Library (8)

MS-IPL (8)

MS-IP

MS-H

HME-P

CC-P

Kennedy Space Center
Dr. Debus/Dr. Gruene, KN-DIR
Dr. Knothe, KN-T
Mr. von Tiesenhausen, KN-DF2

Technical and Scientific Information Facility (25)
P. O. Box 5700
Bethesda, Md.
Attn: NASA Representative (S-AK/RKT)

DISTRIBUTION (Cont'd)

EXTERNAL

Director
Office of Manned Space Flight
NASA Headquarters
Washington, D. C., 20546
Attn: Mr. D. Beattie (2)
Mr. E. Z. Gray (2)
Dr. George Mueller (2)

Office of Advanced Research and Technology (2)
NASA Headquarters
Washington, D. C. 20546

Office of Space Sciences and Applications
NASA Headquarters
Washington, D. C. 20546
Attn: Dr. William B. Foster (2)
Dr. Homer Newell (2)

National Aeronautics and Space Administration (2)
Langley Research Center
Langley Field, Virginia

Goddard Space Flight Center (NASA) (3)
Greenbelt, Maryland, 20771

Jet Propulsion Laboratory (5)
California Institute of Technology
4800 Oak Grove Drive
Pasadena 3, California, 91103

Lewis Research Center, NASA (4)
21000 Brookpark Road
Cleveland 35, Ohio, 44135

Ames Research Center, NASA (3)
Moffett Field
Mountain View, California, 94035

Manned Spacecraft Center, NASA
Houston, Texas, 77001
Attn: Dr. Joseph Shea
Mr. Christopher Craft
Mr. Donald K. Slayton
Mr. John Eggleston (3)
Technical Library (2)
Mr. Edward Wittry

EXTERNAL (Cont'd)

Institute for Space Studies, NASA
475 Riverside Drive
New York 27, New York, 10027

Dr. R. B. Baldwin
Oliver Machinery Co.
Grand Rapids,Michigan, 49502

Dr. Robert Bates
Dept. of Geology
Ohio State University
Columbus, Ohio

Air Force Cambridge Research Laboratories
Bedford, Mass.
Attn: CRFL, Dr. J. W. Salisbury (2)
Technical Library (2)

Dr. Jack L. Hough
Department of Meteorology and Oceanography
University of Michigan
Ann Arbor, Michigan

Bellcomm, Inc.
Washington, D. C.
Attn: Mr. W. W. Elam

Dr. Alex E. S. Green
University of Florida
Physics Department
Gainesville, Florida

Dr. Seymor L. Hess
Florida State University
Department of Meteorology
Tallahassee, Florida